A quantitative study of the effect of process variables on the retention of volatile trace components in drying

Please check the document version of this publication:

• A submitted manuscript is the version of the article upon submission and before peer-review. There can be important differences between the submitted version and the official published version of record. People interested in the research are advised to contact the author for the final version of the publication, or visit the DOI to the publisher's website.
• The final author version and the galley proof are versions of the publication after peer review.
• The final published version features the final layout of the paper including the volume, issue and page numbers.

[Link to publication](#)

A QUANTITATIVE STUDY OF THE EFFECT OF PROCESS VARIABLES ON THE RETENTION OF VOLATILE TRACE COMPONENTS IN DRYING

P.J.A.M. KERKHOF

A QUANTITATIVE STUDY OF THE EFFECT OF PROCESS VARIABLES ON THE RETENTION OF VOLATILE TRACE COMPONENTS IN DRYING

PROEFSCHRIFT

TER VERKRIJGING VAN DE GRAAD VAN DOCTOR IN DE TECHNISCHE WETENSCHAPPEN AAN DE TECHNISCHE HOGESCHOOL EINDHOVEN, OP GEZAG VAN DE RECTOR MAGNIFICUS, PROF.DR.IR. G. VOSSERS, VOOR EEN COM-MISSIE AANGEWEZEN DOOR HET COLLEGE VAN DEKANEN IN HET OPENBAAR TE VERDEDIGEN OP VRIJDAG 20 JUNI 1975 TE 16.00 UUR

door

Petrus Johannes Antonius Maria Kerkhof

geboren te Breda

Dit proefschrift is goedgekeurd door de promotoren :

Prof.dr.ir. H.A.C. Thijssen (1^e promotor)

Prof.dr.ir. S. Bruin (2^e promotor)

aan Rosa
en Peter

ACKNOWLEDGEMENTS

CURRICULUM VITAE

The author was born on December 15, 1945, in Breda, the Nether-
lands. Following his secundary education at the H.B.S. of the
Onze Lieve Vrouwe Lyceum in Breda, he began his studies in the
Chemical Engineering Department at the Technische Hogeschool
Eindhoven in 1963. Graduate work, leading to the title of
"scheikundig ingenieur" in January 1970, was performed under
the guidance of prof.dr.ir. A.I.M. Keulemans. From August 1969
until January 1970 the author was research assistent at the
department of Instrumental Analysis, after which he started
working as "wetenschappelijk medewerker" in the department of
"Fysische Technologie" under the direction of prof.dr.ir. H.A.C.
Thijssen.

CONTENTS

I INTRODUCTION

I.1. General

A very important aspect of food processing is formed by concentration and drying processes, which extend shelf life of foods and allow storage and convenient distribution. Furthermore partial or total removal of water reduces storage and transport volume, and is consequently of considerable economic interest.
In order to design concentration and dehydration processes and to choose between alternative processes insight is required into the following factors:

1. Mass and heat transfer phenomena
2. The relation between composition and stability with respect to microbial spoilage, chemical reactions and physical changes
3. Thermal stability of the food components
4. The relation between composition and physical properties of the concentrated or dried product on one hand, and the quality of the product on the other hand. Factors determing the quality of the product can be: storage stability, nutrient value, flavour, texture, instant properties, free-flowingness, and bulk density
5. Economics of various concentration and dehydration processes.

The contribution of chemical engineering to the field of food dehydration and concentration lies in the study and application of basic chemical engineering principles within the constraints given both by the specific requirements for the product of interest, and by economic factors. An extensive review of these aspects was given by Bomben et al (23).
In this thesis a study is made of the mass and heat transfer in some drying processes for food liquids, and the implication of these transport phenomena for one of the quality aspects, the retention of volatile aroma components.

I.2. <u>Aroma and aroma retention</u>

One of the primary factors determining the quality of many
natural juices and extracts is the flavour pattern. This pattern
is made up by a large number of aroma components. The vast major-
ity of these components are present in very low concentrations
and are very volatile with respect to water (1-4). Upon equili-
brium evaporation of water these components will already be
completely removed from the food liquid, when only part of the
water has been evaporated (1). Experimental investigations into
the retention of volatile flavour components in spray-drying
(1,5-8), have shown that under optimum process conditions aroma
components can be retained to a large extent. Similar results
have been obtained for slab drying (8-12), for extractive drying
(13, this thesis) and for freeze drying (1, 14-18, 68). In the
literature two basic mechanisms are proposed for the retention
of homogeneously dissolved aroma components during the drying
of liquid foods:

1. Selective diffusion concept by Thijssen (19)
2. Microregion concept of Flink and Karel (15,16)

According to the selective diffusion concept as postulated by
Thijssen, the transport of both water and volatile aroma compo-
nents in a drying liquid food in the absence of internal circulat-
ion streams is governed by molecular diffusion. The diffusion
coefficients of water and of aroma decrease strongly with decreas-
ing water concentration; the decrease of the diffusion coefficient
of aroma is, however, much stronger than that of water, as can
be seen from fig. I.1 (1). As water is removed at the surface of
the drying food liquid, water concentration gradients develop.
Some time after the onset of the drying process, the interfacial
water concentration has dropped to such a low value, the "critical
value", that the diffusion coefficients of the aroma compounds are
so much lower than that of water, that virtually no more aroma is
lost. The surface of the food liquid then behaves as a semiperme-
able "dry skin". Experimental and theoretical work on the drying of
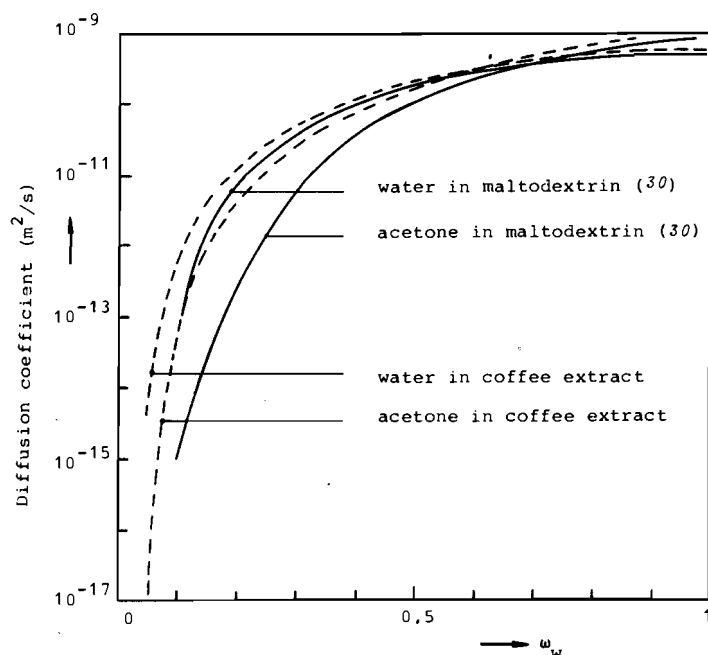
Fig. I-1. Influence of water concentration on the diffusion coefficient of water and of acetone in coffee extract and in aqueous maltodextrin solutions at 25 °C. (Thijssen and Rulkens, (7))

food liquids and model systems has confirmed the relevance of the selective diffusion concept to spray drying, slab drying, extractive drying and slush drying (1,4,7-12,20-22). Reviews of the present knowledge of diffusion coefficients in liquid foods (21,23) reveal that data, describing both the effect of water concentration and the effect of temperature on diffusion coefficients, are scarce.

The microregion concept of Flink and Karel has been used for the description of aroma retention in freeze drying. It postulates that during freezing and subsequent drying microregions are formed inside the liquid food in which aroma molecules may be entrapped. The experimental evidence for this theory has been critically reviewed by King & Massaldi (24), who arrived at the conclusion that the experimental results of Flink and Karel can also be fully explained with the selective diffusion concept. In view of the still not rigorous evidence of the microstructure concept, and because of the fact that at present no quantitative modelling has been performed on this theory contrary to the diffusion concept, the latter theory will be used in what follows.

The foregoing remarks were concerned with aspects of aroma mobility on a molecular scale. Recently the occurrence of aroma in

a dispersed phase has been studied, particularly in freeze dry-
ing (24,25,68,69). The phenomena found in these studies differ
considerably from those found in the studies of homogeneously
dissolved aroma components and also show considerable inter-
action effects between aroma components (68).

I.3. Scope of the present work

As stated above, in this thesis the selective diffusion concept
will be used as a working theory. The following limitations
have been set for this study for pratical reasons:

1. The systems considered are of simple geometry, e.g. slabs,
   cylinders or spheres
2. The aroma components are present in the homogeneously
   dissolved state and do not interact.

Although part of the theoretical treatments to be presented will
also be applicable for more complex systems, the geometrically
more complex freeze drying and the presence or formation of a
dispersed aroma phase will not be discussed.

The first part of this thesis (Chapter II) is concerned with a
study of the theory describing transport of water and aroma
during drying of food liquids. The existing literature is review-
ed, and generalized equations are given for several geometries
of the drying system. Furthermore similarity criteria are deriv-
ed, which enable the translation of the effect of one set of
process conditions into other sets. Finally some numerically
calculated results of ternary diffusion models for the drying of
slabs and of spherical particles are given.

The ternary diffusion models treated in Chapter II account for
the concentration and temperature dependence of the diffusion
coefficients and for the non-ideality of the system with respect
to water and aroma activity. As stated before, the data on
diffusion coefficients in food liquids are scarce. In the second

part of this thesis a method is developed which enables the
prediction of aroma retention from a number of relatively simple
slab drying experiments. The method is based on the observation
(8,9) that the major part of the aroma loss occurs during the
constant-rate period. This constant-rate period is caused by
the typical shape of the water vapour sorption isotherm, as
shown in fig. I-2 for aqueous maltodextrin solutions, measured
by the desiccator method (42). During drying the liquid-side
interfacial water concentration decreases, but the water acti-
vity and consequently the driving force for water removal only
decreases very slightly. Only upon passing a certain critical
value of the water concentration, say 30 wt% for maltodextrin
solutions, the water activity will decrease much faster. At
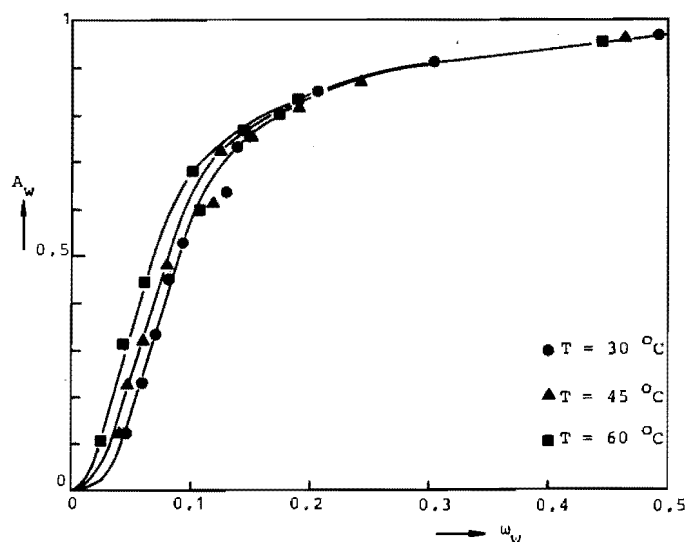
Fig. I-2. Water vapour
sorption isotherm of
aqueous maltodextrin
solution, measured by
the desiccator method

this critical water concentration the ratio of the diffusion
coefficients of aroma and water is already very low, as can be
seen in fig. I-1. In Chapter III from approximating theoretical
models and a large number of computer simulations correlations
are derived for the length of the constant-rate period and for
the effective aroma diffusion coefficient during this period as
a function of process variables. The realistic behaviour of the
ternary diffusion models namely enables the investigation and
correlation of computer-simulated data, instead of performing a
large number of experiments. The use of the correlations in order
to predict aroma retention is also first checked on results of

numerical calculations based on ternary diffusion models.

In Chapter IV the relations found in Chapter III on theoretical grounds are tested experimentally for aqueous maltodextrin solutions with n-alcohols as model aroma components. For this purpose slab drying experiments have been performed. The relations between the length of the constant-rate period and process variables, and the model of an effective aroma diffusion are proven to apply to the experiments. Using the correlations predictions are made of aroma retention in slab drying and spray drying, which are compared with experimental literature data. The foregoing models and correlations are based on simple geometry of the drying system and only take diffusion transport into account. In practice this is the case during a major part of slab drying time. There are however also other factors contributing to aroma loss, such as internal circulation streams inside the drying liquid (7,8) during droplet formation in spray drying, and expansion of droplets followed by crater formation in the dry skin, leading to evaporation from the interior of the particle.

In Chapter V the aroma loss in two new drying processes, dual stage drying and extractive drying, is investigated experimentally. For both processes the loss during the period in which diffusion is the governing mechanism is estimated from the correlations obtained in Chapter III and IV. This loss is designated as the *diffusional loss*. From the experimental results and the diffusional loss, the *additional loss* is calculated for single stage and dual stage spray drying. For both spray drying processes as well as for the extractive drying process with this analysis an evaluation of the merits of the processes is made, and suggestions towards improvement of these drying techniques are given.

II. THEORY OF WATER AND AROMA TRANSPORT DURING DRYING OF FOOD LIQUIDS

II.1. Introduction

Food liquids are generally very complex mixtures, consisting of a large number of components. A rough classification of the mixture on the basis of phase-equilibrium thermodynamical criteria is as follows :

1. a continuous waterphase
2. non-volatile components dissolved in the waterphase
3. volatile components dissolved in the waterphase
4. one or more dispersed phases consisting of partially soluble or insoluble components. In this case a distribution of the other components over the various phases occurs.

As examples of this classification may serve milk, containing dispersed fat, and citrus juices containing citrus oil. For the appropriate design of dehydration processes the knowledge of transport rates inside the material is essential, since the transport of water and heat determine drying time and temperature history, and the transport rate of volatile components determines the aroma loss. The transport rate of each individual component in the food liquid is dependent on the concentrations and transport rates of all other components, and in the case of separate phases also on the distribution of components between phases. As stated in the previous chapter, the influence of one or more dispersed phases will be excluded from the discussion in the following. In general the transport equations for the components in such food liquids are multicomponent equations. Such a multicomponent description however is impractical because of the complexity and the large number of independent relations required for diffusion coefficients, activity coefficients and vapour pressures in dependence on concentrations and temperature (8). Solution of the equations would still only be possible for very simplified conditions.

The work of Menting and of Thijssen and Rulkens (7,9) showed that the behaviour of a complex system such as coffee extract could be approximated by aqueous solutions of maltodextrin containing acetone as a volatile component. This was confirmed by the work of Chandrasekaran and King (11,12,29) on sugar solutions. From theory and experiment also followed that maltodextrin, which is a complex mixture of sugars and polysaccharides (see Appendix 1) could be treated as one component in the theory of transport phenomena in the model system. As the concentrations of aroma components are very low, the influence of these components on the transport rate of water, of dissolved solids and of the other aroma components can be neglected. Therefore the transport rates of water (w) and of dissolved solids (s) can be treated by binary diffusion analysis, and the transport of each individual aroma component (a) as a ternary diffusion problem.

In the literature several approaches have been made towards the theoretical modelling of the drying of liquid foods, as will be discussed briefly in the following.

1. Slab drying

Thijssen and Rulkens (7) and Menting et al (9,10) were the first to publish theoretical models for the drying of slabs. For both the transport of water and the transport of aroma binary diffusion equations were used with water-concentration-dependent diffusion coefficients. Menting et al (30) measured the diffusion coefficients of water and of traces of acetone in aqueous maltodextrin solutions, and determined the water vapour sorption isotherm of this system. Using these experimental data in the numerical solution of the diffusion equations, the above-mentioned authors calculated the drying rate and aroma loss in the isothermal drying of a gelled slab of malotodextrin solution. Good agreement between their results and the experimental curves was found, provided that the shrinkage of the system due to water loss was taken into account.

The binary analysis for the aroma transport mentioned above was later extended by Rulkens and Thijssen (27) who used the ternary Stefan-Maxwell equation for the description of aroma transport. In this model interactions between aroma and the other two components can be distinguished. Calculations based on this model for the same system as mentioned above again showed good agreement with the experimental data.

In the foregoing models the effect of the water concentration on the activity coefficient of aroma and the implication of this effect on aroma transport was excluded. For the system of acetone in aqueous maltodextrin solution this was justified, as shown by Menting (9). To account for this effect Chandrasekaran and King (11,12,19) used a ternary analysis based on the theory of irreversible thermodynamics (31,32,33) in their study of the retention of various volatiles in sugar solutions. Good agreement was observed between their model calculations using experimentally determined data on diffusion and activity coefficients, and experimentally measured concentration profiles in drying gelled slabs.

Rulkens (8) and Kerkhof et al (20) later used the Generalized Stefan-Maxwell equation (37) in their calculations of the effect of process variables on aroma retention. In this model also the effect of water concentration on the aroma activity is included. Using representative relations for diffusion coefficients, water and aroma activity in dependence on water concentration they obtained good qualitative agreement between numerical calculations and experimentally observed influences of process variables on aroma retention in slab drying.

In the treatments given above shrinkage of the slab caused by water loss was taken into account. For the numerical calculations this meant that a coordinate transformation to a dissolved solids based coordinate system was made. For a drying slab this transformation was given by Menting (9) after Crank (34).

2. Drying_of_spherical_particles

The transport of water and aroma in drying droplets was first
discussed utilizing approximate models by Thijssen and Rulkens
(7). For high drying rate they approximated the outer shell of
a drying droplet by a thin slab, and in this way calculated the
length of the constant-rate period. By using a constant effect-
ive aroma diffusion coefficient they calculated the influence
of process variables on aroma retention. Temperature was assumed
to remain constant. Van der Lijn et al (26,35) were the first
to calculate the temperature and drying history of a shrinking
droplet, with a concentration- and temperature-dependent water
diffusion coefficient, as measured for the system water-maltose
by van der Lijn (35). The equations for the coordinate trans-
formation for a spherical particle were derived by van der Lijn
(35). The temperature of the drying particle was derived from
an instationary heat balance. Rulkens (8) solved the water dif-
fusion equation for the non-isothermal drying of a particle,
assuming a water diffusion coefficient dependent on water concen-
tration only, and using the same coordinate transformation as
van der Lijn. He assumed quasi-stationary equilibrium between
the heat and mass flux from the particle to calculate droplet
temperature. Assuming a constant effective binary diffusion
coefficient for aroma transport, he calculated the effect of
process variables on aroma retention. In his discussion of the
effect of process conditions on aroma retention in slab drying
and in spray drying Thijssen (3) also included the effect of
aroma activity coefficients. Kerkhof and Schoeber (21,22) cal-
culated the effect of process variables on drying rate, tempe-
rature history and aroma loss by a binary diffusion equation
for water and the Generalized Stefan-Maxwell equation for the
transport of aroma. The droplet temperature was calculated from
the instationary heat balance.

In the present study the diffusion equations for slabs and drop-
lets will be treated in a general form, including infinite cy-
linders. Also the transformation to dissolved solids based

coordinates will be derived in the general form. Further some similarity rules will be presented, which on one hand show the criteria for similarity between drying samples of different sizes, and on the other hand show the effect of combinations of process variables. Finally some results of numerical calculations for the drying of slabs and of droplets will be discussed briefly. In these calculations a binary diffusion equation is used for the water transport and the Generalized Stefan-Maxwell equation for the aroma transport. Extensive information on the subject is presented by Kerkhof and Schoeber $(21, 22, 28, 36)$.

II.2. Definition of the physical model

A schematic diagram of the system is given in fig. II-1. The
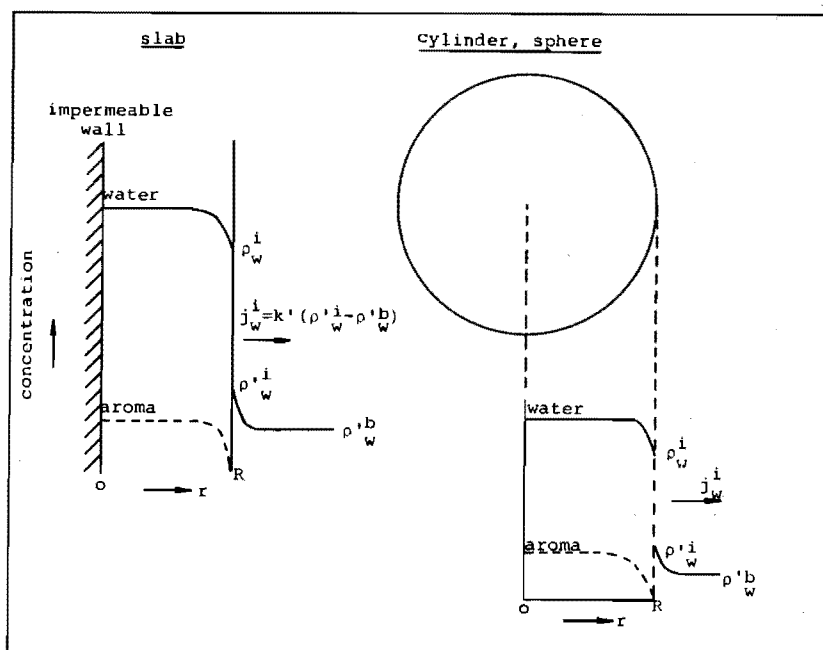
Fig II-1. Diagrammatic representation of drying specimen

drying specimen is thought to be a slab drying from one side, an infinite cylinder, or a spherical particle. In accordance with the the work of other authors the following assumptions are made :

1. The liquid food consists of three components :
   water (w), a dissolved solids component (s) and an aroma
   component present in very low concentration (a).
2. Transport in the liquid food only takes place by molecular
   diffusion and by convective flow due to molecular diffusion.
   Transport only takes place in the r-direction.
3. The drying liquid consists only of one phase : no crystal-
   lization, pore formation, vapour bubble or aroma droplet
   formation takes place.
4. No molecular volume contraction occurs upon mixing. Conse-
   quently the shrinkage of the drying system is equal to the
   volume of the water evaporated. As no net volume flow oc-
   curs through $r = 0$, the volume averaged velocity v^v with
   respect to the linear distance coordinate r is equal to
   zero.
5. At the beginning of the drying process the components are
   homogeneously distributed over the liquid phase.
6. The aroma component has such a high volatility that from the
   onset of the drying process the interfacial aroma concentra-
   tion may be considered to be equal to zero.
7. No temperature gradients are present inside the drying
   specimen.
8. The mass and heat transfer in the continuous phase can be
   described by the well-known film theory.

II.3. Basic transport equations

As in the recent literature both the approach by irreversible
thermodynamics and the Generalized Stefan-Maxwell equation have
been used for the description of transport rates in liquid
foods, both formulations will be treated. Lightfoot et al (37)
showed that the postulates on which the Generalized Stefan-
Maxwell equation is based are in full agreement with the postu-
lates of the theory of irreversible thermodynamics. A different
proof is given in Appendix 2.

II.3.1. Transport of water in the liquid food

Irreversible thermodynamics

On the basis of irreversible thermodynamics follows from the work of Miller (*32,33*) and de Groot and Mazur (*37*) that for the diffusion of water in the ternary system : water, dissolved solids, aroma can be written :

$$j_w^V = - D_{ww} \frac{\partial \rho_w}{\partial r} - D_{wa} \frac{\partial \rho_a}{\partial r} \qquad (II-1)$$

in which :

j_w^V = mass flux of water with respect to volume-averaged
velocity : $j_w^V = \rho_w (v_w - v^V)$ (kg/m^{2}s)

D_{ww}= straight water diffusion coefficient (m^2/s)

D_{wa}= cross water diffusion coefficient (m^2/s)

ρ_w = water concentration (kg/m^3)

ρ_a = aroma concentration (kg/m^3)

r = distance coordinate (m)

D_{ww} and D_{wa} are dependent on concentration and temperature and include relations between activity coefficients and concentrations. For very low aroma concentration, $\rho_a \to 0$, the cross diffusion term can be neglected, giving :

$$j_w^V = - D_{ww} \frac{\partial \rho_w}{\partial r} \qquad (II-2)$$

Generalized Stefan-Maxwell equation

The Generalized Stefan-Maxwell equation for water transport reads (*8,20*) :

$$\rho_w \frac{\partial ln A_w}{\partial r} = \frac{1}{\rho \underline{D}_{wa}} (\rho_a j_w^V - \rho_w j_a^V) + \frac{1}{\rho \underline{D}_{ws}} (\rho_w j_s^V - \rho_s j_w^V)$$

where : (II-3)

A_w = thermodynamic activity of water

$\underline{D}_{wa}$= ternary Stefan diffusion coefficient, representing
mobility of water with respect to aroma molecules
(m^2/s)

$\underline{D}_{ws}$ = ternary Stefan diffusion coefficient, representing mobility of water with respect to dissolved solids (m^2/s)

ρ = total density of the liquid food (kg/m^3)

ρ_s = concentration of dissolved solids (kg/m^3)

j_s^V = mass flux of dissolved solids with respect to volume-averaged velocity (kg/m^2s)

Using the relations $\quad v^V = j_w^V \bar{V}_w + j_s^V \bar{V}_s + j_a^V \bar{V}_a = 0 \qquad$ (II-4)

and $\qquad\qquad\qquad \rho_w \bar{V}_w + \rho_s \bar{V}_s + \rho_a \bar{V}_a = 1 \qquad$ (II-5)

in which

$\bar{V}_i$ = partial specific volume of component i (i = a,w,s) (m^3/kg)

and neglecting the terms involving j_a and ρ_a, after some rearrangement from Equation (II-3) follows :

$$j_w^V = - \underline{D}_{ws} \frac{\partial ln A_w}{\partial ln \omega_w} \frac{\partial \rho_w}{\partial r} \qquad\qquad (II\text{-}6)$$

in which ω_w is the weight fraction of water. Equation (II-6) is identical to Equation (II-2) if

$$D_{ww} = \underline{D}_{ws} \frac{\partial ln A_w}{\partial ln \omega_w} \qquad\qquad (II\text{-}7)$$

As both D_{ww} and $\underline{D}_{ws}$ in general will depend in the same way on water concentration, either of these expressions can be used. It is more practical however to use Equation (II-2).
For the flux of water with respect to the velocity of the dissolved solids can be derived :

$$j_w^S = \frac{-D_{ww} \frac{\partial \rho_w}{\partial r}}{1 - \rho_w \bar{V}_w} \qquad\qquad (II\text{-}8)$$

II.3.2. Transport_of_aroma
Irreversible thermodynamics

Analogous to Equation (II-1) for the transport of aroma can be

written $(3,11,12)$:

$$j_a^v = - D_{aw} \frac{\partial \rho_w}{\partial r} - D_{aa} \frac{\partial \rho_a}{\partial r} \qquad (II-9)$$

in which D_{aw}, D_{aa} = cross and straight aroma diffusion coeffi-
cients respectively (m^2/s)

The diffusion coefficients D_{ww}, D_{wa}, D_{aw} and D_{aa} are related,
for which relation in the case of low aroma concentration a
rigorous treatment is given by Chandrasekaran (12). He showed
that the cross diffusion coefficient D_{aw} is proportional to ρ_a :

$$D_{aw} = D'_{aw} \rho_a \qquad (II-10)$$

in which D'_{aw} only depends on water concentration and temperature,
and is independent of aroma concentration.

Generalized Stefan-Maxwell equation
For aroma transport the Generalized Stefan-Maxwell equation
reads $(8,20)$:

$$\rho_a \frac{\partial ln A_a}{\partial r} = \frac{1}{\rho \underline{D}_{aw}} (\rho_a j_w^v - \rho_w j_a^v) + \frac{1}{\rho \underline{D}_{as}} (\rho_a j_s^v - \rho_s j_a^v) \qquad (II-11)$$

in which $\underline{D}_{aw}$ and $\underline{D}_{as}$ are ternary diffusion coefficients repre-
senting the mobility of aroma with respect to water and dissol-
ved solid respectively, which for low aroma concentration are
independent of this concentration. From the results of Buttery
et al (38) follows that for low aroma concentration the aroma
activity coefficient is independent of aroma concentration.
Substituting the relation

$$A_a = H_a \rho_a \qquad (II-12)$$

in which H_a is a modified activity coefficient (m^3/kg) only
depending on water concentration and temperature, and defining

$$\frac{1}{D_a} = \frac{\omega_w}{\underline{D}_{aw}} + \frac{1 - \omega_w}{\underline{D}_{as}} \qquad (II-13)$$

after (27), Equation $(II-11)$ can be written as :

$$j_a^v = - D_a \frac{\partial \rho_a}{\partial r} - D_a \rho_a \left[\frac{\partial \ln H_a}{\partial \rho_w} + \frac{1}{\rho} D_{ww} (\frac{1}{\underline{D}_{aw}} - \frac{\bar{V}_w}{\bar{V}_s \underline{D}_{as}}) \right] \frac{\partial \rho_w}{\partial r}$$

$$(II-14)$$

Inspection of the relations given by Chandrasekaran (12) reveals that $D_a \equiv D_{aa}$. It can also be seen that the term describing the effect of the water concentration gradient is proportional to ρ_a, as also holds for Equation $(II-9)$. For reasons of notation Equation $(II-9)$ will be used in the following paragraphs.

From the Generalized Stefan-Maxwell equation some limiting cases can be derived. From the physical interpretation of the Stefan diffusion coefficients as relative mobilities of components, Rulkens and Thijssen (27) concluded that for low water concentrations must hold :

$$\underline{D}_{aw} >> \underline{D}_{as} \qquad (II-15)$$

Later this was verified experimentally by membrane permeation experiments by Rulkens (8). From this can be deduced :

$$j_a^v = - D_{aa} \frac{\partial \rho_a}{\partial r} - \rho_a \left[D_{aa} \frac{\partial \ln H_a}{\partial \rho_w} + D_{ww} \frac{\bar{V}_w}{1 - \rho_w \bar{V}_w} \right] \frac{\partial \rho_w}{\partial r} \qquad (II-16)$$

The flux of aroma with respect to the dissolved solids is then given by :

$$j_a^s = - D_{aa} \frac{\partial \rho_a}{\partial r} - D_{aa} \rho_a (\frac{\partial \ln H_a}{\partial \rho_w}) \frac{\partial \rho_w}{\partial r} \qquad (II-17)$$

as also derived by Thijssen (3) from another basis.
In case of small variation of $\ln H_a$ with ρ_w, Equation $(II-17)$ reduces to :

$$j_a^s = - D_{aa} \frac{\partial \rho_a}{\partial r} \qquad (II-18)$$

II.3.3. Mass and heat transfer in the continuous phase

The fluxes of water and heat from the drying specimen to the continuous phase are given by :

$$j_w^i = k' \; (\rho_w'^{\,i} - \rho_w'^{\,b}) \tag{II-19}$$

and

$$j_H^i = \alpha' \; (T^i - T^b) \tag{II-20}$$

with :

k' = continuous phase mass transfer coefficient (m/s)

$\rho_w'^{\,i}$ = continuous phase interfacial water concentration

(kg/m^3)

$\rho_w'^{\,b}$ = continuous phase bulk water concentration (kg/m^3)

α' = continuous phase heat transfer coefficient $(J/m^2 sK)$

T^i = surface temperature of drying specimen (K)

T^b = continuous phase bulk temperature (K)

In the absence of temperature gradients inside the drying specimen, T^i may be replaced by T, the specimen temperature. Both k' and α' are determined by molecular and turbulent film transport phenomena characterized by transfer coefficients k_f' and α_f' and by the net mass flow, for which can be derived :

$$k' = \frac{k_f'}{(1 - \omega_w')_{ln}} \tag{II-21}$$

in which $(1 - \omega_w')_{ln}$ is the logarithmic average of $(1 - \omega_w')$ between the interfacial and bulk continuous phase values, and

$$\alpha' = \alpha_f' \; \frac{\gamma}{\exp(\gamma) - 1} \tag{II-22}$$

with $\gamma = \dfrac{j_w^i \; C_{pw}'}{\alpha_f'}$ (II-23)

in which C_{pw}' is the specific heat of water in the continuous phase (J/kg K).

For the film coefficients correlations are given in literature

18

(40). The coefficients for transfer to an infinite slab are given by the Chilton-Colburn analogy. For the heat and mass transfer to spherical particles the Ranz and Marshall relations apply (41) :

$$Nu = \frac{\alpha_f' \, d}{\lambda'} = 2 + 0.6 \, Re^{0.5} \, Pr^{0.33} \qquad (II-24)$$

$$Sh = \frac{k_f' \, d}{D_w'} = 2 + 0.6 \, Re^{0.5} \, Sc^{0.33} \qquad (II-25)$$

for $0 < Re < 200$ $Sc \simeq 1$, $Pr \simeq 1$

in which

λ'	= continuous phase thermal conductivity	(J/ms K)
D_w'	= continuous phase molecular water diffusion coefficient	(m^2/s)
d	= 2R = sphere diameter	(m)

For cylinders analogous relations to (II-24) and (II-25) hold. Bird et al (40) note that the physical properties to be inserted into the relations (II-24) and (II-25) should be evaluated at the average film temperature and film concentration :

$$T^f = (T^i + T^b)/2 \qquad (II-26)$$
$$\rho'^f = (\rho'^i + \rho'^b)/2 \qquad (II-27)$$

II.4. Diffusion Equations

II.4.1. Water transport

The continuity equation for water in various geometries reads :

$$\frac{\partial \rho_w}{\partial t} = \frac{1}{r^{\nu-1}} \frac{\partial}{\partial r} \left(r^{\nu-1} \frac{\partial \rho_w}{\partial r} \right) \qquad (II-28)$$

in which ν is a geometry factor : $\nu = 1$ for a slab, $\nu = 2$ for an infinite cylinder and $\nu = 3$ for a sphere.
The initial and boundary conditions read :

$$t = 0 \qquad 0 \le r \le R_o \qquad \rho_w = \rho_{w,o} \qquad \text{(II-29)}$$

$$t > 0 \qquad r = 0 \qquad \frac{\partial \rho_w}{\partial r} = 0 \qquad \text{(II-30)}$$

$$r = R \qquad j_w^i = k'(\rho_w'^i - \rho_w'^b)$$

$$\text{with} \qquad j_w^i = j_w^s = \frac{-D_{ww}\dfrac{\partial \rho_w}{\partial r}}{1 - \rho_w \bar{V}_w} \qquad \text{(II-31)}$$

Boundary condition (II-31) stems from the fact that the water flux through the interface is not equal to the flux with respect to stationary coordinates r, but is the water flux with respect to the receding dissolved solids molecules, as given in Equation (II-8). The relation between $\rho_w'^i$ and the liquid side interfacial concentration ρ_w^i is given by the equilibrium curve between the phases. In the case of air drying this relation is given by the water vapour sorption isotherm and the water vapour saturation concentration $\rho_w'^*$ at the specimen temperature :

$$\rho_w'^i = A_w^i \, \rho_w'^* \qquad \text{(II-32)}$$

in which A_w^i is dependent on ρ_w^i and temperature.

The thickness or radius R at time t follows from a balance over the amount of water evaporated :

$$R^\nu = R_o^\nu - \nu \int_0^t R^{\nu-1} j_w^i \, \bar{V}_w \, dt \qquad \text{(II-33)}$$

The relative amount of water WR still present in the drying specimen after time t is given by :

$$WR = \frac{\nu}{\rho_{w,o}R_o^\nu} \int_0^R r^{\nu-1} \rho_w \, dr \qquad \text{(II-34)}$$

II.4.2. Aroma_transport

The continuity equation for aroma reads :

$$\frac{\partial \rho_a}{\partial t} = \frac{1}{r^{\nu-1}} \frac{\partial}{\partial r} \left[r^{\nu-1} (D_{aa} \frac{\partial \rho_a}{\partial r} + D_{aw} \frac{\partial \rho_w}{\partial r}) \right] \qquad \text{(II-35)}$$

The initial and boundary conditions read :

$$t = 0 \qquad\qquad 0 \leq r \leq R_o \qquad\qquad \rho_a = \rho_{a,o} \qquad \text{(II-36)}$$

$$t > 0 \qquad\qquad r = 0 \qquad\qquad \frac{\partial \rho_a}{\partial r} = 0 \qquad \text{(II-37)}$$

$$r = R \qquad\qquad \rho_a = 0 \qquad \text{(II-38)}$$

The aroma retention after time t is given by :

$$AR = \frac{\nu}{\rho_{a,o} R_o^{\nu}} \int_0^R r^{\nu-1} \rho_a \, dr \qquad \text{(II-39)}$$

II.5. Heat and momentum balance

II.5.1. Heat balance

In principle inside a drying material to which heat is supplied by the surroundings, temperature gradients will be present. In this section it will be shown that for the conditions of interest in this thesis no appreciable temperature gradients will be formed. For the heat flux through the interface holds :

$$- \lambda \frac{\partial T}{\partial r} + v^i \rho C_p T^i = \alpha' (T^i - T^b) + j_w^i \Delta H_v \qquad \text{(II-40)}$$

with

λ = thermal conductivity of drying specimen (J/ms K)

v^i = velocity of receding interface (m/s)

C_p = specific heat of specimen at the interface (J/kg K)

To simplify reasoning the extreme case of heat transfer in the absence of water removal will be considered. For the temperature gradient at the interface then can be written :

$$- \frac{\partial (T - T^b)}{\partial r/R} = \frac{\alpha' R}{\lambda} (T^i - T^b) = Bi_H (T^i - T^b) \qquad \text{(II-41)}$$

in which $Bi_H \equiv \frac{\alpha'R}{\lambda}$ is the Biot number for heat transfer. From Equation (II-41) follows that a low Biot number indicates that the dominant resistance to heat transfer lies in the continuous phase, and the temperature gradients inside the material are small. Let the continuous phase be air, flowing with high relative velocity with respect to the drying specimen. For *droplets* just formed in a spray drier a value of Re = 100 is representative (*27*); from Equation (II-24) then follows :

$$Nu = \frac{\alpha'd}{\lambda'} \simeq 8 \qquad \text{(II-42)}$$

Taking representative values for the thermal conductivities of air and of liquid foods (*70*) :

λ' = 0.026 J/ms K

λ = 0.6 J/ms K

for the Biot number is found :

$$Bi_H \simeq 0.17 \quad (\nu = 3) \qquad \text{(II-43)}$$

For cylindrical specimen at Re = 100 follows from the Chilton-Colburn analogy (*40*) that Nu $\simeq$ 5.5 leading to

$$Bi_H \simeq 0.23 \quad (\nu = 2) \qquad \text{(II-44)}$$

For a flat plate of 1 cm thickness, with an air velocity $\bar{w}$ of 10 m/s, the Chilton-Colburn analogy delivers in the turbulent flow regime :

$$j_H = \frac{\alpha'}{\rho' c_p' \bar{w}} Pr^{0.67} \simeq 0.002 \qquad \text{(II-45)}$$

from which follows :

$$\alpha' \simeq 10 \text{ J/m}^2\text{sK} \qquad \text{(II-46)}$$

and

$$Bi_H \simeq 0.16 \quad (\nu = 1) \qquad \text{(II-47)}$$

From the calculated Bi numbers can be seen, that even in the

22

absence of water transport for the case of relatively high velocities of the drying air, the limitation for heat transfer lies predominantly in the continuous phase. For real drying situations in which only part of the heat transferred is available for warming up of the drying specimen thus the assumption of uniform specimen temperature is realistic. As a consequence in the equations will be written T, the specimen temperature.
The overall heat balance over the specimen, in case only heat is transferred by the continuous phase, can be written :

$$\frac{R}{v} \rho C_p \frac{dT}{dt} = \alpha'(T^b - T) - k'(\rho_w'^i - \rho_w'^b) \Delta H_v \qquad (II-48)$$

II.5.2. Momentum balance for spherical particle

For a single spherical particle moving at a relative velocity $\bar{w}$ with respect to a continuous phase, the impulse balance reads:

$$\frac{d\bar{u}}{dt} = (\frac{\rho - \rho'}{\rho}) \bar{g} - \frac{3}{8} \frac{C_d \rho' |\bar{w}| \bar{w}}{\rho R} \qquad (II-49)$$

in which
$\bar{g}$ = gravity acceleration vector $\qquad (m^2/s)$
C_d = drag coefficient
$|\bar{w}|$ = absolute magnitude of $\bar{w}$ $\qquad (m/s)$

The drag coefficient depends on the Re-number :

$$Re = \frac{\rho' |\bar{w}| 2R}{\mu} \qquad (II-50)$$

with μ = continuous phase dynamic viscosity $\qquad (Ns/m^2)$

An extensive treatment and literature review on this subject is given by Kerkhof and Schoeber (27).

II.6. Transformation of the diffusion equations to solute-based coordinates

Here an extension is made of the work of Menting and of van der Lijn (9,35). An alternative formulation of the equation of continuity for a component i (i = w,s,a) is given by :

$$\frac{\partial \rho_i}{\partial t}\bigg|_r = -\frac{1}{r^{\nu-1}} \frac{\partial}{\partial r} (r^{\nu-1} \rho_i v_i)\bigg|_t \qquad (II-51)$$

Let the following coordinate be defined :

$$\sigma = \int_0^r \rho_s \bar{V}_s r^{\nu-1} dr \qquad (II-52)$$

then equal increments in σ correspond to equal increments of dissolved solids volume; as no dissolved solids disappears from the drying specimen, the coordinate denoting the dimension of the specimen will remain constant and equal to σ_o.

For the transformation of $\rho_i(r,t)$ to $\rho_i(\sigma,t)$ the following rules hold :

$$\left(\frac{\partial \rho_i}{\partial r}\right)_t = \left(\frac{\partial \rho_i}{\partial \sigma}\right)_t \left(\frac{\partial \sigma}{\partial r}\right)_t \qquad (II-53)$$

and

$$\left(\frac{\partial \rho_i}{\partial t}\right)_r = \left(\frac{\partial \rho_i}{\partial \sigma}\right)_t \left(\frac{\partial \sigma}{\partial t}\right)_r + \left(\frac{\partial \rho_i}{\partial t}\right)_\sigma \qquad (II-54)$$

From Equation (II-52) follows :

$$\left(\frac{\partial \sigma}{\partial r}\right)_t = \rho_s \bar{V}_s r^{\nu-1} \qquad (II-55)$$

and

$$\left(\frac{\partial \sigma}{\partial t}\right)_r = \left[\frac{\partial}{\partial t} \int_0^r \rho_s \bar{V}_s r^{\nu-1} dr\right]_r = \int_0^r \left(\frac{\partial \rho_s}{\partial t}\right)_r \bar{V}_s r^{\nu-1} dr \qquad (II-56)$$

Substitution of Equation (II-51) into (II-56) gives :

$$\left(\frac{\partial \sigma}{\partial t}\right)_r = -r^{\nu-1} \rho_s \bar{V}_s v_s \qquad (II-57)$$

and so

$$\left(\frac{\partial \rho_i}{\partial t}\right)_\sigma = \left(\frac{\partial \rho_i}{\partial t}\right)_r + v_s \left(\frac{\partial \rho_i}{\partial r}\right)_t \qquad (II-58)$$

Defining new concentrations based on dissolved solids volume :

$$u_i = \rho_i / \rho_s \bar{V}_s \qquad (II-59)$$

24

gives :

$$\left(\frac{\partial u_i}{\partial t}\right)_\sigma = \frac{1}{\rho_s \bar{V}_s} \left[- \frac{\rho_i}{\rho_s} \left(\frac{\partial \rho_s}{\partial t}\right)_\sigma + \left(\frac{\partial \rho_i}{\partial t}\right)_\sigma \right] \qquad \text{(II-60)}$$

After some algebraic manipulation then follows :

$$\left(\frac{\partial u_i}{\partial t}\right)_\sigma = \frac{1}{\rho_s \bar{V}_s r^{\nu-1}} \frac{\partial}{\partial r} (-r^{\nu-1} j_i^s) = \frac{\partial}{\partial \sigma} (-r^{\nu-1} j_i^s) \qquad \text{(II-61)}$$

For water then can be written :

$$\left(\frac{\partial u_w}{\partial t}\right)_\sigma = \frac{\partial}{\partial \sigma} \left[\frac{D_{ww} \, r^{2\nu-2}}{(1 + u_w \bar{V}_w)^2} \frac{\partial u_w}{\partial \sigma} \right] \qquad \text{(II-62)}$$

with initial and boundary conditions :

$$t = 0 \qquad\qquad 0 \leq \sigma \leq \sigma_o \qquad\qquad u_w = u_{w,o} \qquad \text{(II-63)}$$

$$t > 0 \qquad\qquad \sigma = 0 \qquad\qquad \frac{\partial u_w}{\partial \sigma} = 0 \qquad\qquad \text{(II-64)}$$

$$\sigma = \sigma_o \qquad \frac{-D_{ww} \, r^{\nu-1}}{(1 + u_w \bar{V}_w)^2} \frac{\partial u_w}{\partial \sigma} = j_w^i \quad \text{(II-65)}$$

$$\text{with} \qquad j_w^i = k' \, (\rho_w'^i - \rho_w'^b) \qquad \text{(II-66)}$$

For the aroma component follows analogously :

$$\left(\frac{\partial u_a}{\partial t}\right)_\sigma = \frac{\partial}{\partial \sigma}\left[\frac{r^{2\nu-2}}{(1+u_w\bar{V}_w)^2} \left\{ D_{aa} \frac{\partial u_a}{\partial \sigma} + \frac{u_a \bar{V}_w}{1+u_w\bar{V}_w} (D_{ww}-D_{aa}+\frac{D_{aw}}{u_a\bar{V}_w}) \frac{\partial u_w}{\partial \sigma} \right\} \right]$$

$$\text{(II-67)}$$

with initial and boundary conditions :

$$t = 0 \qquad\qquad 0 \leq \sigma \leq \sigma_o \qquad\qquad u_a = u_{a,o} \qquad \text{(II-68)}$$

$$t > 0 \qquad\qquad \sigma = 0 \qquad\qquad \frac{\partial u_a}{\partial \sigma} = 0 \qquad\qquad \text{(II-69)}$$

$$\sigma = \sigma_o \qquad\qquad u_a = 0 \qquad\qquad \text{(II-70)}$$

In these equations the dimension σ_o follows directly from the definition :

$$\sigma_o = \frac{1}{\nu} \rho_{s,o} \bar{V}_s R_o^\nu \qquad \text{(II-71)}$$

As in the transformed equations still the quantity r appears, an expression for r in transformed variables is derived :

$$r^\nu = \nu \int_0^\sigma (1 + u_w \bar{V}_w) \, d\sigma \qquad \text{(II-72)}$$

For the relative amounts of water WR and of aroma AR after time t still present in the specimen holds :

$$WR = \frac{\nu}{\rho_{w,o} R_o^\nu} \int_0^{\sigma_o} u_w \, d\sigma \qquad \text{(II-73)}$$

and

$$AR = \frac{\nu}{\rho_{a,o} R_o^\nu} \int_0^{\sigma_o} u_a \, d\sigma \qquad \text{(II-74)}$$

II.7. Similarity rules

In many heat and mass diffusion problems similarity analysis is applied for the unified treatment of analogous situations, such as analogy between heat and mass diffusion problems, between systems differing in physical properties, between systems of different size, and systems differing in concentration or temperature level. For constant physical properties and simple geometries many problems have been solved analytically (34,71, 72), in which mostly relative concentrations or temperatures are given in relation to a dimensionless Fo time and dimensionless distance scale; also several other dimensionless numbers may occur in the solution such as the Biot number.
In the sysytems under consideration in this thesis, the diffusion coefficients as well as the vapour-liquid equilibria are strong functions of water concentration and of temperature; moreover these relations are different for different substances. Therefore use of dimensionless groups like the Fo or Bi

number will not provide practical information. Also the use of
dimensionless water concentration parameters for a given material,
will not lead to analogous solutions for problems at different
concentration levels. For samples of a given food liquid at a
given initial concentration and temperature however criteria
can be derived for analogy between the behaviour of samples of
different size. In the following these criteria will be derived,
and some of the conclusions following from these criteria will
be discussed. For the ease of argument it will be assumed in
the following that we consider one given material, and thus
that the relations for the diffusion coefficients and all other
physical properties in dependence on concentration and temperature
are fixed, although not necessarily explicitly known.

II.7.1. Water diffusion

Let the following variables be defined :

$$y \quad = \quad r/R_o \tag{II-75}$$

and

$$\phi \quad = \quad t/R_o^2 \tag{II-76}$$

The coordinate y will be denoted by "reduced distance"; although
the variable ϕ is not a reduced variable in the conventional
sense of a dimensionless variable such as the Fourier number,
for the ease of writing it will be denoted by "reduced time",
as its function in the similarity analysis is the same as that
of the Fo-number in other problems.
Substitution of these variables in Equations (II-28) through
(II-31) delivers :

$$\frac{\partial \rho_w}{\partial \phi} \quad = \quad \frac{1}{y^{\nu-1}} \frac{\partial}{\partial y} \left(y^{\nu-1} D_{ww} \frac{\partial \rho_w}{\partial y} \right) \tag{II-77}$$

$$\phi \quad = 0 \qquad 0 \leq y \leq 1 \qquad \rho_w = \rho_{w,o} \tag{II-78}$$

$$\phi \quad > 0 \qquad y = 0 \qquad \frac{\partial \rho_w}{\partial y} = 0 \tag{II-79}$$

$$y = Y = R/R_o \qquad \frac{- D_{ww} \frac{\partial \rho_w}{\partial y}}{1 - \rho_w \bar{V}_w} = k'R_o (\rho_w'^i - \rho_w'^b)$$

(II-80)

with $Y = 1 - \nu \int_0^\phi y^{\nu-1} k'R_o (\rho_w'^i - \rho_w'^b) \, d\phi$ (II-81)

The fractional water retention can be written as :

$$WR = \frac{\nu}{\rho_{w,o}} \int_0^Y y^{\nu-1} \rho_w \, dy$$

(II-82)

For the heat balance follows :

$$\frac{Y}{\nu} \rho C_p \frac{dT}{d\phi} = \alpha'R_o (T^b - T) - k'R_o (\rho_w'^i - \rho_w'^b) \Delta H_v$$ (II-83)

with $\phi = 0 \qquad T = T_o$ (II-84)

From the differential equation with boundary conditions and the heat balance follows that for a given value of $\rho_{w,o}$ and T_o, ρ_w is uniquely determined as a function of ϕ and y, under the restriction that the variables $k'R_o$, $\alpha'R_o$ and $\rho_w'^b$ are either constant, or are prescribed by expressions only containing Y and ϕ as size or time parameters respectively. If these conditions are fullfilled, it can be concluded that :

1. The water concentration profile on a dimensionless scale y only depends on ϕ.
2. The specimen temperature, the reduced specimen thickness Y, and the relative water content WR are only dependent on ϕ.

In the case of air drying under practical circumstances the effects of the rate of mass transfer on k' and α' are small. For the ease of reasoning in the following these effects will be neglected, although a detailed treatment will lead to the same conclusions. Regarding the values of k' and α' two cases can be considered :

1. α' and k' are invariant with time and thickness. This is

28

the case for the drying of slabs with constant external flow conditions.

2. α' and k' are coupled to the dimension R, which is the case for drying cylinders and droplets. For drying cylinders the values of α' and k' are approximately given by :

$$Nu = a \ Re^{0.5} \ Pr^{0.33} \tag{II-85}$$

$$Sh = a \ Re^{0.5} \ Sc^{0.33} \tag{II-86}$$

for Re > 100 (40), and

$$Nu = b \ Pr^{0.3} + c \ Re^{0.52} \ Pr^{0.3} \tag{II-87}$$

for 0.1 < Re < 1000 (46).

For drying spherical particles the Ranz and Marshall equations (II-24) and (II-25) apply, for low Re-numbers leading to :

$$Nu = Sh = 2 \tag{II-88}$$

For the bulk water concentration two cases will be considered :
1. The bulk water concentration $\rho_w'^b$ is constant.
2. The bulk water concentration is coupled to the water concentration in the liquid food by a mass balance. In this case $\rho_w'^b$ can be written in terms of WR, and thus only depends on Y and ϕ, and not on the absolute value of R and t.

From the above for some practical drying situations the following similarity criteria can be deduced :

1. *Slab drying with constant bulk water concentration.*
   As α' and k' are invariant with time, similarity will be observed between samples of different thickness, *if the values of $\alpha'R_o$ and of $k'R_o$ are equal for the two slabs.*
2. *Drying of cylinders under constant external flow conditions; bulk concentration and temperature given by mass and heat balances.*
   For this case can be written :

$$\alpha'R_o = \alpha'R \frac{R_o}{R} = \frac{\alpha'R}{Y} \tag{II-89}$$

For low Re numbers now follows from Equation (II-87) that

$$\alpha'R_O = \frac{\alpha'R}{Y} = (\text{constant})/Y \tag{II-90}$$

and thus $\alpha'R_O$ can be written as $f(Y)$ only, as also follows for $k'R_O$ from the analogy between heat and mass transfer. Thus *for low Re numbers the similarity criteria are fulfilled.*

For high Re numbers from Equations (II-85) and (II-86) follows :

$$\frac{2\alpha'R_O}{\lambda'} = \frac{2\alpha'R}{\lambda'}\frac{R_O}{R} = \text{Nu}/Y = a\,(\text{Re}_O/Y)^{0.5}\,\text{Pr}^{0.3} \tag{II-91}$$

and thus for two cylinders of different radius $\alpha'R_O$ is the same function of Y if the initial Re numbers are equal. So similarity criteria are fulfilled *for high Re numbers if the product of initial diameter and external flow velocity is equal.*

3. *Drying of uniform droplets in spray driers.*
Here the bulk properties $\rho_w'^b$ and T^b can be described by either constant values or are given by simple balances. For small droplets at low velocities holds Equation (II-88) and thus :

$$\alpha'R_O = \alpha'R/Y = \lambda'/Y \tag{II-92}$$

and

$$k'R_O = k'R/Y = D_w'/Y \tag{II-93}$$

Thus also for this case holds, that *for low Re numbers the similarity criteria are fulfilled.*
For free-falling large droplets high Re-numbers are encountered; as the Re number is strongly dependent on the diameter for large droplets the similarity criteria are not fulfilled.

In the above-mentioned practical cases thus the water concentration profiles on dimensionless y-scale are equal at equal reduced times ϕ, and the temperature and relative water content are functions of the reduced time ϕ only, provided the conditions for similarity are fulfilled.

II.7.2. Aroma diffusion

Introducing the relative aroma concentration :

$$w_a = \rho_a / \rho_{a,o} \qquad\qquad (II-94)$$

the diffusion equations for aroma transport can be written as :

$$\frac{\partial w_a}{\partial t} = \frac{1}{y^{\nu-1}} \frac{\partial}{\partial y} \left[y^{\nu-1} \left\{ D_{aa} \frac{\partial w_a}{\partial y} + D'_{aw} w_a \frac{\partial \rho_w}{\partial y} \right\} \right] \qquad (II-95)$$

with initial and boundary conditions :

$$\phi = 0 \qquad 0 \leq y \leq 1 \qquad w_a = 1 \qquad (II-96)$$

$$\phi > 0 \qquad y = 0 \qquad \frac{\partial w_a}{\partial y} = 0 \qquad (II-97)$$

$$y = Y \qquad w_a = 0 \qquad (II-98)$$

The aroma retention is given by :

$$AR = \nu \int_0^Y y^{\nu-1} w_a \, dy \qquad (II-99)$$

D_{aa} and D'_{aw} depend on water concentration and temperature. If for the water transport the similarity criteria are fulfilled then formally can be written :

$$D_{aa} = D_{aa}(\phi, y) \qquad (II-100)$$

and

$$D'_{aw} = D'_{aw}(\phi, y) \qquad (II-101)$$

As follows from Equations (II-95) through (II-99) in this case also w_a can be solved in dependence on y and ϕ only, and AR is only a function of ϕ.

II.7.3. Practical consequences

The following practical rules can be distilled from the fore-

going :

1. In slab-drying doubling the mass transfer coefficient in the gas phase has the same effect on aroma retention as doubling the slab thickness. In the latter case the process takes place four times slower.

2. In drying cylindrical specimen or droplets at not too high Re numbers a doubling of the initial diameter extends the time scale at which the drying process takes place, by a factor 4. Aroma retention is independent of the diameter.

As can be seen from Equation (II-49) the deceleration or acceleration of droplets under the action of gravity cannot be included in the similarity analysis, as the impulse balance will still contain free R or R_0 terms.
In Chapter III this analysis will be used and extended for the discussion of the constant-rate period.

II.8. Numerical solution of the diffusion equations

For the numerical solution of the diffusion equations by finite-difference methods standard algorithms fail, because of the sharp concentration profiles and strong variation of the diffusion coefficients with distance and time. It was therefore necessary to use distance and time grids in which the size of the discretization steps is adapted. Experience has shown that it is necessary to employ implicit or semi-implicit methods (35,26, 22,8). The difference schemesused for the calculations on slab drying and droplet drying in this thesis are discussed extensively by Kerkhof et al (20) and Schoeber (22) respectively. It should be noted that due to the strong variation of diffusion coefficients with concentration and temperature, no stability and convergence criteria are known, and thus stability and convergence have to be determined by trial and error.

II.9. Solutions of the diffusion equations

With the aid of numerical programs, written in Algol-60, solutions to the diffusion equations were obtained, of which extensive use is made in Chapter III for correlation purposes.
In order to illustrate these calculations some typical features are discussed here for the drying of slabs and of droplets. As in Chapter III the results of the numerical calculations will also be used for the simulation of drying processes for different materials, calculations have been performed for several dependences of the physical properties, including diffusion coefficients, on water concentration and temperature. A detailed survey of these dependences is given in appendix 3. It was assumed that activation energies for water and aroma diffusion coefficients increase with increasing dissolved solids concentration (29), and that the interaction between aroma and dissolved solids molecules is much stronger than between aroma and water molecules. Part of the work has been published by Kerkhof et al (20) and by Kerkhof and Schoeber (21,22,28).

The results of the computations can be divided in three parts :

1. concentration profiles of water and aroma compounds
2. dependence of several variables on time, such as temperature, water and aroma retention
3. influence of process variables on key drying results such as the length of the constant-rate period, and on final aroma retention.

II.9.1. Drying of slabs

The isothermal drying of a slab was calculated numerically with the physical properties of appendix 3, table 2.

Concentration profiles

In fig. II-2 typical water and aroma concentration profiles are given in reduced distance coordinate for two values of $k'R_o$:
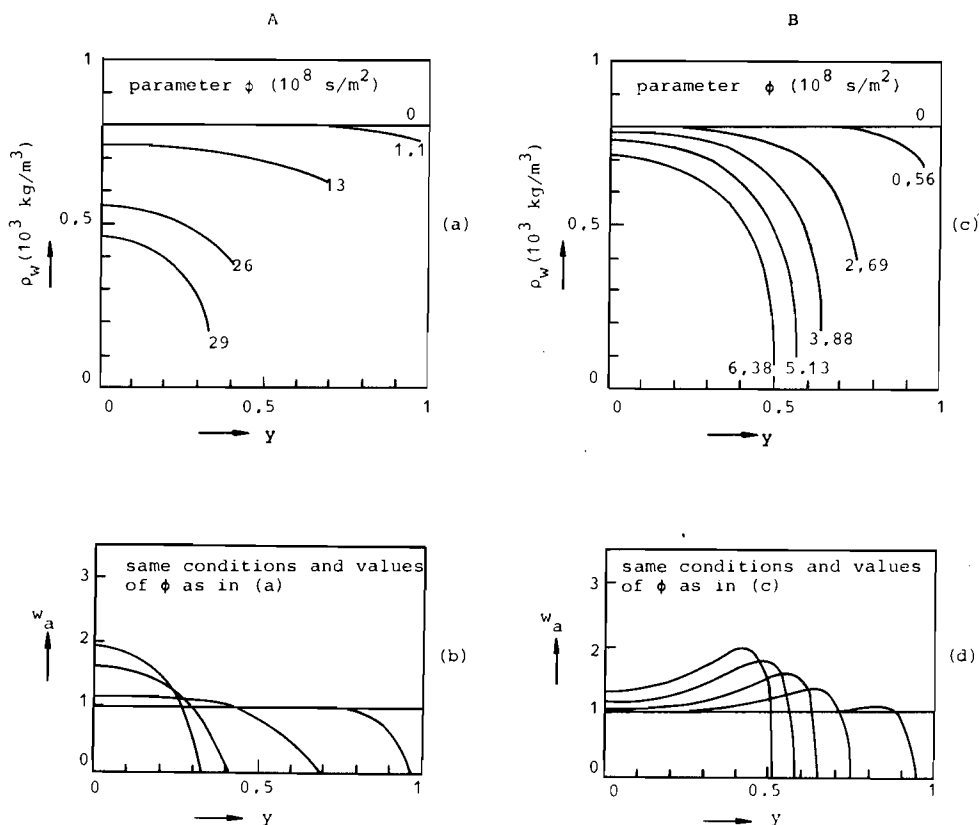
Fig II-2. Water and aroma concentration profiles in a drying slab as calculated by Kerkhof et al (20). Slab temperature 25°C initial water concentration 800 kg/m^3, zero humidity of drying air. $\underline{A}$: $k'R_0 = 10^{-5}$ m/s; $\underline{B}$: $k'R_0 = 4 \times 10^{-5}$ m/s. Physical properties according to appendix 3, table 2.

$-.-.-.-$

A : $k'R_0 = 10^{-5}$ m^2/s

B : $k'R_0 = 4 \times 10^{-5}$ m^2/s

This figure shows that increasing the factor $(k'R_0)$ leads to steeper water concentration profiles inside the drying slab, causing a more pronounced decrease of the surface water concentration in terms of reduced time ϕ. In case A the centre water concentration decreases with a rate more or less comparable with that of the interfacial water concentration. In case B on the contrary the centre water concentration only has decreased slightly when the interfacial water concentration has already decreased almost to zero. From additional calculations we concluded that steeper concentration profiles also occur at higher

initial dissolved solids concentration. The explanation for this effect can easily be read from Equation (II-80) :

$$y = Y \qquad \frac{- D_{ww} \frac{\partial \rho_w}{\partial y}}{1 - \rho_w \bar{V}_w} = k'R_o (\rho_w'^i - \rho_w'^b)$$

Increasing $k'R_o$ leads to higher values of $- \frac{\partial \rho_w}{\partial y}$ at the interface. As at higher initial dissolved solids content D_{ww} is lower from the beginning of the process, also the concentration gradient will be larger for equal values of the RHS of Equation (II-80).

The aroma concentration profiles in fig. II-2(b), for case A, for short contact times shows a penetration type behaviour, gradients becoming smaller with time. After some time however gradients become steeper again and the aroma concentration in the centre rises. This can be explained by the fact that once the water concentration has fallen below a certain critical level at the interface the aroma loss becomes negligible, and as the amount of aroma remains constant, the shrinkage of the slab leads inevitably to an increase in aroma concentration.
In case B a maximum is observed in the aroma concentration profiles. This phenomenon, which was also found experimentally (11,12) has been extensively discussed in the literature (3,11, 12,20), and is explained both by the effect of shrinkage and of the negative influence of ρ_w on the aroma activity coefficient. It is seen to occur only for sharp water concentration profiles (20).
Clearly it can be observed from the two cases that the increase in $k'R_o$ leads to an increase of the final aroma retention.

Water and aroma content in relation to time

In fig. II-3 the calculated fractional water content WR and the fractional aroma content AR are given in relation to reduced time ϕ, for the two values of $(k'R_o)$ mentioned above. Clearly a period of approximately constant drying rate can be observed, as denoted by ϕ_c, which decreases strongly with an increase of $(k'R_o)$. Also the effect found experimentally by Menting (9),
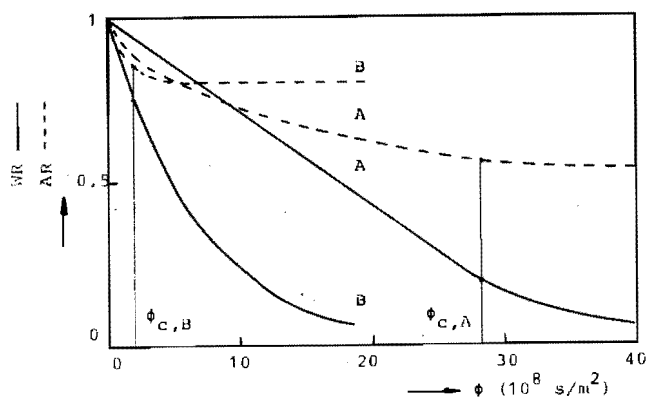
Fig II-3. Calculated water and aroma content in relation to reduced time ϕ for isothermal slab drying; same conditions as in Fig II-2

that after the constant-rate period only little aroma is additionally lost, can be observed, and in the case of the highest value of $(k'R_o)$ the highest aroma retention is found. Clearly the increase of the external rate of water removal causes a more rapid decrease of the surface water concentration of the slab, resulting in a more rapid dry skin formation and consequently in lower aroma loss. In fig. II-4 the interfacial water concentration is given in dependence of ϕ for some more values of $(k'R_o)$. It is observed that an increase of $(k'R_o)$ leads to a more rapid decrease of $\rho_{w,i}$ in terms of reduced time ϕ. Further a sharp decrease in interfacial water concentration is seen
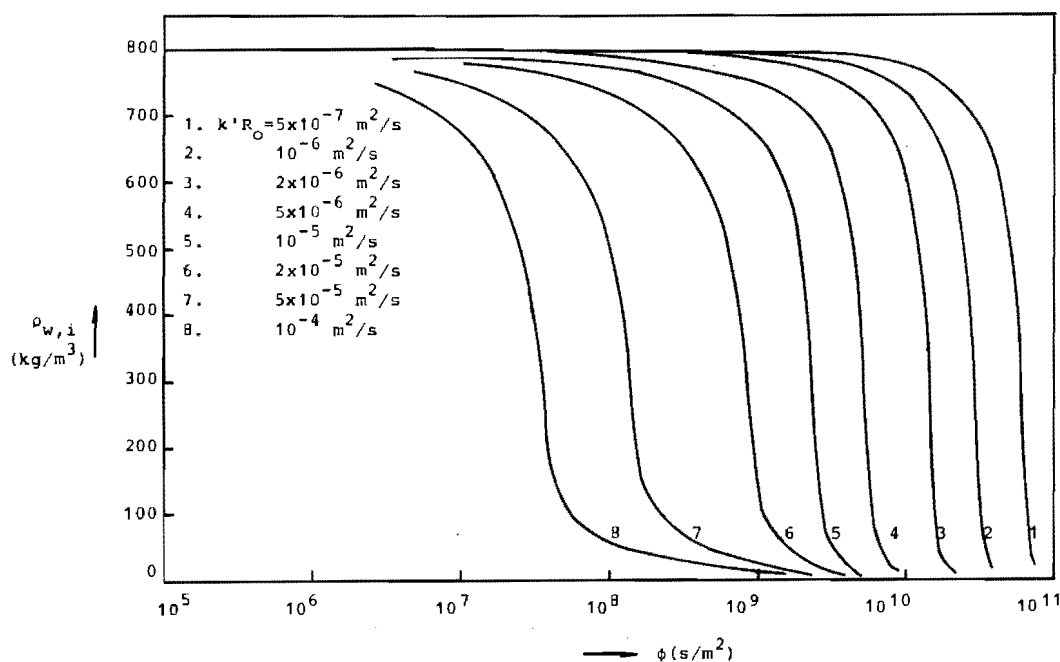
Fig II-4. Calculated interfacial water concentration as a function of reduced time in slab drying. $\rho_{w,o} = 800$ kg/m^3; $\rho'^{b}_{w} = 0$; T = 25°C. Same physical properties as in Fig II-2

between $\rho_{w,i}$ = 400 kg/m^3 and $\rho_{w,i}$ = 200 kg/m^3. In fig. II-5 the interfacial water activity A_w^i is plotted as a function of time, for three values of (k'R$_o$). From this figure can be read that the activity starts to decrease rapidly once it has passed the 90% level. As the activity is decreasing from the onset of dry-ing, the evaporation rate will constantly decrease; above 95% water activity however rather slowly. The constant-rate period is now defined as the length of time during which the interfa-cial water activity is higher than about 90%. From the figure can be read that the difference between the time necessary to reach a water activity of 0.95 or of 0.85 is only small, so that the choice of the water activity at which the constant-rate period ends is not very critical. This also means that the time to reach selective permeability which is different for different components (Thijssen(3)), may in good approximation be taken equal for all components.
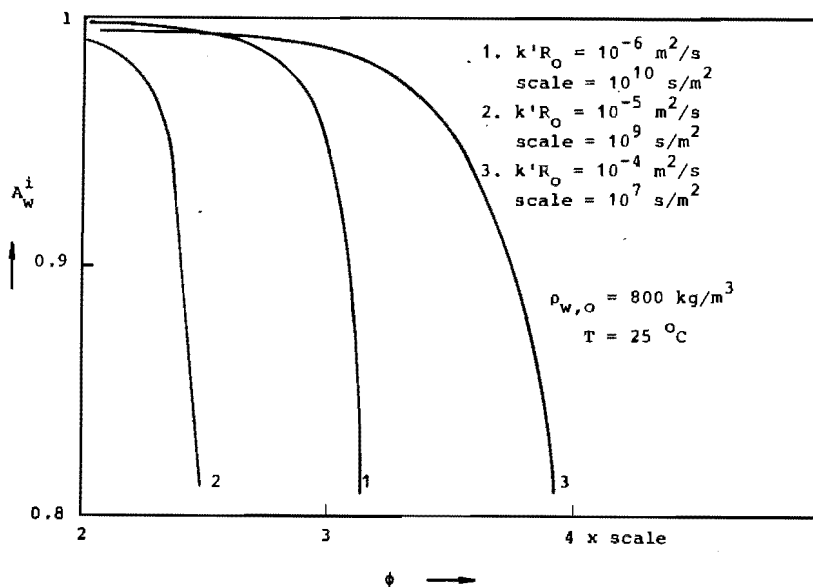
Fig II-5. Numerically calculated interfacial water activity A_w^i in dependence on reduced time, for different values of k'R$_o$. Other conditions and physical properties of Fig II-2.
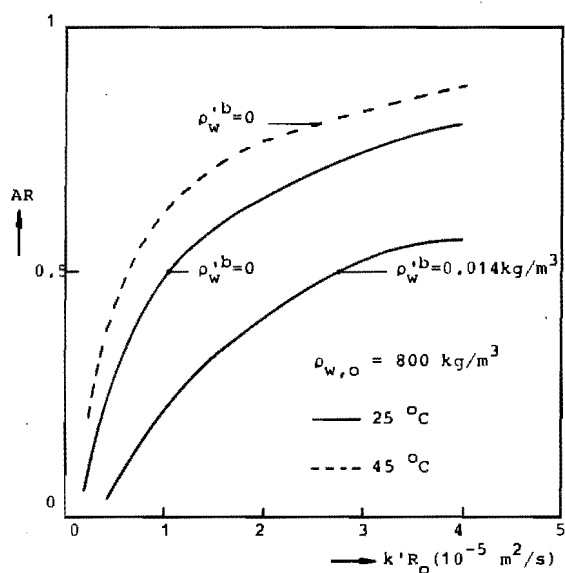
Fig II-6. Numerically calculated effect of $(k'R_o)$ on final aroma retention in slab drying. Same physical properties as in Fig II-2

Effect of process variables on final aroma retention

In fig. II-6 the effect of $(k'R_o)$ on final aroma retention is given, with gas phase bulk humidity and temperature as parameters. From this figure can be read that aroma retention increases with :

- increasing value of $(k'R_o)$
- decreasing gas phase bulk humidity
- increasing temperature

In fig. II-7 the effect of the initial water concentration on
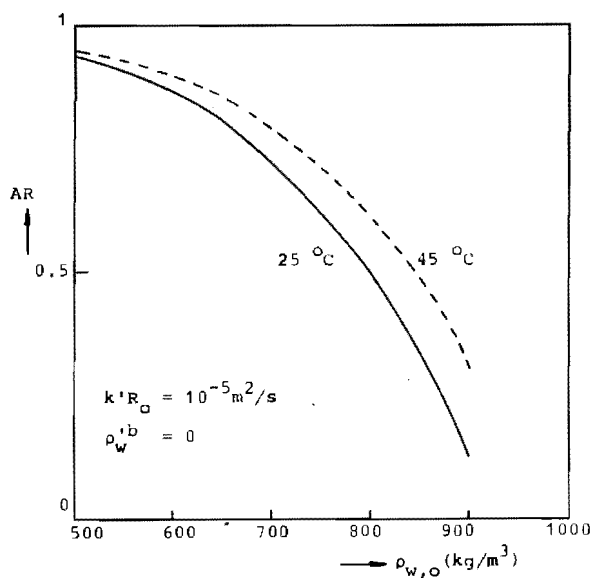
Fig II-7. Numerically calculated effect of initial water concentration on final aroma retention. Physical properties as in Fig II-2.

the final aroma retention is given, for two slab temperatures.
It is observed, that aroma retention increases with :

- decreasing initial water concentration

and again the increase with increasing temperature is found.
As will be discussed more extensively in Chapter III, these
effects can be split up into three main factors, each leading
to higher aroma retention :

- an increase of k', R_o and a decrease in bulk water concen-
tration all lead to a higher value of $k'R_o(\rho_w'^i - \rho_w'^b)$, and thus
to sharper water concentration profiles and a shorter reduced
time ϕ_c.

- a decrease in initial water concentration will result in a
smaller distance between initial and critical water concentra-
tion, and to a lower initial value of D_{ww}, leading to sharper
water concentration profiles; both factors lead to a decrease
of ϕ_c. As also the initial value of D_{aa} is lower at lower ini-
tial water content, an increase in retention is found.

- an increase in temperature at other process conditions
constant leads to an increase of the water vapour pressure and
thus of the water flux, which tends to shorten ϕ_c. Also the dif-
fusion coefficient of water increases, which would tend to en-
large ϕ_c. Furthermore the diffusion coefficients of aroma in-
crease. Discussion of the effect of these partly competing in-
fluences is best done on basis of quantitative data on tempera-
ture influences; this will be done in Chapter IV for the model
system of aqueous maltodextrin solutions with n-alcohols as
model aroma components.

The effects found are fully in agreement with the experimental
results of Rulkens (8) on the slab drying of the model system
named above.

II.9.2. The_drying_of_spherical_particles

Numerical solutions to Equations (II-62) through (II-74), inclu-
ding the heat balance (II-48) were calculated for the physical
properties of appendix 3, table 3 (21,22,28,36). For some calcu-
lations also the impulse balance (II-49) was included in the
calculations.

The concentration profiles of water and of aroma during the
non isothermal drying of droplets are similar to the ones dis-
cussed in slab drying. Again steeper water concentration profi-
les are encountered at higher rate of water removal from the
surface, and lower initial water concentrations.

The variation of temperature, fractional water content and aro-
ma retention with time is illustrated in fig. II-8. First a
warming-up period towards wet-bulb temperature is observed, then
a period of approximately constant wet-bulb temperature, after
which the temperature rises again. As in this case the droplet
enters below dew-point temperature of the drying air, the frac-
tional water content shows initially a slight increase until
the dew point is reached, after which water is lost. Aroma loss
approximately levels out at the time that the temperature starts
to deviate from the wet-bulb temperature, thus coinciding with
the decrease in water activity causing the temperature rise.
Thus the aroma loss also here mainly takes place during the pe-
riod of approximately constant water activity, which is also in
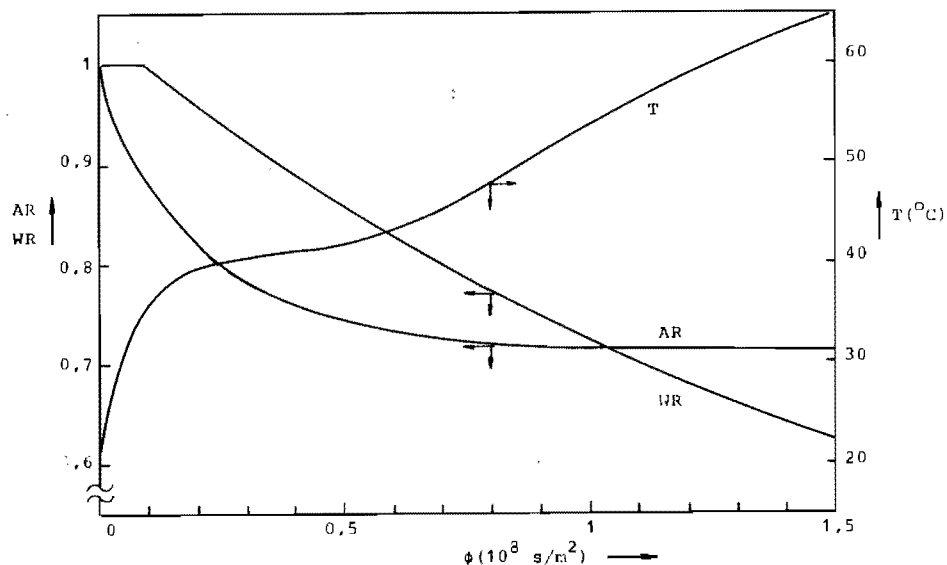
Fig II-8. Numerically calculated temperature, water and aroma
content in relation with time for drying droplet (27). Initial
water content $\omega_{w,o}$ = 0.45; initial droplet temperature 20°C;
air temperature 100°C; air humidity 0.03 kg/kg dry air; air
ideally mixed; Nu = Sh = 2

droplet drying commonly denoted by the in principle erroneous name : "constant-rate period". From the following equations derived for water removal from droplets for $A_w^i = 1$ at wet-bulb temperature and $Sh = 2$:

$$\frac{1}{\bar{V}_w} \frac{dR}{dt} = j_w^i = k' \ (\rho_w'^i - \rho_w'^b) = \frac{D_w'}{R} \ (\rho_w'^i - \rho_w'^b) \qquad (II-102)$$

$$\frac{1}{\bar{V}_w} \frac{dR^3}{dt} = 3R^2 \ j_w^i = 3 \ D_w' \ R \ (\rho_w'^i - \rho_w'^b) \qquad (II-103)$$

follows that due to shrinkage neither the water flux, nor the overall evaporation rate are constant during drying, and so the term "constant-rate" period would better be replaced by "constant-activity" period. However, because of the general use of the term, the name "constant-rate" period will be used in the following.

From calculations for a number of process conditiond the final aroma retention in dependence on these variables was calculated. The results are shown in fig. II-9 (22,28). From these graphs can be read that according to the theoretical model, aroma retention increases with :

- decreasing air humidity
- increasing air outlet temperature
- decreasing initial water content
- increasing particle radius in the case of high initial velocity $\bar{v}_o$
- increasing initial velocity $\bar{v}_o$

The effects of the dissolved solids concentration, air humidity and velocity agree with experimental findings of Rulkens for spray drying (8) and of Menting for droplet drying (10). The explanation of the effects of initial dissolved solids concentration and air humidity is the same as in the last section. The velocity effect can be explained from the fact that for two particles of different size with the same initial velocity the initial Re-number, and consequently also the Sh and Nu numbers
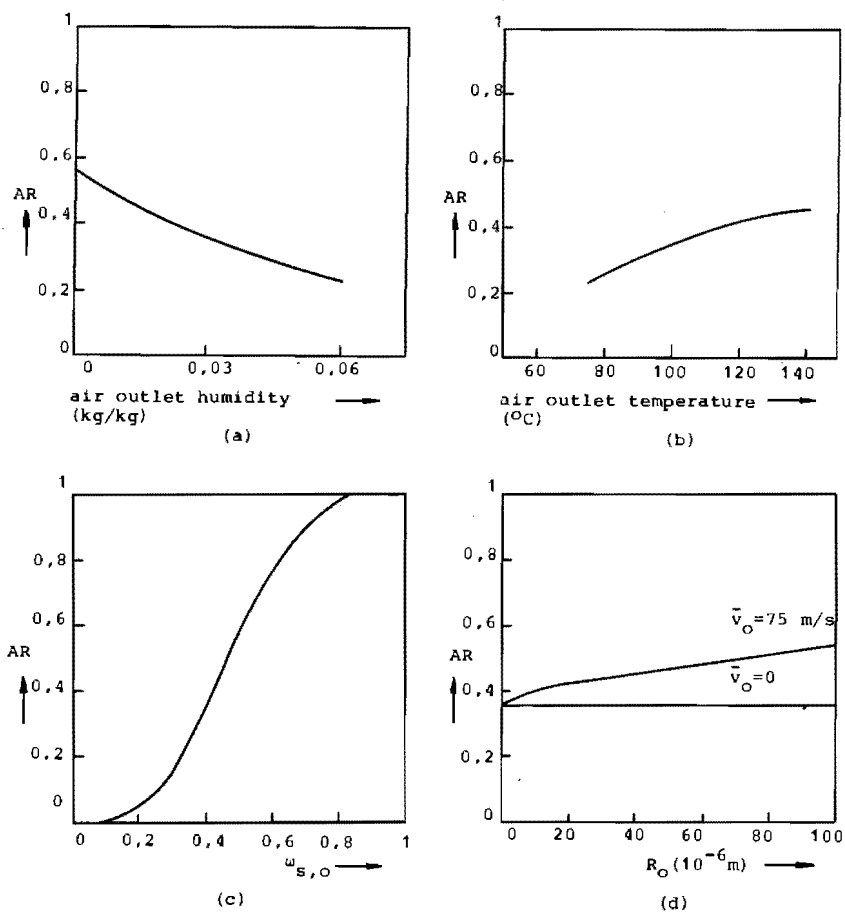
Fig II-9. Numerically calculated effect of process conditions on aroma retention in droplet drying $(22,28)$. Ideally mixed air flow ; feed temperature $20^{\circ}C$.

(a) air temperature $100^{\circ}C$; $\omega_{s,o} = 0.4$; Sh = Nu = 2

(b) air humidity 0.03 kg/kg dry air; $\omega_{s,o} = 0.4$; Sh = Nu = 2

(c) air temperature $100^{\circ}C$; air humidity 0.03 kg/kg dry air; Sh = Nu = 2

(d) air temperature $100^{\circ}C$; air humidity 0.03 kg/kg dry air; $\omega_{s,o} = 0.4$; $\bar{v}_o$ is initial droplet velocity; Nu and Sh given by (II-24) and (II-25)

42

are the largest for the largest particle; as also the terminal Re-number is larger for the larger particle during the whole process the values of Nu and Sh are higher, causing a shorter length of the constant-rate period and thus higher aroma retention. The increase of aroma retention with increasing air temperature which causes higher drying rate, was also found experimentally by Menting at air temperatures below about 100 ^{o}C. Higher temperatures led to boiling inside the droplets and an increasing aroma loss with temperature. This was also found in the experimental spray drying work of Rulkens and Thijssen (*8,7*).

II.10. <u>Conclusions</u>

In this chapter the diffusion equations have been given in general form, including geometrical factors. Also general rules for the coordinate transformation to dissolved solids based coordinates have been given, which are necessary for ·the numerical programming of the equations.
From similarity analysis it was shown that the effect of the gas phase mass transfer coefficient and the initial thickness or radius of a drying specimen upon drying behaviour and aroma retention can be combined to the effect of one variable; the use of reduced distance and time coordinates gives insight into the similarity between drying of samples of different sizes. Finally the effect of process variables on drying behaviour and aroma loss of drying slabs and droplets has been given, as calculated from ternary diffusion equations. The comparison of the theoretically obtained results with experimental data from literature generally shows good agreement.

III CORRELATION OF THE LENGTH OF THE CONSTANT-RATE PERIOD AND
    AROMA RETENTION WITH PROCESS CONDITIONS; DEVELOPMENT OF A
    SIMPLE PREDICTION METHOD FOR AROMA RETENTION

III.1 Introduction

The theoretical models discussed in Chapter II enable accurate
calculation of drying rate and aroma loss in drying liquid foods.
The models treated can easily be extended to more complex drying
situations, in which external conditions vary with time. Also
the calculation of thermal degradation reactions as performed
by Schoeber and Kerkhof (21,22,28,44) only requires a relatively
small extension of the computer program. Thus the theoretical
models provide a very powerful tool for fundamental studies,
enabling the investigator to simulate the effect of process
variables on drying rate, aroma retention and thermal deteriorat-
ion also for complex drying conditions.

To perform the above mentioned sutdies for a specific liquid
food requires the knowledge of basic diffusion and activity
data, as discussed in Chapter II. The determination of such data
is very time-consuming. If one is only interested in approximate
estimation of aroma retention for not too complicated drying
conditions, the determination of the relations for the water and
aroma diffusion coefficients in relation to temperature and water
concentration, the implementation of rather complicated computer
programs, and the requirement to study multicomponent diffusion,
are not worth the effort. In such cases measurement of aroma
retention in relation to process variables, although also requir-
ing a considerable experimental effort, may be an easier and
faster approach to the problem. However, every change in process
conditions or in composition of the feed requires new drying
experiments.

In this chapter a simplified method of predicting aroma loss
is developed which circumvents the above mentioned difficulties
(45). By developing approximate models and by analysis of a large
number of computer simulations with the model of Chapter II,

correlations are developed which relate the length of the con-
stant-rate period, and the effective aroma diffusion coefficient
during this period, to process variables. The correlations are
of a general nature, and for a given liquid food the constants
occurring in the correlations can be determined from a small
number of simple slab drying experiments. The only additional
physical data needed are water vapour sorption isotherms and
the partial specific volume of the dissolved solids.

The first part of this chapter deals with the development of the
correlations, the second part with testing of the predictive
value of the correlations on some computer simulations. In Chap-
ter IV the experimental verification of the method is discussed.

III.2 Approximate models for the length of the constant-rate
period

In the following the same assumptions will be made as in Chapter
II for the ternary diffusion models. Additionally it will be
assumed that during the constant-rate period the temperature of
the drying specimen is constant.
The constant-rate period is considered to end, once a critical
liquid-side interfacial water concentration $\rho_{w,c}$ has been reached.
Analogously to section II.7, also in this section it is assumed
that one given liquid food is considered and that the relations
for the diffusion coefficients and vapour liquid equilibria in
dependence on water concentration and temperature are thereby
fixed.
In Appendix 7 the solution to the problem of a slab with con-
stant diffusion coefficient, thickness and surface flux (CDTF-
model) is given, as it is illustrative also for the case of
variable diffusion coefficient and thickness.

III.2.1 The semi-infinite slab

Let us consider a semi-infinite slab as given in fig. III-1.
For the sake of simplicity the coordinate system has been fixed
to stationary coordinates, and the origin is placed somewhere
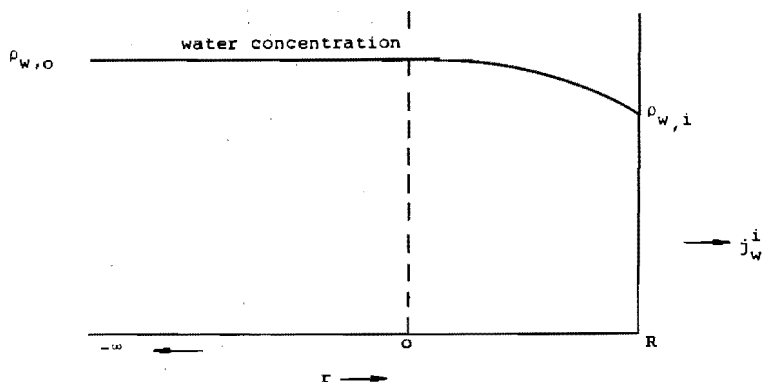
Fig. III-1. Diagrammatic representation of semi-infinite slab

in the drying slab. For the diffusion of water Eq (II-28) holds
with the following initial and boundary conditions:

$$t = 0 \qquad - \infty < r < R_o \qquad \rho_w = \rho_{w,o} \qquad \text{(III-1)}$$

$$t > 0 \qquad r = - \infty \qquad \rho_w = \rho_{w,o} \qquad \text{(III-2)}$$

$$\frac{-D_{ww} \dfrac{\partial \rho_w}{r}}{1 - \rho_w \overline{V}_w} = j_w^i \qquad \text{(III-3)}$$

Let the flux j_w^i be taken constant and equal to $j_{w,o}^i$. For a
given initial water concentration at a given temperature the
solution of this equation in terms of $\rho_w = \rho_w(r,t)$ depends upon
the flux $j_{w,o}^i$. By means of the substitutions:

$$w = r \, j_{w,o}^i \qquad \text{(III-4)}$$

and

$$v = t \, (j_{w,o}^i)^2 \qquad \text{(III-5)}$$

the differential equation with boundary conditions goes over in:

$$\frac{\partial \rho_w}{\partial v} = \frac{\partial}{\partial w} \left(D_{ww} \frac{\partial \rho_w}{\partial w} \right) \qquad \text{(III-6)}$$

$$v = 0 \qquad - \infty < w < R_o j_{w,o}^i \qquad \rho_w = \rho_{w,o} \qquad \text{(III-7)}$$

$$v > 0 \qquad w = - \infty \qquad \rho_w = \rho_{w,o} \qquad \text{(III-8)}$$

46

$$w = R \, j_{w,o}^i \qquad \dfrac{-D_{ww} \dfrac{\partial \rho_w}{\partial w}}{1 - \rho_w \bar{V}_w} = 1 \qquad \text{(III-9)}$$

from which follows that the solution can be written as $\rho_w = \rho_w(v,w)$, independent of $j_{w,o}^i$. Consequently the value v_c of the transformed time coordinate v required to reduce the interfacial water concentration from $\rho_{w,o}$ to $\rho_{w,c}$ is constant; and thus t_c is inversely proportional to the square of the water flux $j_{w,o}^i$:

$$t_c = \dfrac{v_c}{(j_{w,o}^i)^2} = \dfrac{\text{constant}}{(j_{w,o}^i)^2} \qquad \text{(III-10)}$$

in which the value of the constant depends on $\rho_{w,o}$ and $\rho_{w,c}$, and on the relation between D_{ww} and ρ_w.

The physical interpretation of Equation (III-10) is as follows. The steepness of the concentration profile is inversely proportional to the water flux $j_{w,o}^i$, and consequently the distance of penetration of the concentration profile and the amount of water evaporated when reaching the critical surface concentration, are inversely proportional to $j_{w,o}^i$. Since the amount of water evaporated is equal to $j_{w,o}^i t_c$, it follows that t_c is inversely proportional to $(j_{w,o}^i)^2$.

In practice this situation is encountered if the water concentration profile has not penetrated towards the impermeable side of a drying slab. Thus in terms of reduced quantities in this case can be written:

$$\phi_c = \dfrac{F_w}{\varepsilon^2} \qquad \text{(III-11)}$$

in which $\varepsilon = j_{w,o}^i R_o \bar{V}_w = k' R_o (\rho_w'^i - \rho_w'^b) \bar{V}_w \qquad \text{(III-12)}$

The quantity ε will be denoted by the term "reduced flux parameter". A similar dependence as given by Equation (III-11) is found in the CDTF-model, as given in Appendix 7, Equation (10).

II.2.2 The slab with flat water concentration profile

If the external rate of water removal from a drying slab is so low that the internal water diffusion can level off the concentration differences in the liquid, the water concentration profiles will be flat. This will be the case for very low drying rates or for very thin slabs. If the water flux is again taken constant, the water loss during the constant-rate period is given by:

$$j^i_{w,o} \, t_c = R_o \, \rho_{w,o} - R_c \, \rho_{w,c} \qquad \text{(III-13)}$$

in which R_c is the thickness of the slab at time t_c . R_c is given by a solute balance:

$$R_c \, \rho_{s,c} = R_o \, \rho_{s,o} \qquad \text{(III-14)}$$

Substituting the relation $\rho_s \bar{V}_s = 1 - \rho_w \bar{V}_w$ (III-15)
and Eq (III-14) in (III-13) the following result is obtained:

$$t_c = \frac{R_o}{j^i_{w,o}} \, \frac{\rho_{w,o} - \rho_{w,c}}{1 - \rho_{w,c} \bar{V}_w} \qquad \text{(III-16)}$$

or in reduced variables:

$$\phi_c = \frac{1}{\varepsilon} \, \frac{(\rho_{w,o} - \rho_{w,c}) \bar{V}_w}{1 - \rho_{w,c} \bar{V}_w} = \frac{B_1}{\varepsilon} \qquad \text{(III-17)}$$

It is obvious but still interesting to note that B_1 only depends on $\rho_{w,o}$ and $\rho_{w,c}$, and not on any other material property or on temperature. The same type of dependence is found in the CDTF-model (see appendix 7, Equation (6)).

III.2.2 The constant-rate period for drying spherical particles

One extreme situation of the drying of spherical particles is encountered if the water concentration profile has only penetrated to a very small distance from the interface. In this case the outer layer of the sphere will behave as a semi-infinite slab, and the same relations as found for slabs, (Equations (III-10) and (III-11) will apply. This clearly will only be the case for very steep concentration profiles, as in that case no

effects of spherical geometry occur.

At a very low water flux the other extreme, flat water concentration profiles, occur. Let Sh = 2 be assumed, which for small droplets at not too high velocity is a reasonable assumption. At a constant value of D_w' and constant driving force the group

$$k'R \ (\rho_w'^i - \rho_w'^b) = j_w^i R = j_{w,o}^i R_o \qquad \text{(III-18)}$$

will remain constant during the constant-rate period. The shrinkage due to water loss can be written:

$$\frac{d}{dt} \ (\frac{4}{3} \pi R^3) = -4\pi \ R^2 \ j_w^i \ \overline{V}_w \qquad \text{(III-19)}$$

Substitution of $\varepsilon = j_{w,o}^i \ R_o \ \overline{V}_w = j_w^i \ R \ \overline{V}_w$ (III-20)

gives:

$$R \ \frac{dR}{dt} = - \ \varepsilon \qquad \text{(III-21)}$$

Integration and re-arrangement gives:

$$\phi_c = \frac{1}{2\varepsilon} \ (1 - \frac{R_c^2}{R_o^2}) \qquad \text{(III-22)}$$

From the solute balance:

$$\frac{4}{3}\pi \ R_o^3 \ (1 - \rho_{w,o}\overline{V}_w) = \frac{4}{3}\pi \ R_c^3 \ (1 - \rho_{w,c}\overline{V}_w) \qquad \text{(III-23)}$$

R_c can be eliminated and for ϕ_c the following relation results:

$$\phi_c = \frac{1}{2\varepsilon} \left[\ 1 -\left(\frac{1 - \rho_{w,o}\overline{V}_w}{1 - \rho_{w,c}\overline{V}_w} \right)^{2/3} \ \right] = \frac{B_2}{\varepsilon} \qquad \text{(III-24)}$$

In this case too ϕ_c is inversely proportional to ε and the proportionality constant again only depends on initial and critical water concentration.

III.3 Effective aroma diffusion coefficient

In order to define an effective aroma diffusion coefficient for the loss of aroma components during the constant-rate period the following simple system is considered:

Aroma loss from a slab or a sphere, with constant dimension R_o, occurs during a time t_c, and can be described by a constant diffusion coefficient $D_{a,eff}$. The interfacial aroma concentration is equal to zero. The diffusion equations for this case have been solved analytically by Crank (34). The solution can be obtained as an expression of the aroma retention in dependence on the Fourier-number:

$$Fo_c = D_{a,eff} \, t_c \, / \, R_o^2 = \phi_c \, D_{a,eff} \qquad \text{(III-25)}$$

and reads:

$$slab: \quad AR = \frac{8}{\pi^2} \sum_{n=0}^{\infty} \frac{1}{(2n+1)^2} \exp \left[-(2n+1)^2 \, \pi^2 \, Fo_c/4 \right] \qquad \text{(III-26)}$$

$$sphere: \quad AR = \frac{6}{\pi^2} \sum_{n=0}^{\infty} \frac{1}{n^2} \exp \left[- n^2 \, \pi^2 \, Fo_c \right] \qquad \text{(III-27)}$$

Approximations for short times and for long times are given by:

$$slab: \quad AR = 1 - 2(Fo_c/\pi)^{1/2} \quad \text{for } Fo_c < 0,2 \qquad \text{(III-28)}$$

$$AR = \frac{8}{\pi^2} \exp (-\pi^2 \, Fo_c/4) \quad \text{for } Fo_c > 0,2 \qquad \text{(III-29)}$$

$$sphere: AR = 1 - 6(Fo/\pi)^{1/2} \quad \text{for } Fo < 0,022 \qquad \text{(III-30)}$$

$$AR = \frac{6}{\pi^2} \exp (-\pi^2 \, Fo) \quad \text{for } Fo > 0,022 \qquad \text{(III-31)}$$

In both cases the boundary between the long and short times approximations lies at $AR \simeq 0,5$; the maximum error in the aroma retention is of the order of 10% relative error.

III.4. Determination of correlations from computer simulations

III.4.1. The constant-rate period for drying slabs

With a digital computer program the drying of slabs, as described by the diffusion equations of Chapter II, was simulated for a

number of process conditions with varying R_o, k', $\rho_{w,o}$ and $\rho_w'^b$. The dependence of the diffusion coefficients of water and of aroma on water concentration and temperature, and relations for water and aroma activity are presented in appendix 3, table 1. As critical water concentration the value of $\rho_{w,c} = 250$ kg/m^3 was used, corresponding to an equilibrium water activity $A_w = 0.92$.

In fig. III-2 a logarithmic plot is presented of ϕ_c vs ϵ for two values of $\rho_{w,o}$ and a slab temperature of 25 ^{o}C. The points represent the values calculated numerically. The full lines are given by Eq (III-17), the dotted lines by Eq (III-11). The value of F_w was derived for each concentration from the numerically calculated value of ϕ_c at very high ϵ-value.

It is clear that for very high and for very low values of ϵ the numerically calculated results coincide with either Eq (III-11) or Eq (III-17) respectively, which describe the extreme situations. The largest deviation occurs at the intersection point of the two lines, which is given by

$$\epsilon_{is} = F_w \, / \, B_1 \qquad\qquad (III-32)$$

and

$$\phi_{c,is} = B_1^2 \, / \, F_w \qquad\qquad (III-33)$$

From the figure can be read that the deviation is given by:

$$\phi_c(\epsilon=\epsilon_{is}) = 0.7 \, \phi_{c,is} \qquad\qquad (III-34)$$

To investigate the deviation also for other product properties, also for a number of other dependences of the diffusion coefficient on water concentration the ratio $\phi_c/\phi_{c,is}$ was determined. *In all cases, including even a constant diffusion coefficient, it was found that relation (III-34) was valid.* An explanation for this effect may be given by considering the way in which the water concentration profile at ϕ_c for $\epsilon = \epsilon_{is}$ is formed. For a higher value of ϵ the length of the constant-rate period approaches the values given by the semi-infinite slab; this means that during a considerable part of the constant-rate period the water concentration has not penetrated towards the
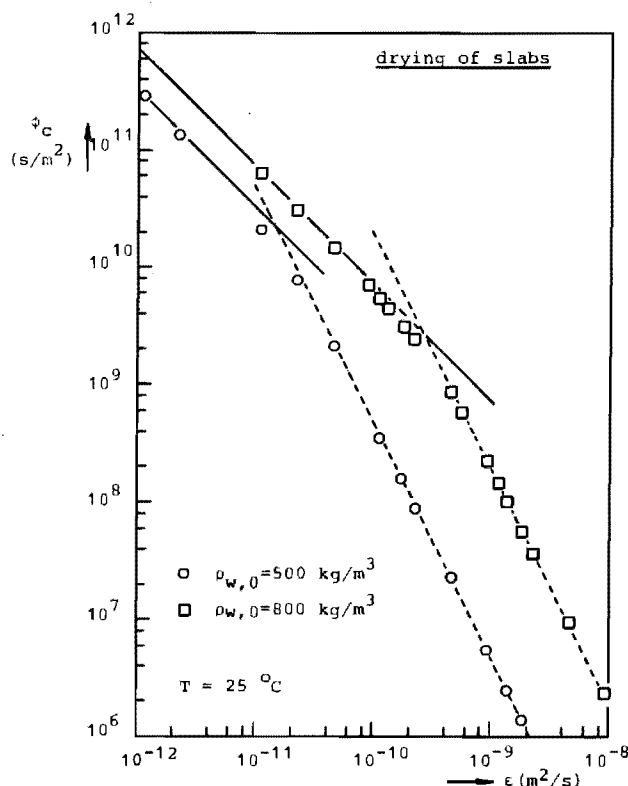
Fig.III-2. Reduced length
of constant-rate period ϕ_c
in relation to reduced
flux parameter ϵ.
Points represent diffusion
model of Chapter II.
——— Eq(III-17)
---- Eq(III-11)
Physical properties from
Appendix 3, Table 1.

centre of the drying slab. For values of $\epsilon < \epsilon_{is}$ the behaviour
is more like that of the case for flat water concentration pro-
files. This means that during the main part of the constant-
rate period the centre concentration has decreased at a rate
comparable with the interfacial water concentration.
The history of the concentration profile at $\epsilon = \epsilon_{is}$ now repre-
sents an intermediate situation between the two extremes. Thus
the concentration profile at ϕ_c for $\epsilon = \epsilon_{is}$ is curved near the
interface, but the centre concentration has also decreased con-
siderably. A measure for the penetration of the concentration
profile is the ratio of the amount of water evaporated at ϕ_c,
and the amount which would evaporate in the case of flat water
concentration profiles. Easily can be derived that this ratio,
which will be denoted as the "profile penetration number" N_{pp},
is equal to:

$$N_{pp} = \frac{\epsilon \phi_c}{B_1}$$

(III-35)

The result described by Eq (III-34) thus implies:

$$N_{pp} \ (\varepsilon = \varepsilon_{is}) = 0.7 \qquad\qquad (III-36)$$

which result is apparently valid for strongly varying material properties. The apparent uniformity of this phenomenon is a subject of further study, and will be included in the work of Schoeber (73).

Computations were also made for other initial water concentrations and temperatures, and the results showed similar trends as the points in fig. III-2. With the aid of these results the dependence of F_w on initial water concentration and temperature was investigated, as is illustrated in fig. III-3. Apparently the factor F_w is an exponential function of $\rho_{w,o}$, and the effect of temperature is nearly independent of $\rho_{w,o}$. Additional calculations for a temperature of 37.5 $^{\circ}$C showed that the effect of temperature could best be described by an Arrhenius equation, and so the following correlation was obtained:
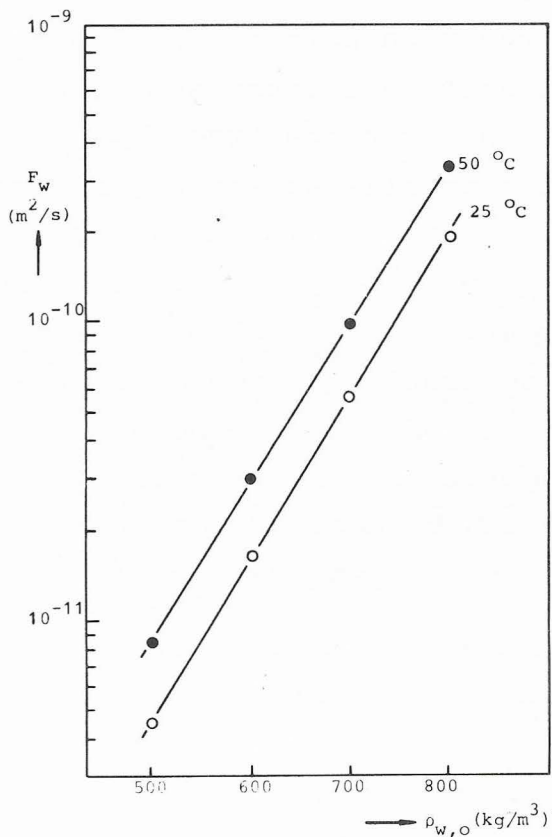
Fig.III-3. Dependence of F_w on initial water concentration and temperature, as found from numerical calculations.

$$F_w = F_w{}^o \exp \left(- \frac{E}{RT_k} + f_{ww}\rho_{w,o}\bar{V}_w\right) \qquad \text{(III-37)}$$

in which R   = gas constant (J/mole K)

        E   = activation energy (J/mole)

        T_k = absolute temperature (K)

        F_w = constant (m^2/s)

        f_{ww} = constant (-)

III.4.2. The aroma loss from drying slabs

In a number of the before-mentioned numerical computations the transport of an aroma component was also simulated. The physical properties chosen for these calculations are again tabulated in appendix 3, table 1. It was established that the major loss of aroma took place during the constant-rate period, except for high bulk humidity where aroma loss after the constant-rate period was also considerable. This could be expected since at high humidity the interfacial concentration decreases only slowly past the critical value. From the calculated values of the aroma retention AR at t_c, values of the Fourier-time Fo_c where calculated with the aid of Eqs (III-28) and (III-29), and
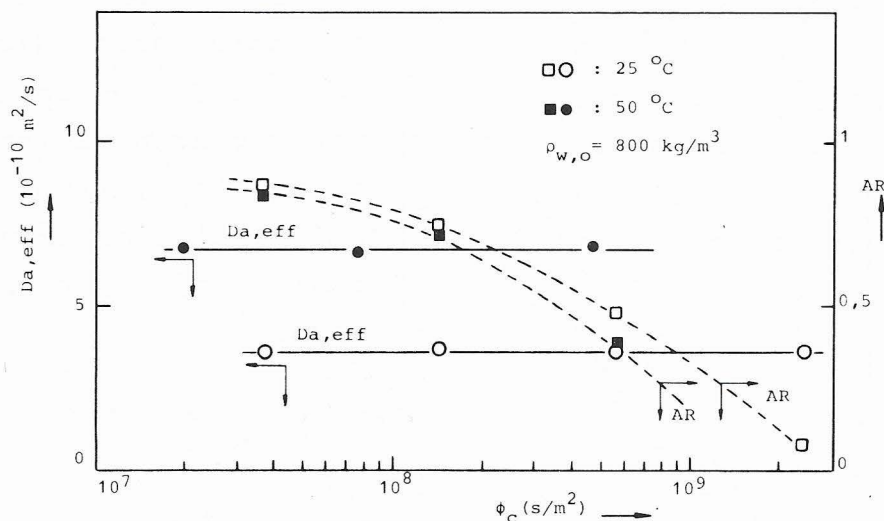
Fig III-4. Aroma retention AR and effective aroma diffusion coefficient $D_{a,eff}$ in dependence on ϕ_c, as found from numerical calculation of ternary diffusion model in slab drying.

subsequently the values of $D_{a,eff}$ where calculated. In fig.III-4 the aroma retention AR and $D_{a,eff}$ are given in relation to ϕ_c, for $\rho_{w,o}$ = 800 kg/m^3 and temperatures of 25 $^\circ$C and 50 $^\circ$C. From this figure follows that $D_{a,eff}$ is independent of ϕ_c, or of AR, and increases with increasing temperature. Interesting is the comparison between $D_{a,eff}$ and D_{aa}. For the initial concentration $\rho_{w,o}$ = 800 kg/m^3 D_{aa} is equal to 5.4 x 10^{-10} m^2/s, at $\rho_{w,c}$ D_{aa} = 7.7 x 10^{-13} m^2/s, and at $(\rho_{w,o} + \rho_{w,c})/2$ follows D_{aa} = 4.3 x 10^{-11} m^2/s. Thus follows that $D_{a,eff}$ cannot be approximated by D_{aa} at the initial or the average value of the water concentration. Computations for other initial water concentrations also showed no relation between $D_{a,eff}$ and ϕ_c, but showed a sharp increase of $D_{a,eff}$ with initial water concentration, as is illustrated in fig. III-5. Like the coefficient F_w, $D_{a,eff}$ is also seen to be approximately an exponential function of $\rho_{w,o}$, and the effect of temperature is seen to be virtually independent of initial water concentration. Thus the following correlation for $D_{a,eff}$ is found:

$$D_{a,eff} = D_a^O \exp \left(- \frac{E_a}{RT_k} + f_{aw} \rho_{w,o} \bar{V}_w \right) \qquad \text{(III-38)}$$
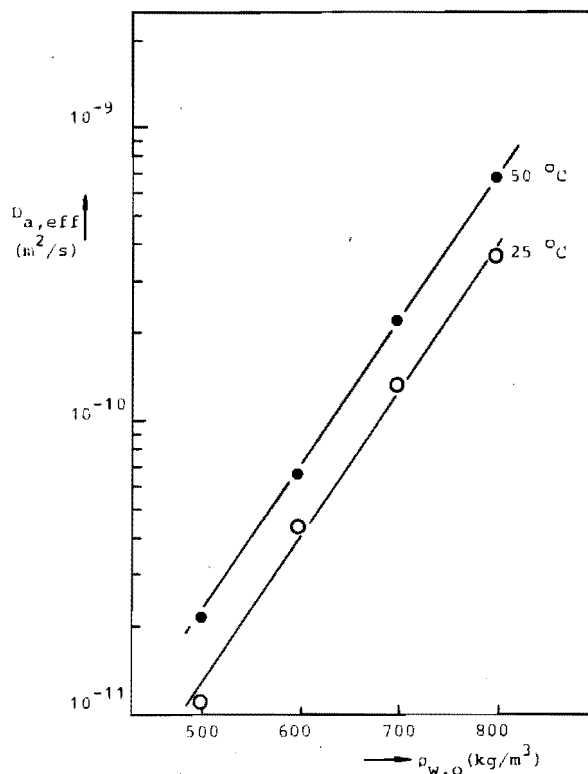
Fig III-5. Dependence of effective aroma diffusion coefficient on initial water concentration and temperature, from numerical calculation of ternary diffusion model for drying slab.

III.4.3. Constant-rate period and effective aroma diffusion coefficient for drying spheres

With aid of a digital computer program the diffusion equations
for water and aroma were solved for spherical particles at con-
stant temperature, assuming the same physical properties as for
the slab drying calculations. Some results obtained are repre-
sented as points in fig. III-6. In this figure the full lines
represent Eq (III-24), derived for flat water concentration
profiles. The dotted lines represent Eq (III-11), as derived
for infinite slabs, with the constant F_w found from the slab
drying simulations. For both concentrations the values of ϕ_c
obtained for very low or very high values of ε with respect to
ε_{is}, agree well with the lines describing the extreme situations.
The deviation observed around $\varepsilon = \varepsilon_{is}$ is larger than in the case
of slab drying, which is caused by the effects of the spherical
geometry. The maximum deviation is again found at the inter-
section point, given by:

$$\varepsilon_{is} = F_w / B_2 \qquad\qquad (III-39)$$

and
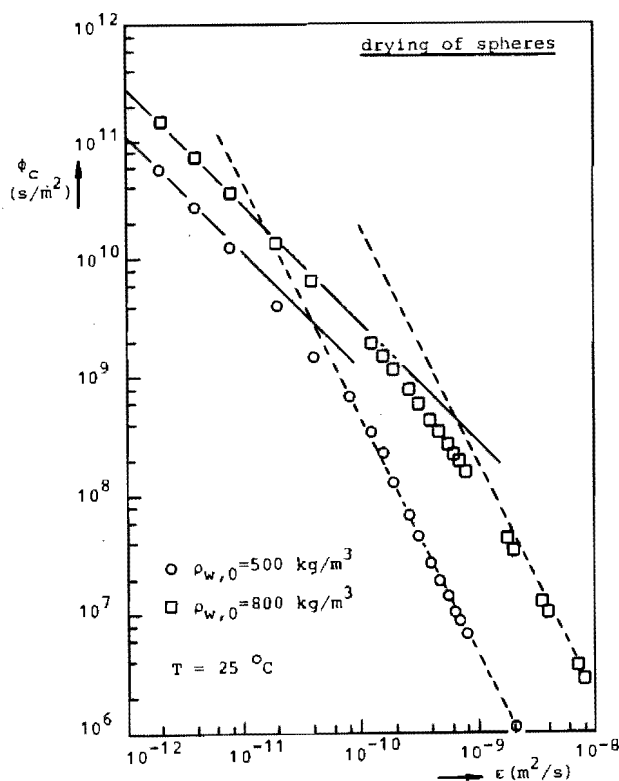
Fig III-6. Relation between
reduced length of constant-
rate period ϕ_c and reduced
flux parameter ε. for the
drying of spherical particles.
Points represent diffusion
model of Chapter II.
—— Eq(III-24)
--- Eq(III-11)

56

$$\phi_{c,is} = B_2^{\,2} / F_w \tag{III-40}$$

In the cases given in the figure, as well as for cases calculated for other dependences of the diffusion coefficient on water concentration and for other concentrations, it was found that:

$$\phi_c \ (\varepsilon = \varepsilon_{is}) = 0.5 \ \phi_{c,is} \tag{III-41}$$

For the relation between ϕ_c, $\phi_{c,is}$ and N_{pp} can be derived:

$$N_{pp} = \frac{1}{1 - \beta} \left[1 - \left\{ 1 - \frac{\phi_c}{\phi_{c,is}} (1 - \beta^{2/3}) \right\}^{3/2} \right] \tag{III-42}$$

with

$$\beta = \frac{1 - \rho_{w,o} \, \bar{V}_w}{1 - \rho_{w,c} \, \bar{V}_w} \tag{III-43}$$

Substitution of (III-41) in (III-42) delivers for $\rho_{w,o}$ varying between 500 and 900 kg/m^3 and $\rho_{w,c}$ = 250 kg/m^3 a value of N_{pp} varying from 0.52 to 0.57.

From the aroma transport calculations for drying spheres the values of Fo_c and of $D_{a,eff}$ were calculated with relations (III-30) and (III-31). The interesting result was obtained that for equal initial water concentration and temperature *the value of $D_{a,eff}$ found for spheres was equal to that found in slab drying*.

III.5. Prediction of aroma retention with correlations

From the foregoing it follows that in principle from only a few slab drying data for a given material the correlation constants can be determined, and predictions of aroma retention in slab drying and the drying of droplets under other circumstances can be made. The methods for this purpose are summarized points-wise in the following.

III.5.1. Determination of correlation constants

1. For a given food liquid the value of $\rho_{w,c}$ can be determined from the water vapour sorption isotherm. It is recommended that $\rho_{w,c}$ be determined at a water activity of about 90%.

2. For given values of $\rho_{w,o}$ and $\rho_{w,c}$ the constants B_1 and B_2, for the drying of slabs and of spheres respectively, can be calculated.

3. The dependence of F_w on concentration and temperature is characterized by three constants. To determine these constants three slab drying experiments, performed at two concentration and two temperature levels, are in principle sufficient. It is essential that the measurements are performed in such a way, that the slab behaves as an infinitely thick slab. This requirement was determined to be met if

$$N_{pp} < 0.5 \qquad\qquad\qquad (III-44)$$

Thus if condition (III-44) is fulfilled for the three experiments, the three constants in Eq (III-37) can be determined.

4. By analyzing one or more key aroma components, the constants in the correlation for $D_{a,eff}$ can also be determined from the three slab drying experiments mentioned under 3.

Although in principle three slab drying experiments would suffice, the best results will be obtained by analyzing more experiments. The experimental procedure is described in Chapter IV.

III.5.2 Prediction_of_aroma_retention

1. Determine B_1 or B_2 for the drying of slabs or of spheres respectively, according to Equation (III-17) or (III-24), from $\rho_{w,o}$ and $\rho_{w,c}$.

2. Calculate the value of F_w at the temperature and initial water concentration of interest, with Equation (III-37).

3. Calculate ε_{is} according to either Equation (III-32) for drying slabs, or Equation (III-39) for drying spheres.

4. Calculate the value of ε from R_o, k', $\rho_w'^b$ and $\rho_w'^i$ at the prevailing temperature.

4. Determine ϕ_c with
   Eq. (III-11) if $\varepsilon > \varepsilon_{is}$
   Eq. (III-17) (slabs) $\Big\}$ if $\varepsilon < \varepsilon_{is}$
   Eq. (III-24) (spheres)

6. From $\rho_{w,o}$ and T calculate $D_{a,eff}$ according to the correlation (III-38).

7. Calculate the Fourier time Fo_c for aroma loss from
$$Fo_c = D_{a,eff} \; \phi_c \quad (III-25)$$

8. Calculate the aroma retention AR with the aid of one of the relations (III-28) through (III-31).

As can be seen from the procedures given in this paragraph, calculations are very simple, and can be carried out by means of a simple desk calculator or even with a slide rule.

III.6 <u>Test of predictive value of correlations on computer simulated data</u>

The correlations in the preceeding sections have been based on data, calculated with the ternary diffusion models for <u>one</u> <u>dependence of the diffusion coefficients of water and aroma on</u> <u>water concentration and temperature</u>. In this section it is assumed that the form of the correlations is general, and *the prediction method is tested* on results from the ternary diffusion model, but *with other dependences of the diffusion coefficients*. Therefore numerically calculated results of the slab drying are taken as *simulated experiments*.

III.6.1 <u>Drying of slabs</u>

From the ternary slab-drying calculations reported in Chapter II, three simulated "experiments" were taken for which the requirement $N_{pp} < 0.5$ was met. From these three data, as tabulated in Appendix 4, table 1, the values of the constants F_w^o, E, f_{ww}, D_a^o, E_a and f_{aw} were calculated according to the procedures of section III.5. The data are tabulated in Appendix 4, table 2. With the aid of these constants the influence of the initial water concentration on final aroma retention was calculated for two temperatures, 25 ^oC and 45 ^oC, and two values of the gas phase relative humidity: 0% and 60%, based on slab temperature. Further process conditions were: $R_o = 10^{-3}$ m and k' =

10^{-2} m/s. The critical water concentration was taken to be 250 kg/m^3. Following the procedure from III.5.2, the values of F_w, B_1 and $D_{a,eff}$ were calculated for each condition. After the determination of ε and ε_{is} for each condition the appropriate relation for ϕ_c was chosen, and ϕ_c, Fc_c and AR were calculated. The values for the calculations at 25 $^{\circ}$C are compiled in Appendix 4, table 3. In fig. III-7a the points obtained by the prediction method are compared with the final aroma retention, numerically calculated with the ternary diffusion model by Kerkhof et al (20). Generally the agreement is very good, except for $\rho_{w,o}$ = 500 kg/m^3 and RH = 0.6. Inspection of the ternary diffusion calculations learned, that for this case considerable aroma loss occurs after ϕ_c, and that the value of AR at ϕ_c was approximately equal to the one found from the prediction method. The explanation of this effect, as mentioned earlier, is that,

(a)   (b)
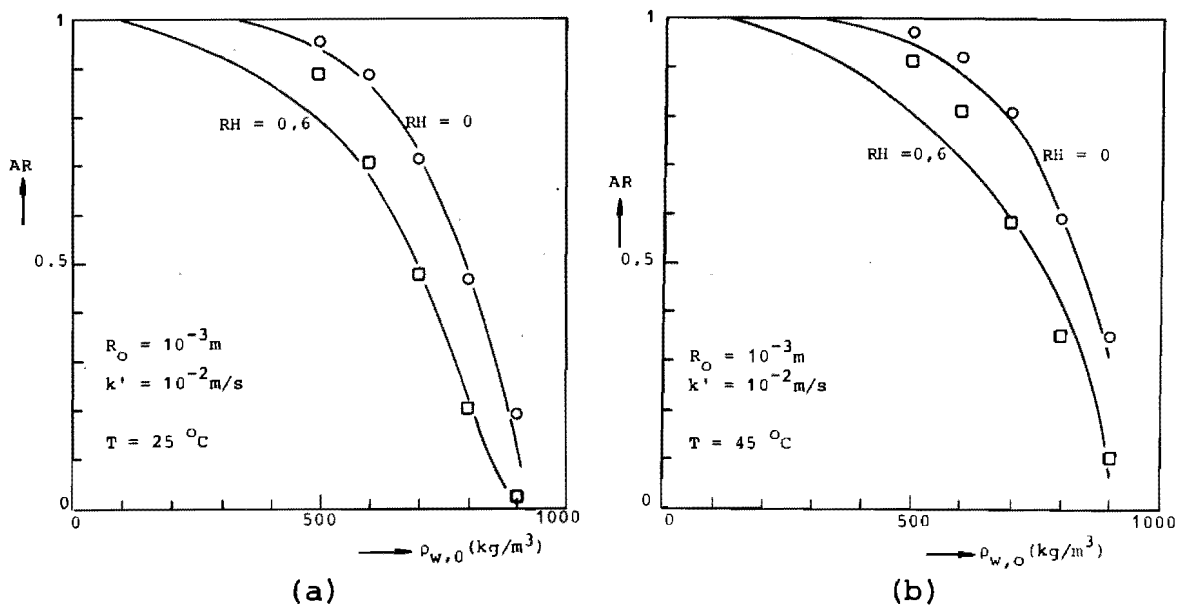
Fig. III-7. Comparison between predicted aroma retention and numerically obtained values for slab drying. Points represent predicted values, full lines numerically calculated data from ternary diffusion model. Physical properties from Appendix 3, Table 2. O RH = 0; □ RH = 0.6. Predictions made with correlation constants in Appendix 4, Table 2.

(a) slab temperature 25 $^{\circ}$C, comparison with (20)

(b) slab temperature 45 $^{\circ}$C

at equal value of ϵ, the decrease of the water concentration ρ_w^i
with ϕ after ϕ_c is considerably lower for high bulk himidities
than for low humidity and thus aroma loss will continue for some
time after t_c. That the effect is stronger for $\rho_{w,o}$ = 500 kg/m^3
than for $\rho_{w,o}$ = 600 kg/m^3, and is negligable for higher initial
water concentration, is caused by the fact that, *relative to* ϕ_c,
the decrease in ρ_w^i below $\rho_{w,c}$ is slower for the lower initial
water concentration. Still, although the error in the aroma loss
is of the order of 100%, aroma retention is predicted within 15%
accuracy. In fig. III-7b an analogous comparison is made between
the points predicted from the correlations and the curves repre-
senting numerical ternary diffusion calculations, for the same
physical properties, but at a slab temperature of 45 ^{o}C. Again
the general agreement is good, except for the lower initial wa-
ter concentration at high humidity. Again the relative error in
AR does not exceed 15%.

III.6.2 Drying of spherical particles

In the calculations of Schoeber and Kerkhof as discussed in
Chapter II, also the temperature rise of the droplets was taken
into account. With the physical data used by these authors, as
given in Appendix 3, table 3, three slab drying experiments were
again simulated. The values derived from these simulations are
tabulated in Appendix 4, tables 4 and 5. The influence of the
initial water concentration, this time expressed as the initial
weight fraction $\omega_{w,o}$ was again used to test the predictive value
of the correlations. At the conditions used by Schoeber and Kerk-
hof (air temperature = 100 ^{o}C, bulk air humidity = 0.03 kg H$_2$O/
kg dry air) the wet bulb temperature of a drying droplet is 43
^{o}C, as can be read from the psychrometric chart (Perry and Chil-
ton (43)). Taking Sh = 2, the value of ϵ can be calculated for
the droplet. For each concentration F_w and B_2 were determined
and the intersection point ϵ_{is} was calculated. As for all con-
centrations $\epsilon < \epsilon_{is}$, Eq. (III-24) was used for the prediction of
ϕ_c. The values of AR were then calculated according to III.5.2.
In fig. III-8 the predicted values of AR are compared with the
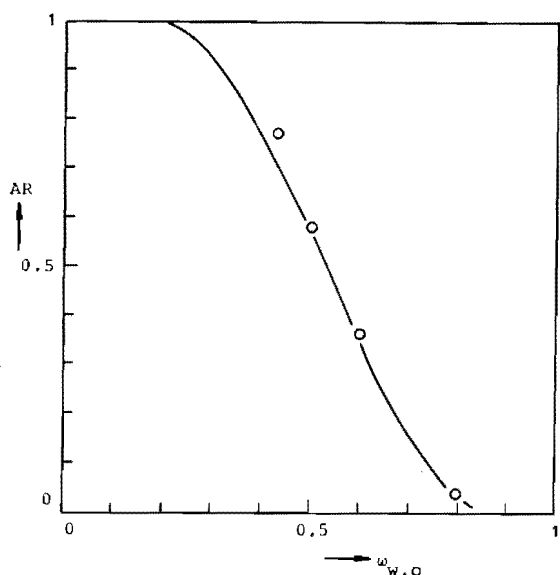
Fig. III-8. Comparison between predicted aroma retention and numerically obtained values from ternary diffusion model, for the air drying of spherical particles.

O predicted from three simulated slab drying experiments

——— calculated by Schoeber and Kerkhof

air temperature : 100 ^{o}C

air humidity : 0.03 kg/kg

Sh = Nu = 2

numerically calculated values. Excellent agreement can be observed.

III.7 Discussion

From the foregoing it can be concluded that the prediction method, as developed from approximating models for the length of the constant-rate period and aroma transport during this period, can be used for prediction of final aroma retention within only small deviation from results calculated with the ternary diffusion models discussed in Chapter II. Some remarks can be made with regard to the accuracy. As the method only predicts aroma loss during the constant-rate period, a too high prediction of AR will be found for those cases in which after this period still an important loss occurs. It has been recognised that this occurs for low initial water concentration and high bulk water concentration in the gas phase a situation improbable to occur in practice. Another factor influencing the accuracy of AR is the accuracy with which the length of the constant-rate period can be predicted. In the following the maximum deviation is estimated. The maximum deviation occurs at the transition between the two extreme

models, and is given by:

$$\phi_c / \phi_{c,is} = \alpha \qquad\qquad (III-45)$$

with $\alpha = 0.7$ for drying slabs, and $\alpha = 0.5$ for drying spherical particles. For AR > 0.5 holds that the aroma loss is proportional to $Fo_c^{1/2}$, and thus the relative deviation in the aroma loss is half of the deviation in Fo_c. Assuming no error in $D_{a,eff}$, the relative deviation in $1 - AR$ made by the prediction method, is at the intersection point equal to $\sim$ 21% for slabs, and $\sim$ 50% for drying spherical particles. For AR < 0.5 it follows that the relative error in AR is proportional to the absolute error in the Fourier-number:

$$\frac{\Delta AR}{AR} = - \frac{\pi^2}{4} \Delta Fo_c \approx - 2.5 \; \Delta Fo_c \qquad \text{for a slab} \qquad (III-46)$$

and

$$\frac{\Delta AR}{AR} = - \pi^2 \; \Delta Fo_c \approx - 10 \; \Delta Fo_c \qquad \text{for a sphere} \qquad (III-47)$$

For a given relative error in Fo_c this means that the relative error in AR increases with increasing Fo-number. Taking AR $=$ 0.1 as a typical lower bound for practical interest, the maximum deviation then for both geometries becomes approximately:

$$\frac{\Delta AR}{AR} \approx - 1 \qquad\qquad (III-48)$$

And thus instead of AR $=$ 0.1 a value of AR $\approx$ 0.05 will be predicted. At AR $=$ 0.5 the relative deviation is:

$$\frac{\Delta AR}{AR} \approx - 0.2 \qquad\qquad (III-49)$$

for both geometries, leading to prediction of AR $=$ 0.4 instead of AR $=$ 0.5. It is stressed here that the deviation derived here represent the maximum deviation, obtained at the most unfavourable situation, for the prediction namely at the transition of the two extreme models. For all other cases the deviation will be less; this can clearly be seen from figs. III-2 and III-6.

IV EXPERIMENTAL INVESTIGATION OF THE PREDICTION METHOD

IV.1 Introduction

In order to test the validity of the correlation and prediction methods derived from theoretical considerations and numerical evaluations of theoretical models in Chapter III, a number of slab drying experiments was performed. As a model system gelled slabs of aqueous maltodextrin solutions were used, with methanol (C_1), n-propanol (C_3) and n-pentanol (C_5) as model aroma components, added in low concentration. As stated before, the correlation method was devised to provide estimates of aroma retention within reasonable accuracy with the aid of very simple equations and calculations. This only can be useful, if also the experimental set-up and methods required for the determination of correlation constants are as simple as possible. Therefore a method was chosen in which slabs are dried with air of constant temperature, and in which slab temperature was measured in order to determine the length of the constant-rate period. When this period had clearly been passed, samples were analyzed for aroma content. For each experimental condition the water flux was determined by drying slabs of 1% aqueous agar-agar solutions.

The experiments are interpreted by the rules from Chapter III It will be shown that the behaviour found from the theoretical models is also observed experimentally. Predictions with the experimentally obtained correlation constants are compared with literature data on aroma retention in drying maltodextrin solutions, and will be seen to agree well.

Finally some remarks will be made with regard to the relative effect of process variables upon aroma retention.

IV.2 Experimental set-up and methods

IV.2.1 Sample preparation

1. *Solutions for determination of water flux*

In 100 ml of tap water 1 g of agar-agar and 0.1 g of benzoic

acid were dissolved by boiling. The benzoic acid was used as a preservating agent. After boiling the liquid was cooled to about 50 ^{O}C, at which the liquid is viscous but not fully gelatinated.

2. *Solutions for measurement of constant-rate period and aroma-retention*

To 100 ml of tap water the desired amount of maltodextrin was added, together with 1 g of agar-agar and 0.1 g of benzoic acid. After initial mixing at room temperature, the mixture was heated and kept boiling until total dissolution had been reached. The solution was then cooled till about 50 ^{O}C, and 2 ml of a mixture of methanol, n-propanol and n-pentanol was added. For specification of the maltodextrin see Appendix 1. The alcohols used were of analytical grade.

3. *Sample holder*

The sample holder, shown in fig. IV-1, consists of a perspex ring with an inner diameter of 30 mm and an outer diameter of 38 mm, with a thin red copper bottom plate of 32 mm diameter and a thickness of 0.03 cm. In the perspex ring with a height of 6 mm a circular groove of a width of 2 mm and a depth of 4 mm was fraised in order to minimize heat capacity and heat transfer through the wall.

The samples were prepared by injecting 2 ml of the warm solution into the sample holders, which were placed on a flat heat exchanger, thermostated slightly above the desired drying tempe-
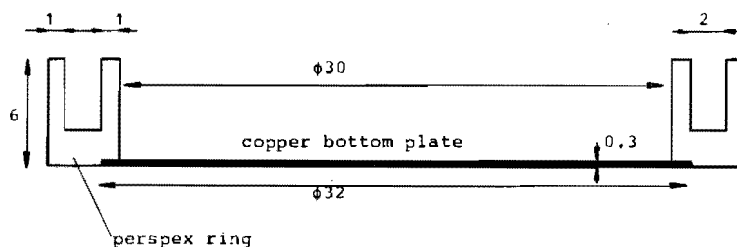
Fig. IV-1. Diagram of sample holder for slab drying experiments. All dimensions in mm.

rature. Immediately after injection of the liquid, the sample
holders were closed by means of brass cover plates, which had
been preheated at 70 $^{\circ}$C to prevent condensation during the
cooling of the samples. During cooling the lids were kept at a
temperature slightly higher than the thermostate temperature
by means of a lamp placed over the covered samples. The samples
were allowed to cool for one hour, which time can be calculated
to be amply sufficient for the nivellation of the temperature
gradients. As the head space over the samples is very small,
the disturbance of the concentration profiles of water and aroma
can be neglected. All samples were weighed after cooling.
For a given initial water concentration at two values of the
mass transfer coefficient three drying and two flux experiments
were done in most cases, thus requiring 6 maltodextrin samples,
and 4 agar-agar samples. Also in such an experimental run two
2 ml samples were injected into weighing flasks, one for the
determination of the water content and one for aroma analysis.

IV.2.2 Drying_apparatus_and_experimental_methods

A diagrammatical presentation of the experimental set-up is
given in fig. IV-2. The drying experiments were conducted in a
perspex cylinder with an internal diameter of 15 cm and a height
of 4 cm; the bottom consisted of a 2 cm thick layer of insulating
styrene foam, the top of a brass plate, equipped with a flat
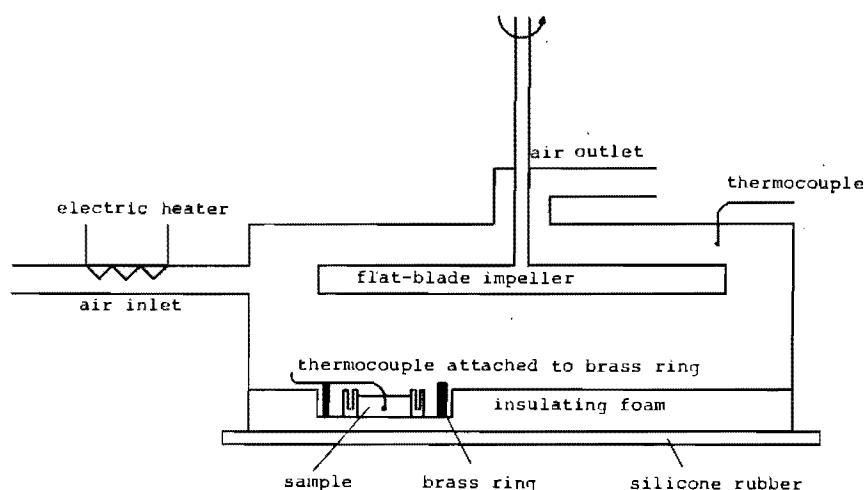
Fig. IV-2. Diagram of drying apparatus for slab drying
experiments.

blade impeller of 10 x 1 cm^2. The impeller speed could be varied
in order to change the mass transfer coefficient in the gas
phase. The foam plate was placed on a silicone rubber plate
resting on a laboratory jack table, thus providing easy sample
exchange, but airtight closure. Around the samples a brass ring
could be placed to which a thermocouple wire had been attached
in such a way that by placing the ring around the sample holder,
the thermocouple junction was inserted into the gelled solution.
The place of the sample was chosen excentrically in order to
obtain equal mass transfer rates over most of the sample area
(8); the distance between the centres of the sample and of the
drying chamber was 5.5 cm. The inlet air stream of 10^{-3} m^3/s
was heated by an electrical heater controlled by a variable
transformer. The air was obtained from the laboratory low pressure
circuit, and in one case was humidified. The air temperature was
measured by means of a thermocouple placed near the impeller tip.

By placing an agar-agar sample in the drier, the heater was
adjusted in such a way that the desired slab temperature was
obtained. The drying apparatus was then accomodated at the
given air inlet temperature. Consecutively an agar-agar sample
was placed in the drying chamber and allowed to dry for some time.
From the weight loss over the drying time the flux was determined.
After that a maltodextrin sample was placed in the drier; when
the temperature of the drying slab had increased more than 15%
of the initial temperature difference between sample and drying
air, the sample was removed and put in a weighing flask. For most
initial water concentrations 3 maltodextrin samples and two agar-
agar samples were dried at two impeller speeds.

IV.2.3 Analysis

The water content of the feed samples was determined by heating
in a stove at 80 ^{O}C for 24 hrs. and subsequent heating at 100 ^{O}C
for 24 hrs. From the weight loss the water content was calculated.
The retention of the model aroma components was determined gas-

chromatographically by methods analogous to those of Rulkens
(8). To the dried samples and to the feed samples 10 ml of a 2
^{O}/oo aqueous n-butanol solution was added, and the samples were
weighed. The gelled layers were detached from the sample holders
and stirred shortly. Then the samples were left standing for
24 hrs. in order to obtain equilibrium between the gelly phase
and the water phase. It was verified that indeed equilibrium was
reached within this time. From the solution 0.1 μL samples were
injected on a Becker Multigraph gas chromatograph equipped with
a 1.5 m Porapak ST column operated at 180 ^{O}C and an air inlet
pressure of 0.5 ato. Peak areas were determined with an Info-
tronics CRS 208 electronical integrator.

At a slab temperature of 20 ^{O}C 5 runs were carried out at diffe-
rent initial water concentrations, and 3 runs at a slab tempe-
rature of 30 ^{O}C. Due to some technical troubles not in all cases
aroma retentions have been determined, and in some cases aroma
retentions were rather inaccurate due to bad reproducibility of
the chromatographic equipment.

IV.3 Experimental results and determination of correlation constants

A full survey of the experimental results is given in Appendix
5, tables 1 and 2.

IV.3.1 Temperature-time curves

In fig. IV-3 some typical curves are given for the slab tempe-
rature in relation to drying time. It can be seen that the
temperature decreases initially, for the high initial water con-
centration remains more or less constant for some time, and
thereupon starts to increase. The increase is seen to be approxi-
mately linear with time for the first part of the heating period.
In the case of the lower initial water contents the constant
temperature period is much shorter, as could be expected.
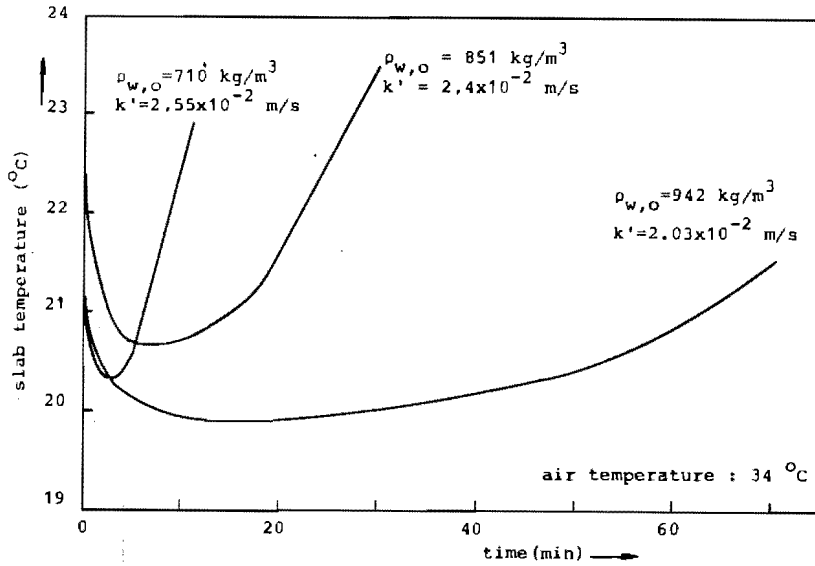
Fig IV-3. Typical temperature readings during slab drying experiments.

IV.3.2 Length of the constant-rate period

As stated also in Chapter II, the end of the constant-rate period should be defined by a critical value of the water activity at the evaporating interface. For the present analysis the critical water activity was taken to be equal to 0.90, corresponding to an interfacial water concentration of 30 wt%, or 405 kg/m^3, as can be read from the sorption isotherm (fig. I-2). Based on the observation of the approximately linear warming-up rate of the slab, in Appendix 6 a relation is derived from which the slab temperature at $A_w^i = 0.9$ can be calculated; also a sample calculation is included. From these calculated "critical" temperatures the value of t_c can be determined by monitoring the slab temperature. A tabulation of t_c is also given in Appendix 5. The value of t_c and of $j_{w,o}^i$ were converted into values of ϕ_c and ε. For each run the value of $N_{pp} = \varepsilon\phi_c/B_1$ was calculated, as also tabulated in Appendix 5. As can be seen, for most cases $N_{pp} < 0.5$, and so for these experiments the slab should behave as infinitely thick, and the relation:

$$\phi_c = \frac{F_w}{\varepsilon^2}$$

(III-11)
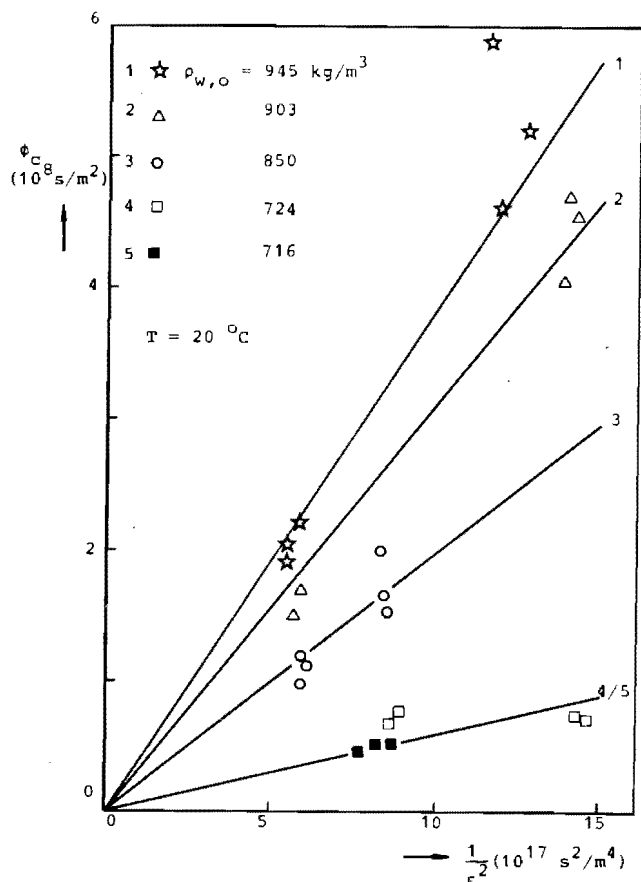
Fig. IV-4. Experimentally
observed dependence of
reduced length of con-
stant-rate period ϕ_c on
reduced flux parameter
ε for drying of slabs
of aqueous maltodextrin
solution. Slab temperature
20 °C.

should hold. In figs. IV-4 and IV-5 the values of ϕ_c are plotted
vs $\frac{1}{\varepsilon^2}$ for the different initial water concentrations. As can be
seen from these figures, indeed in good approximation relation
(III-11) applies. One of the causes of the scattering of the
data is the fact that during the constant-activity period some
cooling down occurs from the initial temperature, which initial
temperature is not exactly equal for all samples. Also replacing
of the samples may give slightly different flow and mass and heat
transfer conditions. From the data presented in figs. IV-4 and
IV-5, the value of F_w was calculated by least-squares fitting
for each concentration and temperature. The data for 724 and
710 kg/m^3 initial water concentration were combined and treated
as values at the average concentration. The values of F_w thus
obtained are tabulated in Appendix 5, table 3, and are repre-
sented graphically in fig. IV-6, in which a semi-logarithmic
plot of F_w vs $\rho_{w,o}$ is given. Clearly the exponential relation
between F_w and $\rho_{w,o}$ can be observed, for both temperature levels,
and also here the dependence of F_w on $\rho_{w,o}$ may in good approxi-
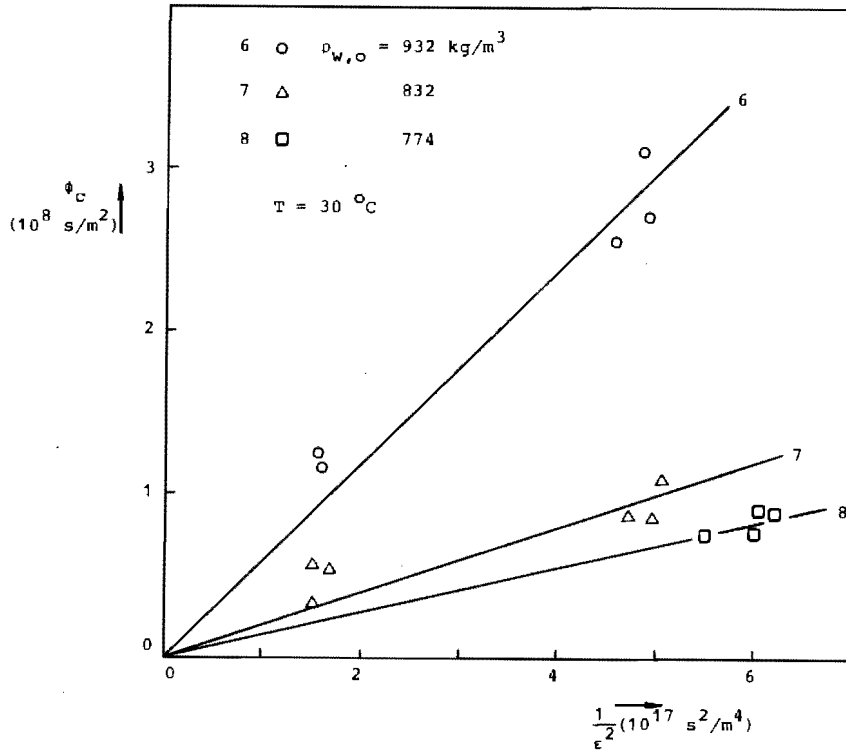
Fig IV-5. Experimentally observed dependence of reduced length of constant-rate period ϕ_c on reduced flux parameter ε for drying of slabs of aqueous maltodextrin solution. Slab temperature 30 $^\circ$C.

mation be treated independent of the temperature influence. Thus good agreement in behaviour between the relations found in Chapter III from the theoretical models and the experimental results is found. The following correlation was found to fit the results:

$$F_w = 1.346 \times 10^{-9} \exp \left[8.781 \, \rho_{w,o} \overline{V}_w - \frac{2764}{T_k} \right] \qquad \text{(IV-1)}$$

in which T_k is the absolute temperature (K).

IV.3.3 Effective aroma diffusion coefficient

As can be seen in tables 1 and 2 of Appendix 5, between duplicate experiments some difference in the values of the aroma retention is observed. This can be due both to errors in the determination of AR, and to differences in t_c; the latter should give higher values of AR at shorter times t_c. A simple investigation shows that there is no systematic correlation between the
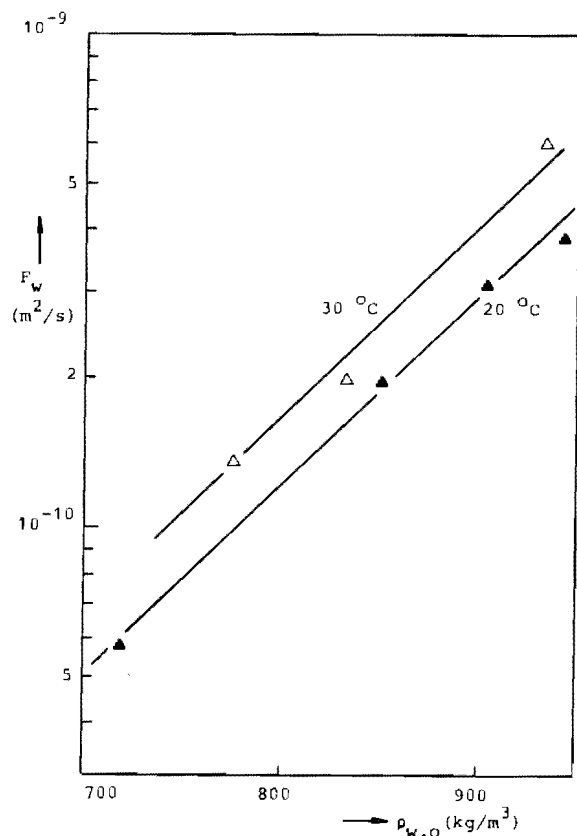
Fig. IV-6. Experimentally observed values of F_w in dependence on initial water concentration and temperature, in slab drying of aqueous maltodextrin solutions.

fluctuations in t_c and in AR for duplicate experiments, and so the fluctuations are due to other experimental errors. Therefore, the values of AR were for each component averaged over each series of duplicate experiments, such as 1a, 1b, etc. From these averaged aroma retention data Fo_c-numbers were calculated according to Eqs. (III-28) and (III-29). Taking also average ϕ_c data for the duplicates, the values of $D_{a,eff}$ were calculated, as tabulated in Appendix 5, table 4. It was found that considerable scattering occurred in the values of $D_{a,eff}$, especially in the values obtained for 30 $^{\circ}$C. Consequently the determination of activation energies for each aroma component could not be performed with reasonable reliability. Therefore, as an approximation, the same energy of activation was taken for all three aroma components, which enabled a more accurate determination of this average temperature effect. It was found that a value of $E_a = 1.0 \times 10^4$ cal/mole = 4.2×10^7 J/kmole gave a good description of the temperature effect. This can be seen in fig. IV-7 in which for all three components the value of $\ln D_{a,eff} + \frac{E_a}{RT}$ is plotted
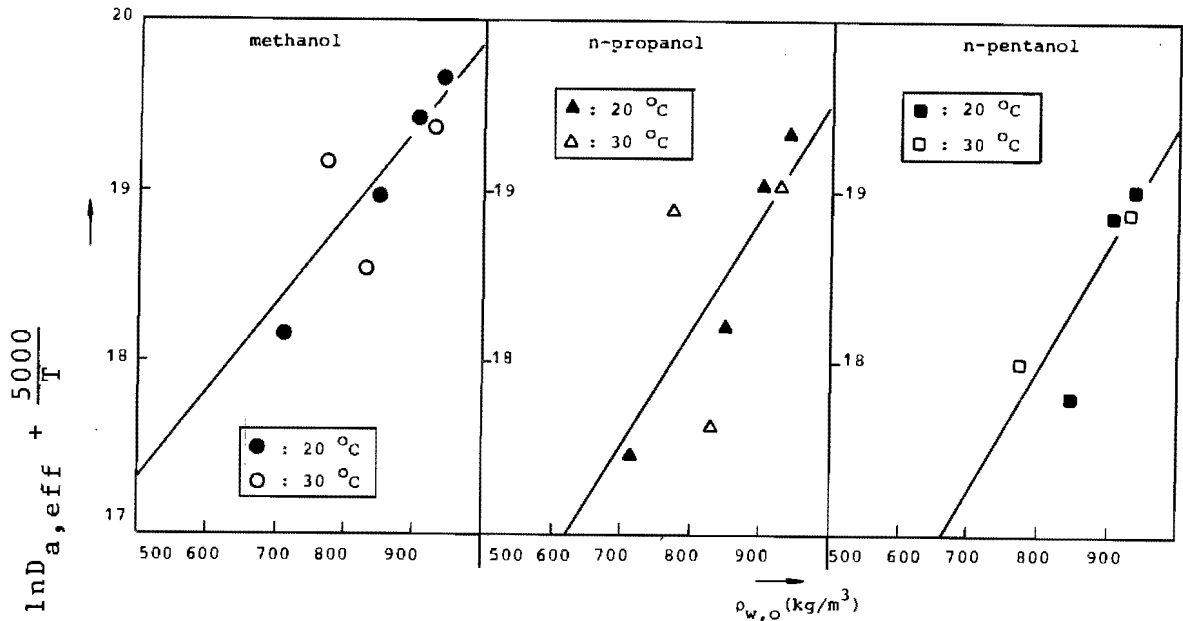
Fig. IV-7. Effective diffusion coefficients of n-alcohols in aqueous maltodextrin solutions in dependence on initial water concentration and temperature, as determined from slab drying experiments.

vs $\rho_{w,o}$. The exponential relation between $D_{a,eff}$ and $\rho_{w,o}$, as found in Chapter III from numerically calculated values, is seen to be also a good approximation to the experimental values, and for both temperatures can be approximated by the single straight lines. From these graphs correlation constants for $D_{a,eff}$ were determined, as tabulated in table IV-1, together with the correlation constants for water.

water	$F_w^o = 1.35 \times 10^{-9}$ m^2/s	$E/R = 2764$ K^{-1}	$f_{ww} = 8.78$
methanol	$D_a^o = 1.86 \times 10^{-4}$ m^2/s	$E/R = 5.10^3 K^{-1}$	$f_{aw} = 5.41$
n-propanol	$D_a^o = 3.84 \times 10^{-5}$ m^2/s	$E/R = 5.10^3 K^{-1}$	$f_{aw} = 6.65$
n-pentanol	$D_a^o = 2.26 \times 10^{-5}$ m^2/s	$E/R = 5.10^3 K^{-1}$	$f_{aw} = 7.04$

Table IV-1. Correlation constants found from slab drying experiments of aqueous maltodextrin solutions, with n-alcohols as model aroma components. Correlation constants to be used in Eqs. (III-37) and (III-38).

Both from the graphical representation and from the values of f_{aw} presented in table IV-1, it can be seen that the effect of

initial water concentration on the effective aroma diffusion coefficient increases with increasing molecular weight of the aroma component. Chandrasekaran and King (29) found experimentally that the influence of the water concentration on the straight diffusion coefficient D_{aa} of various aroma components could be described by one relation, only differing for the various aroma components by a factor D_{aa}^O, the diffusion coefficient in pure water. As follows from the work of Thijssen (3,23), who defined the critical water concentration by $D_{aa}/D_{ww} = 0.01$, this critical water concentration will be higher for lower absolute values of D_{aa}, and thus will increase with increasing molecular weight. The difference between the initial water concentration and the critical water concentration and thus the time necessary to pass through this concentration range at the interface, will be smaller and so more influenced by the initial water concentration with increasing molecular weight of the aroma components. Operating on the basis of one value of t_c for all aroma components, as is done in this thesis, thus leads to a stronger influence of the initial water concentration on the effective aroma diffusion coefficient $D_{a,eff}$ with increasing aroma molecular weight.

IV.4 Comparison of predictions from correlations and experimental observations

IV.4.1 Slab drying

Experiments in this thesis

For all conditions under which the slab drying experiments reported in this chapter have been performed, values of ϕ_c and of AR were calculated with the correlation method of Chapter III, and the experimentally determined constants as tabulated in table IV-1. In fig. IV-8 the aroma retention computed with the correlations is compared with the experimentally observed values. From this figure follows, that the correlations give a very satisfactory description of the experimental values.
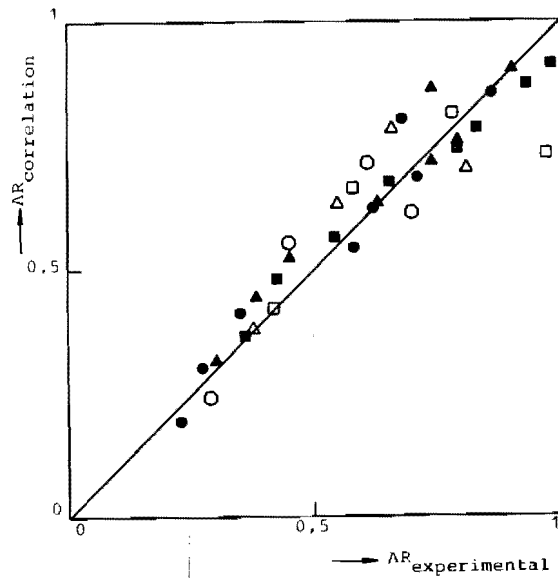
Fig. IV-8. Comparison of aroma retention of n-alcohols calculated from correlations, and experimentally observed values for the slab drying of aqueous maltodextrin solutions, as reported in this thesis.

	C_1	C_3	C_5
20 ^{O}C	O	△	□
30 ^{O}C	●	▲	■

Experiments of Rulkens (8)

Rulkens performed studies of the drying rate and aroma loss as functions of time during drying slabs of aqueous maltodextrin solutions, using n-alcohols as model aroma components. A comparison will be made between his experimental data for gelled slab and calculations with the correlation method. As final aroma retention data from his experiments, the averages of the aroma retention after t_c were taken. In fig. IV-9 the curves represent the predictions from the correlations, and the points represent Rulkens' experimental observations. From these figures it can be concluded that in general good agreement exists between predicted and experimental values.

Experiments of Menting (9)

Menting experimentally studied the retention of acetone in drying gelled slabs of aqueous maltodextrin solutions, and reported data on the dependence of the acetone retention on the relative humidity of the drying air. Taking the experimentally determined value of the acetone diffusion coefficient D_{aa} at the initial water concentration, and determining the length of the constant-rate period from recorder readins, he calculated acetone retention also from the simplified model, as given in III.3. He showed that these simplified calculations gave good agreement with his
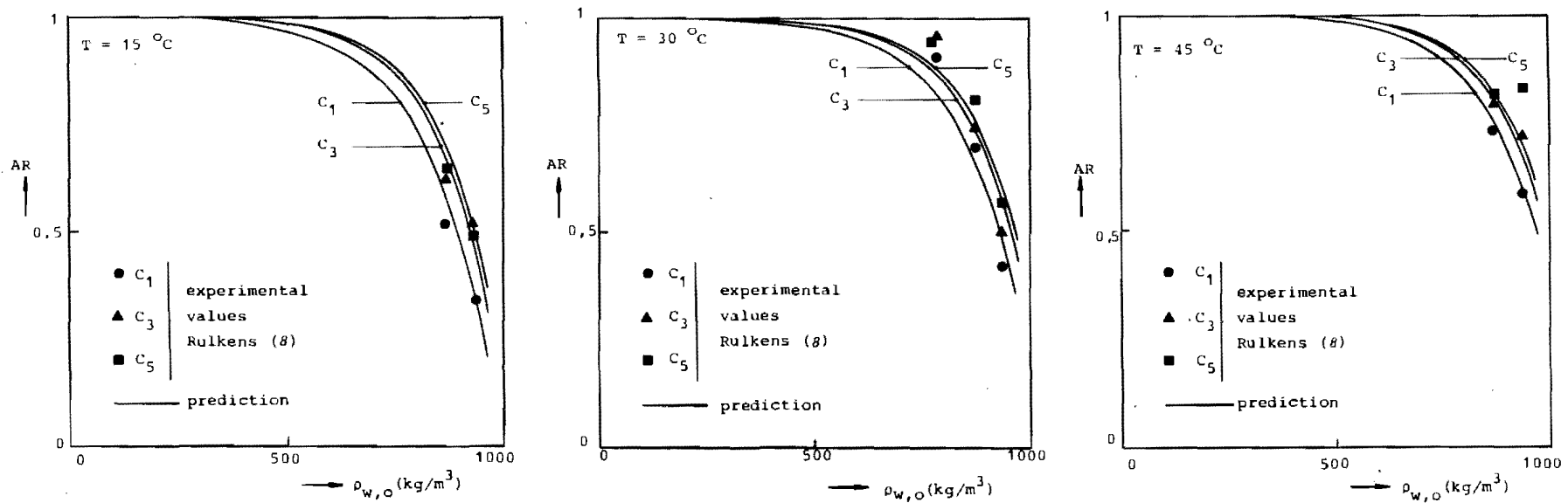
Fig. IV-9. Comparison of predicted values of aroma retention, as obtained from correlations and correlation constants in this thesis, with experimental values of Rulkens (8), for the drying of gelled slabs of aqueous maltodextrin solutions with lower n-alcohols as model aroma components.

experimental observations. In the present study the length of the
constant-rate period for his experimental conditions was cal-
culated with the correlation method of Chapter III and the con-
stants given in this chapter. Using the same diffusion coefficient
as Menting, the full line in fig. IV-10 was obtained. As follows
from the good agreement between prediction and experimental va-
lues, the prediction of the length of the constant-rate period
was also for this case of good accuracy.
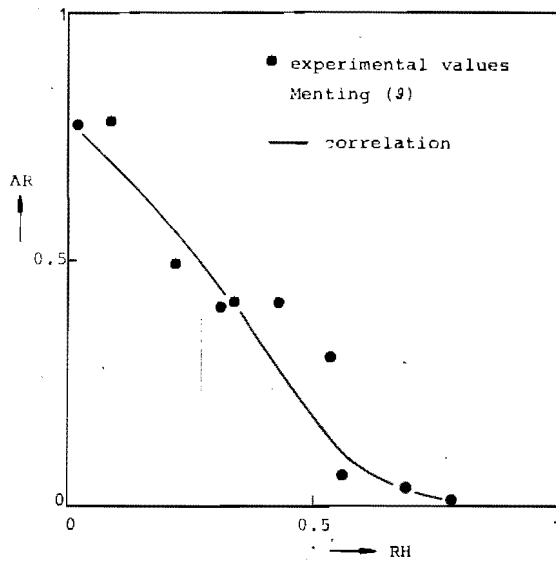
Fig. IV-10. Acetone retention
in drying gelled slabs of
aqueous maltodextrin solution
in dependence of the relative
humidity of the drying air.
Initial water concentration
750 kg/m^3, slab temperature
21,5 $^{\circ}$C. Comparison of predict-
ion method with experimentally
observed values of Menting (9).

From the calculations followed that for the conditions studied
by Rulkens (8) and in this thesis the slab behaved as infinitely
thick. The values of ε were at least 1.5 x the values of ε_{is},
and so it may indeed be expected that the error in ϕ_c is low.
In Mentings experiments ε_{is} is found for RH = 0.60, and thus
the maximum error in ϕ_c occurs at this point, where the aroma
retention is very low. For lower RH, and higher aroma retention
again $\varepsilon > 2\varepsilon_{is}$, and thus low error in ϕ_c can be expected. The
fact that good agreement is found between predicted and experi-
mentally observed values of AR in slab drying also indicates,
that the determination of the effective aroma diffusion coeffi-
cients has been accurate enough for practical purposes.

IV.4.2 Spray_drying

Rulkens and Thijssen ($7,8$) present data on the retention of n-
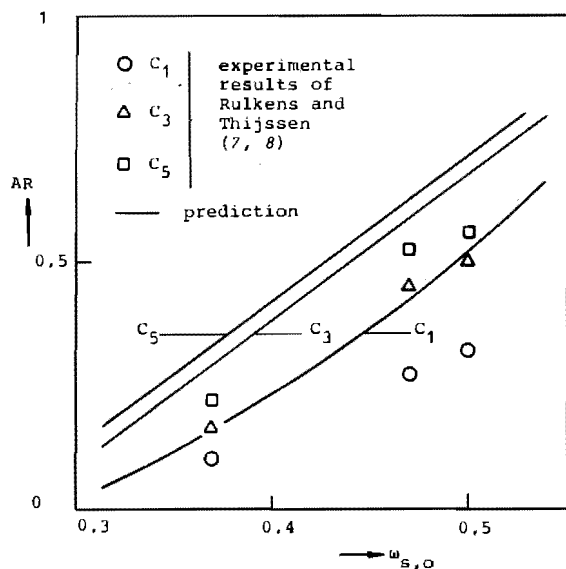
Fig. IV-11. Comparison between predicted and experimentally observed values of retention of n-alcohols in spray drying aqueous maltodextrin solutions.

alcohols in spray drying aqueous maltodextrin solutions in dependence on initial water concentration. Their conditions and apparatus will extensively be discussed in Chapter V. In this analysis it is assumed that the air in the spray drier was ideally mixed, which according to temperature measurements seems a reasonable approximation (8). As in the experimental set-up used by these authors large heat losses occur through the drier wall, the air outlet temperature is nearly independent of the amount of water evaporated. From a mass balance the outlet humidity can be determined. For the air inlet an absolute humidity of 0.01 kg/kg dry air was assumed, corresponding to 50% RH at 25 $^\circ$C. The wet-bulb temperature was read from the psychrometric chart, and the values of F_w and $D_{a,eff}$ were calculated. The value of ε was calculated, and subsequently ϕ_c and AR were determined according to the methods of Chapter III. In fig. IV-11 the predicted values are represented as solid lines, and the experimentally observed values as points. It can be seen that the predicted values of AR are higher than those observed experimentally. Several possible causes for deviations can be distinguished:

1. Error in ϕ_c due to intrinsic error of correlation method
2. Error in ϕ_c caused by the assumption of wet-bulb temperature (47 $^\circ$C) and thereby neglecting the effect of warming-up of the droplets from feed temperature (20 $^\circ$C)

3. Error in ϕ_c due to neglect of initial velocity effect
4. Different behaviour of the droplets from the model; this includes additional losses during the spray drying process, such as aroma loss during the very turbulent droplet formation, and crater formation upon overheating of the particles.

The contribution of 1. would be an underestimation of AR, as argumented earlier. However, for the conditions studied, $\varepsilon \approx 5\varepsilon_{is}$, so this effect can only be very small. The second effect would lead to an underestimation of ϕ_c, and consequently an overestimation of AR. From numerical calculations as mentioned in Chapter II, in which transient particle temperature was included, it followed that also this effect was small (27). The third cause will also lead to underestimation of AR, as shown in fig. II-9. Thus the discrepancies between the real drying behaviour of droplets and the theoretical model will be the main cause of the differences between prediction and experiment. The losses due to turbulent mass transfer upon droplet formation, and the loss due to crater formation and aroma evaporation from the particle interior can be considerable, as found by Rulkens and Thijssen (7,8). In Chapter V an extended discussion of these effects is given. Keeping in mind these extra factors that are responsible for aroma loss, the predicted values are again a reasonable estimate of the experimental results. It should be remarked here that also the much more sophisticated ternary diffusion model of Chapter II can by nature only predict aroma loss from the rigid sphere, and cannot account for extra losses.

IV.5 Discussion

IV.5.1 Experimental results and correlations

The results regarding the determination of the length of the constant-rate period are subjected to some scattering, for which the initial temperature history and the replacement of the samples may be the main cause. In spite of this inaccuracy the results are seen to obey the relations derived in Chapter III from the theoretical calculations, and can well be approximated by the

correlations.

The results of the effective diffusion coefficients show considerable scattering, as due to technical difficulties leading in some cases to inaccurate determinations of AR. Still the results can be reasonably approximated by the correlations of Chapter III, be it that no activation energy could be determined for each aroma component separately. It is preferable to perform improved aroma retention measurements, so as to obtain more accurate relations.

The predictions made with the correlations and correlation constants obtained from the measurements have been shown to be in good agreement with literature data for slab drying. In view of the additional losses occurring in spray drying, the predicted values of aroma retention in this process are also satisfactory estimates.

IV.5.2 Combined influences of process variables on aroma retention

In this paragraph the relative effects of process variables on aroma retention will be estimated, as based on the correlations. As a reference system the retention of n-propanol in aqueous maltodextrin solutions will be considered.

Let some standard situation be given, characterized by a given temperature T^S, a given water flux ε^S, and an initial water concentration $\rho_{w,o}^S$. Let R_o be fixed, and let only small variations of process variables be considered. Increasing the temperature at constant external conditions leads to an increase of water vapour pressure, characterized by an activation energy ΔH_v, and so for ε approximately holds:

$$\varepsilon = \varepsilon^S \exp\left[-\frac{\Delta H_v}{R}\left(\frac{1}{T} - \frac{1}{T^S}\right)\right]$$

$$\approx \varepsilon^S \exp\left[\frac{\Delta H_v}{R}\frac{(T-T^S)}{(T^S)^2}\right] \tag{IV-2}$$

Also external changes can lead to increase ε, as indicated by:

$$\varepsilon = \alpha \varepsilon^S \exp\left[\frac{\Delta H_v}{R} \frac{(T-T^S)}{(T^S)^2}\right] \tag{IV-3}$$

For F_w follows:

$$F_w = F_w^S \exp\left[f_{ww} \bar{V}_w (\rho_{w,o} - \rho_{w,o}^S) - \frac{E}{R}\left(\frac{1}{T} - \frac{1}{T^S}\right)\right]$$

$$\approx F_w^S \exp\left[f_{ww} \bar{V}_w (\rho_{w,o} - \rho_{w,o}^S) + \frac{E}{R} \frac{(T-T^S)}{(T^S)^2}\right] \tag{IV-4}$$

and for $D_{a,eff}$:

$$D_{a,eff} \approx D_{a,eff}^S \exp\left[f_{aw}(\rho_{w,o} - \rho_{w,o}^S)\bar{V}_w + \frac{E_a}{R} \frac{(T-T^S)}{(T^S)^2}\right] \tag{IV-5}$$

Let for the small variations in $\rho_{w,o}$ the effect on B_1 or B_2 be neglected. For the Fourier number now follows:

$$Fo_C = \frac{B.D_{a,eff}}{\varepsilon}$$

$$= Fo_C^S \exp\left[f_{aw} (\rho_{w,o} - \rho_{w,o}^S)\bar{V}_w + \frac{(E_a - \Delta H_v)(T-T^S)}{R\,(T^S)^2}\right] \tag{IV-6}$$

for flat water concentration profiles, and:

$$Fo_C = \frac{F_w D_{a,eff}}{\varepsilon^2}$$

$$= Fo_C^S \exp\left[(f_{aw} + f_{ww})(\rho_{w,o} - \rho_{w,o}^S)\bar{V}_w + \frac{(E + E_a - 2\Delta H_v)(T-T^S)}{R\,(T^S)^2}\right]$$

$$\tag{IV-7}$$

for the limiting case of the infinitely thick slab.

Substituting the data of n-propanol in aqueous maltodextrin solution as determined in this chapter (IV-6) and (IV-7) go over in:

$$Fo_C = Fo_C^S \exp\left[6.56(\rho_{w,o} - \rho_{w,o}^S)\bar{V}_w - \frac{220\,(T-T^S)}{(T^S)^2}\right] \tag{IV-8}$$

and

$$Fo_C = Fo_C^S \exp \left[15.43 (\rho_{w,o} - \rho_{w,o}^S) \bar{V}_w - \frac{2700(T-T^S)}{(T^S)^2} \right] \qquad \text{(IV-9)}$$

respectively.

From these relations immediately follows that an increase in temperature leads for both extreme situations to shorter Fo-time, and thus a decrease in aroma loss; the effect is much stronger for the semi-infinite slab approximation.
Also the effect of initial water concentration on Fo_C is much more pronounced for the semi-infinite case. In order to reduce the Fo_C number from Fo_C^S to $0.8 \, Fo_C^S$, the following separate influences follow at $T^S \approx 300$ K.

	$\rho_{w,o} - \rho_{w,o}^S$	$T - T^S$	α
flat profile	-33 kg/m^3	$+ 90$ K	$1,25$
semi-infinite slab	-14 kg/m^3	$+ 7$ K	$1,12$

Thus for the case of flat water concentration profiles the influence of temperature is very low, and increasing the retention of aroma can much more effectively be attained by an increase of initial dissolved solids concentration, or by changing the external conditions so that the flux is increased. For the extreme of the semi-infinite slab it follows that an increase of 7 K in temperature has the same effect as a decrease of 14 kg/m^3 in initial water concentration or an increase of the flux by a factor 1.12, accomplished by a change in the external conditions.

The above presented very simple analysis may for a given material provide a means of fast analysis of the steps to be taken in improvement of aroma retention.

V INVESTIGATION OF AROMA LOSSES IN TWO NEW DRYING PROCESSES FOR AROMA-CONTAINING LIQUID FOODS : DOUBLE-STAGE SPRAY DRYING AND EXTRACTIVE DRYING

V.1 Introduction

From experimental results on spray drying (7,8), slab drying (8) and the drying of single droplets (9) it can be concluded that during an important part of the process the transport of water and of aroma components is controlled by molecular diffusion processes, as described in Chapter II. Aroma loss during this part of the process can be calculated with the ternary diffusion model or with the correlation method presented in this thesis. From the studies mentioned it also followed that a considerable part of the aroma loss may occur during other parts of the process, such as droplet formation and internal circulation in the first stages of spray drying and loss by evaporation from the particle interior upon expansion and crater formation, caused by overheating of the particles near the end of the spray drying process (7,8,9). From a simplified theoretical model aroma losses during internal circulation of droplets, as caused by the high shear stress due to the high relative velocity of just-formed droplets with respect to the air in spray driers, were estimated to be in the order of 10 to 30%, over a distance of a few centimetres covered in a few milliseconds (27). Losses during formation of droplets with a pressure nozzle atomizer in the order of 10% were found experimentally (47). Aroma losses due to puffing may be seen to be in the order of 10-20%.

From these data clearly follows that optimization of aroma retention should be performed by minimization of the losses during the molecular diffusion period, which will be denoted as "*diffusional loss*", and minimization of the other losses, denoted by "*additional loss*". For the final aroma retention can be written:

$$AR = (1 - L_{diff})(1 - L_{add}) \qquad (V-1)$$

in which L_{diff} is the fractional diffusional loss, as occurring from the rigid particle, and L_{add} is the fractional additional loss. The fractional diffusional loss can be estimated by the correlation methods presented in the previous chapters; by analyzing the overall aroma loss, thus the additional loss can also be estimated. In this chapter the diffusional and additional losses, and the minimization of these losses, is investigated for two processes:

1. *double-stage spray drying*

   In this process the material is only partly dried in normal spray drying conditions, is then removed from the drying chamber and after-dried on a bed drier at lower temperature.

2. *extractive drying at room temperature*

   The droplets of the liquid food are dispersed in a hygroscopic liquid at room temperature, which liquid acts as dehydrating agent instead of air. Also in this process partial dehydration may be performed during extraction, and after-drying may be done in a bed drier with air (13).

In the double-stage spray drying it would in principle be possible to exclude overheating and thus aroma loss during puffing. In extractive drying at room temperature overheating effects are also excluded, and provided an appropriate extractant is used, also much higher rates of water removal can be achieved than in spray drying, thus also minimizing the diffusional loss.

V.2 Double-stage spray drying

V.2.1 Introduction

As stated before, after the constant-rate period the temperature of a drying droplet in air drying will increase due to the decrease of the interfacial water activity and consequently decreasing water evaporation rate. Thus the particle may reach almost air temperature. This was clearly shown experiment-

tally by Menting (9), and theoretically by van der Lijn (26,35). Apart from the mentioned aroma loss, the combination of high droplet temperature and intermediate water content in the particle centre may lead to detrimental chemical reactions, such as enzyme inactivation, lipid oxidation, proteine denaturation and Maillard reactions. Surveys of the typical water concentration and temperature dependence of these reactions are given by Karel (48,49) and Labuza (50). Also for not very heat-sensitive liquid foods high temperatures may be undesirable, as the expansion causes low bulk density of the product (51). Also several liquid foods such as orange and tomato juices cannot successfully be spray dried in pure form due to the very sticky character of the product, even at low water concentrations and slightly elevated temperatures (51,52) and either the use of additives or special drier arrangements are necessary.

To overcome these disadvantages, several modifications of the spray drying process have been proposed and developed recently (51,53-57), in which the drying process is accomplished in two or more stages. The first stage is the atomization and partial drying in a hot air chamber, in the second and possible following stages the product is after-dried in bed driers, such as moving-belt driers or fluidized bed driers, at lower temperatures. Extensive reviews of these processes and applications are given by Meade (57) and Kjaergaard (51). The latter author reports that in double-stage spray drying enzymes were dried with an inactivation of only 1-5%, compared to an inactivation of about 30% during single-stage spray drying.
Apart from the mentioned advantages of the controlled particle temperature another advantage of the multiple-stage drying processes is the high product hold-up in the final drying stages, thus requiring for this period only a very small apparatus volume compared to spray drying. Although at present multistage spray drying processes are in commercial use for several products, thus far no investigation has been made towards possible improvement of aroma retention with this technique. In this study the NIRO laboratory spray drier,

86

used by Rulkens and Thijssen $(7, 8)$ in their single-stage spray drying investigations, was modified for the study of double-stage spray drying and experiments were made under similar conditions as in the single-stage experiments.

V.2.2 Experimental apparatus and procedures

Feed preparation

As model food constituents again maltodextrin, water and n-alcohols were used. The feed solution was prepared by dissolution of the desired amount of maltodextrin in tap water at room temperature, after which the solution was filtered and pumped to the feed tank. Then the solution was heated to 85 $^{\text{O}}$C by means of a steam jacket around the feed tank; when that temperature had been reached, about 0.1 wt% on dissolved solids base of each of the aroma compounds was added.
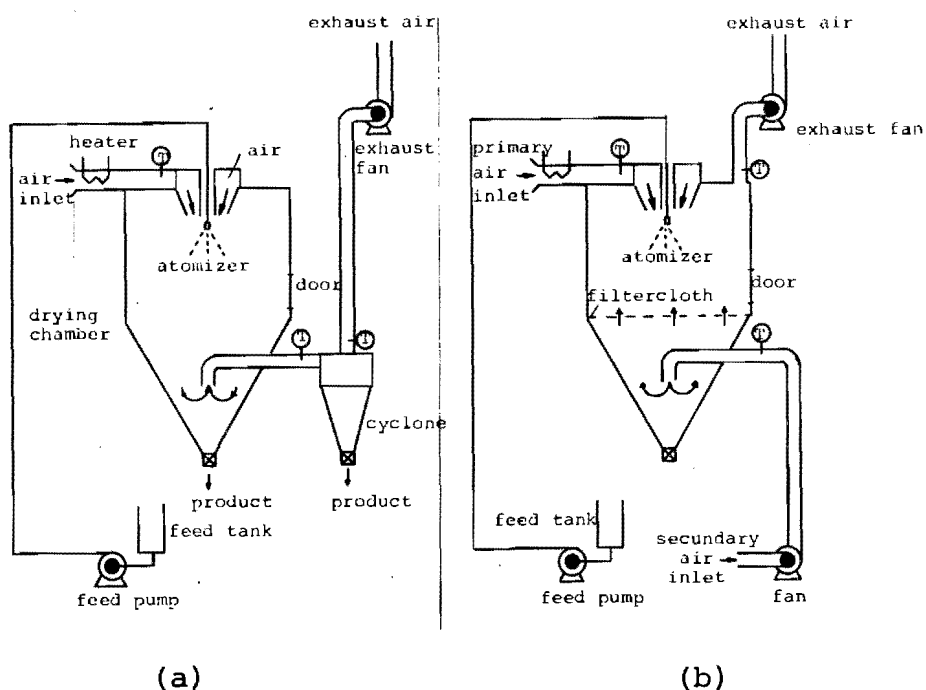
Fig. V-1. Diagram of experimental set-up for single-stage spray drying (a) and double-stage spray drying (b).

Drying apparatus and procedures

In fig. V-1 schematic diagrams of the single-stage spray drier
and of the modified spray drier are given. In the cylindrical
part, with a diameter of 2.5 m and a height of 2 m, hot air
was introduced tangentially through an annular opening around
the SPRAYING-SYSTEMS pressure nozzle atomizer. At the bottom
of the cylindrical part a linen filtercloth was placed, through
which air of approximately 40 ^{O}C was lead for the after-drying
of the particles. The flow rate of primary hot air was about
600 Nm^3/hr, the flow rate of secundary cold air was about 300
Nm^3/hr. The exhaust air was removed from the top of the drier
by means of an exhaust fan. Air inlet and outlet temperatures
were measured with thermocouples. The feed was pumped from the
feed tank by means of a positive displacement pump, at a rate
of 0.03 m^3/hr. In all drying experiments the apparatus was
accomodated by atomization of water. Product samples were
taken at least 15 min after the start of the drying process
at each condition by quickly placing a piece of fine metal
gauze on the filtercloth and collecting product for 5 min.

Bulk density was determined by vibrating a cylinder filled
with dried product for 10 min at a fixed frequency.
Moisture content was analyzed by heating the sample for 24 hrs
at 80 ^{O}C followed by 24 hrs at 120 ^{O}C. This procedure was used
for both feed liquid and dried samples.
Aroma retention was determined by vacuum distillation of the
samples, if necessary dissolved in water, followed by gaschro-
matographic analysis with n-butanol added as internal standard.
For a detailed description the reader is referred to Rulkens (8).

V.2.3 Results and discussion

Air temperature distribution

Temperature measurements without drying gave typical curves as
presented in fig. V-2. From this figure follows that the pri-
mary drying air forms a hot core of approximately 25 cm diame-
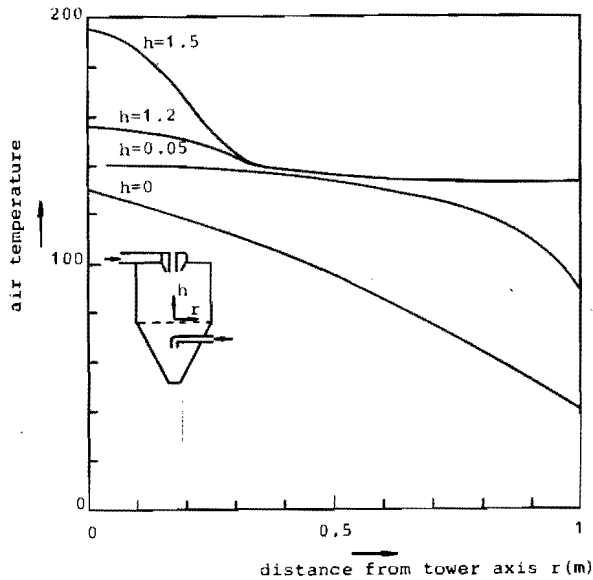
Fig. V-2. Temperature profiles measured in modified NIRO spray drier without drying. Primary air inlet temperature 235 $^{\circ}$C, secundary air inlet temperature 30 $^{\circ}$C.

ter and a height of about 30 cm. At half height of the cylindrical part the air temperature is nearly uniformly distributed. On the filtercloth however also a radial distribution is found. Probably the method of introduction of the secundary air causes an uneven flow distribution of secundary air, leading to preferent flow at larger radial distance. Therefore product samples were always taken at r ≃ 0.8 m.

For the air outlet in dependence on air inlet temperature, approximately the same relation was found as given by Rulkens (8), as illustrated in fig. V-3. Although a substantial part
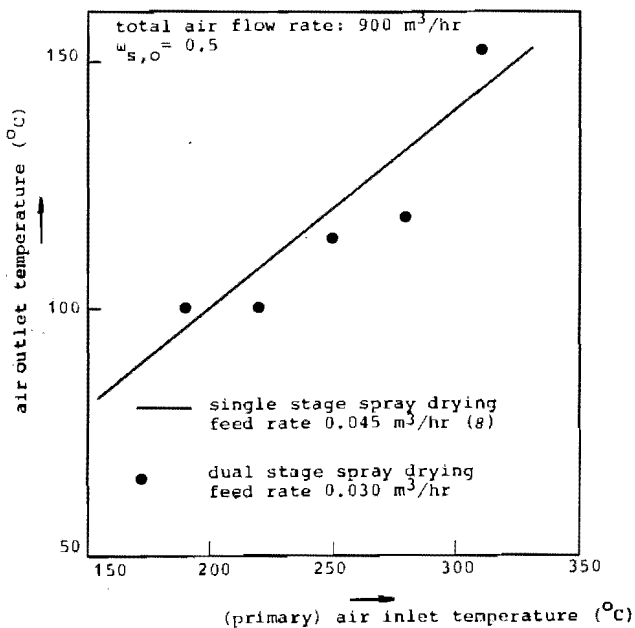
Fig. V-3. Relation between air outlet temperature and (primary) air inlet temperature for single-stage and dual-stage spray drying experiments.

of the air is fed at low temperature, this is compensated by
a decrease of about 30% in the area over which heat can be
lost to the exterior.

Bulk density

In fig. V-4 the bulk density of the product is given in relation
to the hot air inlet temperature. Agreeing with the observations
of Thijssen and Rulkens, the bulk density is seen to decrease
strongly with increasing air temperature, and approximately
bear the same relationship to the air inlet temperature as in
the case of the single-stage spray drying experiments. High
bulk densities are found for low primary air temperatures, at
which in the single-stage spray drying no dry product was ob-
tained.
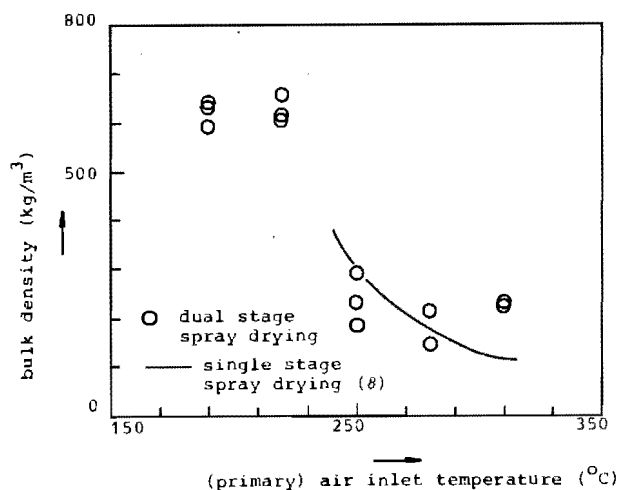
Fig. V-4. Bulk density of
spray dried maltodextrin
powder in relation to
(primary) air inlet tem-
perature.

Particle size and moisture content of the product

Analogous to the findings of Rulkens and Thijssen, it was found
that there was a large spread in particle size, but there was
an increase in particle size with increasing initial dissolved
solids content and increasing air inlet temperature, as observed
from microscope photographs (47). At low primary air inlet tem-
peratures hardly any particle expansion is observed but the
particles show generally to be shrunken.
No correlation could be found between particle moisture content
and process conditions.
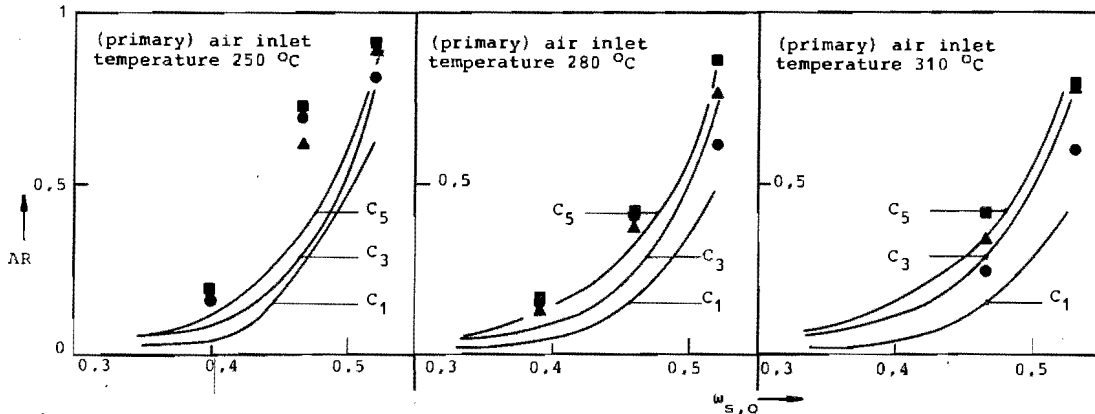
Fig. V-5. Aroma retention in dependence of initial dissolved
solids content in feed at different air inlet temperatures
in single-stage and double-stage spray drying.

● methanol, ▲ n-propanol, ■ n-pentanol in double-stage spray
drying at feed rate 0.030 m^3/hr; —— single-stage spray
drying ($8,58$) at feed rate 0.045 m^3/hr. Feed temperature 85 $^{\circ}$C.

Aroma retention

In fig. V-5 the effect of the initial dissolved solids content
on aroma retention is given for different hot air inlet tempe-
ratures. In the same diagrams data of Rulkens (8) and of
Herczog (58) are given. From the figure can be seen that aroma
retentions obtained for the double-stage drying experiments
are somewhat higher than the data obtained in the single-stage
drying process. As in the present experiments a lower feed rate
was used than in the experiments of Rulkens and Herczog, causing
lower air outlet humidity and thus higher water evaporation
rate, on the basis of final aroma retention data alone no con-
clusions towards the merits of the dual-stage process can be
drawn. A better comparison of both processes is obtained if
the aroma loss is split up into the diffusional loss and the
additional loss, and if additional losses are compared. For the
diffusional loss L_{diff} an estimate was made by means of the
correlations of the foregoing chapters. For this estimation it
was assumed that the droplets remained at wet-bulb temperature
form the beginning of the "rigid-sphere" or "diffusional" period,
and that Sh = Nu = 2. It is clear that due to the real feed

temperature of 85 $^{\circ}$C and the high initial velocities of the droplets, the diffusional loss L_{diff} will be overestimated and thus L_{add} will be underestimated. The data can however be used for the comparison of the additional losses in both drying techniques. In fig. V-6 the calculated additional loss factor, L_{add} is presented in relation to initial dissolved solids concentration at the various primary air inlet temperatures. It can be seen that L_{add} decreases strongly with increasing initial dissolved solids concentration. At high initial dissolved solids concentration an increase is found in L_{add} with increasing air temperature, while for low initial dissolved solids content there is virtually no effect in the single-stage process, but an increase is found for the double-stage process. Comparison of the additional loss factor L_{add} in both processes shows that the additional loss is about equal for high initial dissolved solids content, but for lower feed concentration is less in the double-stage drying process. This can be understood by the fol-

	C_1	C_3	C_5
single-stage	O	△	□
double-stage	●	▲	■
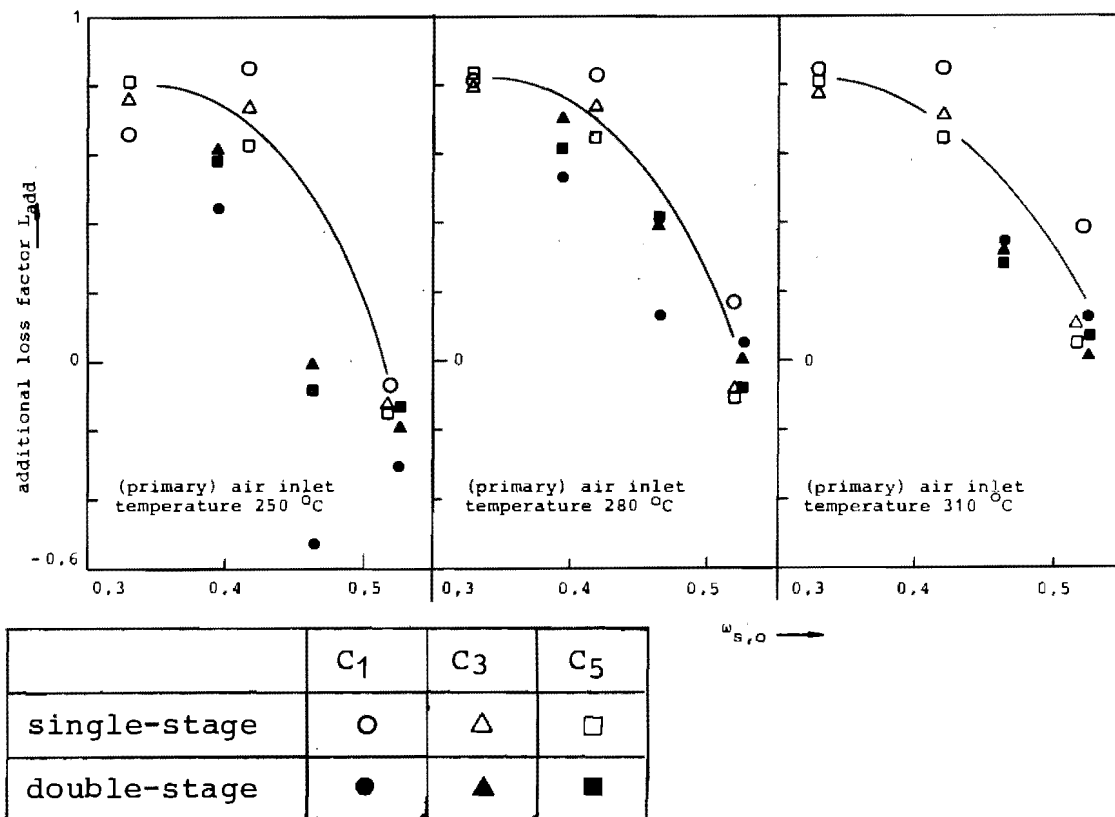
Fig. V-6. Additional loss factor in spray drying, in dependence on initial dissolved solids concentration and temperature.

lowing reasoning. For low initial dissolved solids concentrat-
ion aroma loss due to internal circulation streams just after
formation can be high because of the low viscosity of the drop-
lets (8). The constant-rate period is rather extended and warm-
ing-up is relatively slow, so that high temperatures are only
reached when the particles are nearly dry, thus limiting expans-
ion phenomena. At these low initial dissolved solids contents
thus the effect of double-stage drying will not improve very
much on aroma retention. At high initial dissolved solids con-
centration the major part of the loss is due to expansion and
crater formation, as circulation streams will be damped out
rapidly in the highly viscous droplets. As the length of the
constant-rate period is short at high initial dissolved solids
concentration, and temperature rise is fast, in the experiment-
al set-up used probably in both drying techniques expansion
and aroma loss occurs at only a short distance from the atomi-
zer, and thus no result of low temperature after-drying is
found. Thus the following conclusions can be drawn:

1. At low initial dissolved solids concentration the major-
   ity of the additional losses take place during the form-
   ation period and the internal circulation period. For
   minimization of the additional losses, attention should
   be paid to this first period. It is not clear whether
   larger or smaller droplets are preferable. Larger drops
   will be more influenced by shear stress, and thus L_{add}
   will increase with increasing droplet diameter. On the
   other hand the diffusional loss will decrease with in-
   creasing droplet diameter, because of the effect of the
   Re-number on continuous phase mass transfer, as found in
   chapter II.

2. At higher initial dissolved solids concentration the use
   of double-stage drying may indeed provide a decrease in
   the additional aroma losses, as in this case the major
   part of this loss is due to expansion phenomena upon over-
   heating. A necessary requirement is for this case that
   conditions are chosen in such a way that the particles
   reach the second stage before puffing. This requires

careful investigation of proper atomization conditions
and droplet size for a given liquid food at a given
initial dissolved solids concentration.

V.3 Extractive drying at room temperature

V.3.1 Introduction

From the foregoing it follows that in spray drying aroma reten-
tion can be optimized by using high initial dissolved solids
concentration and high driving force water transport, thus
decreasing L_{diff}, and by using special techniques for the mini-
mization of additional losses L_{add}. In practice however for
several food liquids limits are encountered to the dissolved
solids concentration obtained in concentration processes and
to air temperatures which may be applied. In that case theore-
tically possible aroma retentions in spray drying may not be
realized, and other drying techniques or combinations of drying
techniques should be used, such as freeze drying, slab drying
and slush drying (72). Freeze drying is an expensive operation,
while slab drying and slush drying are at present not economic-
al due to the low specific area employed in these processes.

Now an alternative way of processing may be that before drying
the aroma components are removed from the liquid food and are
concentrated. The bulk of the liquid food is then spray dried
without preconcentration, and the concentrated aroma is encap-
sulated in another process, in which high volatile retention
can be achieved. At the end of the processes both dry products
can be mixed again.

Recently microencapsulation processes, which generally consist
of the incorporation of an active material in an inert solid
medium, have attracted much interest and found very wide-spread
application, as was shown by Balassa and Brody (59), Balassa
and Weiss (60) and Nack (61). An extensive review of the appli-
cation of microencapsulation processes in the food industry
was given by Balassa (62). Although most of the applications
concern the encapsulation of discrete particles of droplets in

protecting capsules, an interesting aspect of the micro-encap-
sulation technique is the encapsulation of volatile aroma com-
ponents from aqueous solutions, which contain the volatiles
and the capsuleforming solid in the homogeneously dissolved
state. This aspect was patented among other things by the Bal-
chem Corp. (63). According to the Balchem patent aqueous solut-
ions of dextrin with 1% added pineapple aroma were dried by
dispersing them in polyethylene glycol with a molecular weight
ranging from 106 to 2000. The flavour retention was reported
to be good.

In the present study an investigation was made of the retention
of aroma compounds in model food solutions with PEG 400 as
extractant. The model solutions consisted of aqueous solutions
of dextrin, maltodextrin or mixtures of these carbohydrates
and methanol, n-propanol, and n-pentanol as model aroma com-
ponents. These aroma components were in all but one experiment
added in low concentrations.

V.3.2 Experimental

Extraction experiments

A schematic drawing of the experimental set-up is given in
fig. V-7. All experiments were carried out in a 1 litre tank,
equipped with 4 baffles and an 8-blade turbine impeller. The
maximum speed of the impeller motor was 1500 rpm. From a 100
ml perspex container to which air pressure could be applied
the feed solution flowed through a 0.4 mm needle, from the end
of which the droplets formed. Droplet size ranged from 0.2 to
2 mm, depending upon feed viscosity.

The feed liquid consisted of an aqueous solution of a mixture
of dextrin and maltodextrin, methanol, n-propanol and n-pentanol
were added in concentrations of 0.3 wt% on dissolved solids
base, except for one experiment. Waterfree PEG 400 was used as
extraction liquid; in each experiment about 55 ml of feed so-
lution was used and 1 litre of PEG. Extraction took place at
room temperature.
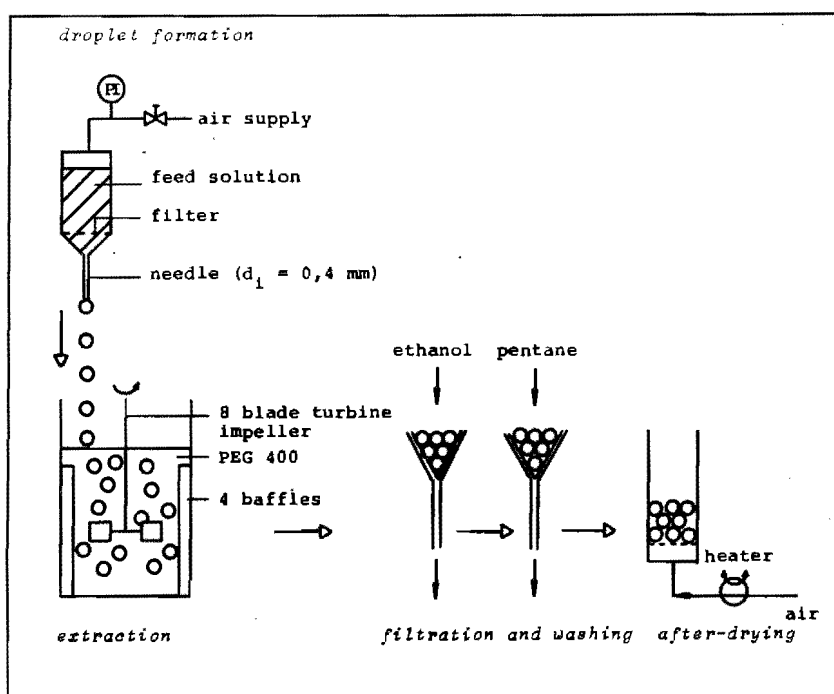
Fig. V-7. Diagram of the experimental set-up for extractive drying process.

After extraction for 30 min the product was filtered off and quickly washed first with dry ethanol to remove adhering PEG and subsequently with pentane to remove the ethanol. Then the product was placed in a small bed drier and dried with dry air for several hours at a temperature of about 30 ^{o}C. Aroma retention was measured by gaschromatographic determination of the amounts of aroma present in the feed liquid and in the product by the distillation method mentioned before.

The influence on aroma retention of the following process conditions was investigated:

1. dissolved solids composition: 0,25,50,75 and 100 wt% maltodextrin on solute basis; total dissolved solids concentration in feed solution 50 wt%.

2. dissolved solids concentration: 50 and 60 wt% total dissolved solids in feed, solute composition 75 wt% maltodextrin.

3. stirrer speed: 150 - 1500 rpm.

4. aroma concentration: in one experiment 15 wt% total

aroma was added to a 60 wt% dissolved solids feed with
a solute composition of 75% maltodextrin and 25% dextrin.
More detailed information is given by (64).

Transport properties

The following properties of PEG 400 were determined:
1. water vapour sorption isotherm, determined by a dessicator method with saturated salt solutions
2. water diffusion coefficient at low water concentration, determined by measuring the water content as a function of time after a sudden change in humidity over a layer of PEG
3. viscosity and density of PEG at low water concentration.

V.3.3 Results

Extraction experiments

1. Dissolved solids composition
In fig. V-8 the effect of the dissolved solids composition on aroma retention is shown at a total solute concentration of the feed of 50 wt%. With this solute concentration the alcohol retention attains a maximum at a solute composition of 75% maltodextrin and 25% dextrin. The retentions found with 100% maltodextrin are very low with respect to the optimum solute composition. Visual observation learned that at 50% solute concentration the droplets more or less retained their spherical shape upon entering the extraction liquid at up to 50 wt% maltodextrin on dry basis, whereas at higher ratios of maltodextrin to dextrin in the feed, deformation of the droplets occurred, which effect grew worse with increasing maltodextrin content, resulting in full distortion to threads at 100% maltodextrin. This is accompanied by a sharp decrease in viscosity of the feed liquid at maltodextrin fractions of more than 75%.

The deformation of the droplets upon contact with the PEG can be explained by the low interfacial tension between the two phases. For the system dextrin-PEG-water, Ryden and Albertson
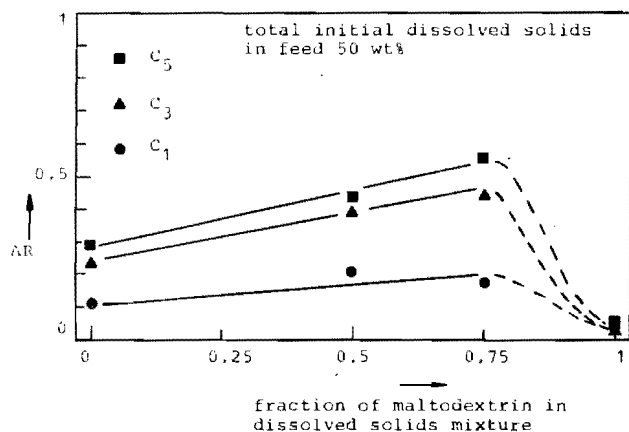
Fig. V-8. Experimental values of retention of n-alcohols as a function of composition of dissolved solids, for 50 wt% total dissolved solids during extractive drying with PEG 400

(65) reported values of the interfacial tension smaller than 0.1 dyne/cm. Thus a droplet can only remain spherical if its viscosity is high compared with the viscosity of the surrounding continuous phase.

The partial substitution of dextrin by maltodextrin has a positive effect on aroma retention, provided the viscosity remains high enough. Apparently the selectivity of the surface of the drying droplet is improved by the addition of maltodextrin. Probably the combination of the lower molecular carbohydrates with the high molecular dextrin results in a less open structure at the same water concentration, thus reducing the mobility of the aroma molecules.

2. Stirrer speed

From the above it can be concluded that a fair part of the aroma loss is due to droplet deformation (and distortion). At a constant maltodextrin fraction of 75 wt% on dissolved solids base the effect of stirrer speed on aroma retention was investigated for total solute concentrations of 50 and 60 wt% of the feed. The results are shown in fig. V-9. For the 50 wt% solution there is a definite drop in aroma retention with increasing stirrer speed, whereas at 60 wt% no influence was found. Apparently the droplets formed with the 60 wt% solution already have such a high viscosity, that the shear forces exerted on the droplet are not strong enough to induce deformation.

98
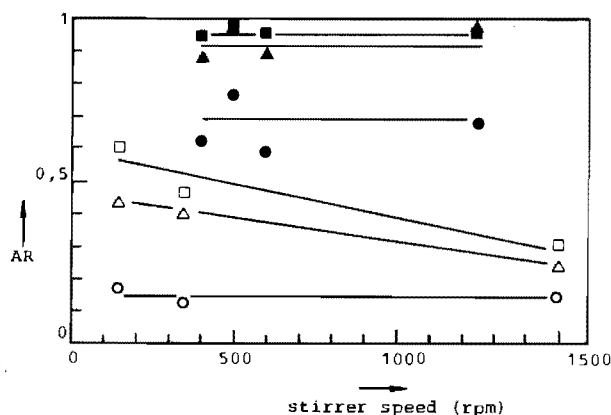
	C_1	C_3	C_5
$\omega_{s,o} = 0.50$	O	△	□
$\omega_{s,o} = 0.60$	●	▲	■

Fig. V-9. Experimentally observed retention of n-alcohols in extractive drying of aqueous solutions of a mixture of dextrin and maltodextrin (ratio 1 : 3), in dependence of stirrer speed.

3. Dissolved solids concentration in feed
The effect of the total solute concentration of the feed on aroma retention can also be derived from fig. V-9. At 60 wt% the retention of n-propanol and n-pentanol was 90% and 95% respectively, while the retention of methanol was about 70%. These values are much higher than those found for 50 wt% dissolved solids. The retention is not only higher because of less deformation of the droplets, but also because of the shorter time needed to attain selective permeability at the surface.

4 Aroma concentration
To a 60 wt% dissolved solids solution with a 3:1 ratio of malto-dextrin and dextrin in the solids an amount of 5 wt% on total dry basis of each aroma component was added. The retentions found were:
-methanol   31% (0.016 kg/kg on dry basis)
-n-propanol   59% (0.030 kg/kg on dry basis)
-n-pentanol   55% (0.028 kg/kg on dry basis)
The addition of the alcohols to the mixture reduced the dissol-

ved solids concentration to 55 wt%, which caused a drop in vis-
cosity, thus allowing a somewhat stronger deformation. Moreover
it is not likely that at such high alcohol concentrations the
selectivity of the "dry skin" is as high as at low concentrations.
An interesting aspect of this experiment is the absolute amount
of aroma retained in the product, which equalled a total aroma
content of 7.4 wt% on dry basis.

Transport properties

The *sorption isotherm* of polyethylene glycol was determined ex-
perimentally with the desiccator method. From this sorption
isotherm and the sorption isotherm of maltodextrin (fig. I-2)
the equilibrium curve between the two phases was calculated, as
given in fig V-10.
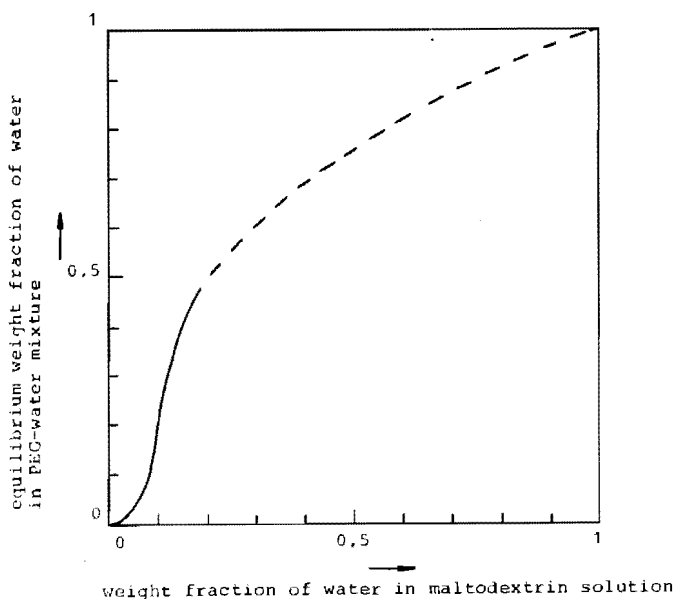
Fig. V-10. Experimentally
determined equilibrium
curve for water in PEG and
maltodextrin

The *diffusion coefficient of water* in PEG 400 as determined
from the initial slope of the water content vs the square root
of time after a sudden change in humidity was at low water con-
centrations equal to $D_w' = 2 \times 10^{-10}$ m^2/s.
The *viscosity* of PEG 400 was measured with a Brookfield visco-
simeter, and was equal to 80 cP at low water concentrations.
The *density* of PEG 400 at low water concentrations was about
1000 kg/m^3.

V.3.4 Discussion

The most important contribution to additional loss in the extractive drying experiments performed here is the deformation of the droplets if the feed viscosity is too low. For high dissolved solids content and high feed viscosity it is seen that also for extractive drying the selective diffusion theory applies as aroma retention increases with increasing dissolved solids concentration and with increasing molecular weight of the aroma components.

From the transport properties determined an estimation of the diffusional loss from a droplet of maltodextrin in the absence of deformation can be made. For the mass transfer to particles in stirred vessels, correlations have been presented by Barker and Treybal (66) and by Huige (67). From these correlations follows for water transport in PEG 400 to particles of 2 mm at a stirrer speed of 600 RPM, that Sh ≃ 80. Over the trajectory from 50 wt% water to 30 wt% water follows from fig. V-10 an average driving force of about 700 kg/m^3, for water transport from a maltodextrin droplet to dry PEG. Herewith follows ε = 1.1x10^{-8} m^2/s. From the correlations of Chapter III and IV now follows for the retention of methanol in a 50 wt% maltodextrin solution, that AR ≃ 0.975. The fact that also in the absence of droplet distortion methanol loss is still about 30% clearly confirms the conclusion that the selectivity of the mixture of dextrin and maltodextrin is much worse than that of pure maltodextrin, as was also seen from the effect of dissolved solids composition on aroma retention.

For optimum aroma retention thus high feed viscosities and high selectivities are required; a further investigation into the simultaneous realization of these two effects is necessary.

V.4 Conclusions

V.4.1 Spray drying

An analysis has been made from single-stage and double-stage

spray drying results, using the correlation methods described in earlier chapters of this thesis. From this analysis it has become clear that at low initial dissolved solids concentration in the feed the aroma loss predominantly takes during droplet formation and internal circulation, while at high initial dissolved solids concentration the evaporation of aroma due to particle expansion and puffing is the main cause of aroma loss. In the latter case under proper conditions double-stage spray drying may lead to increasing aroma retention.

V.4.2 Extractive drying

The main cause of aroma loss during extractive drying of model solutions at low feed viscosity is the deformation of the droplets. At high initial dissolved solids concentration high aroma retentions can be achieved even at high aroma concentration level. Improvements still can be achieved by proper choice of the composition of the dissolved solids. As the process is simple and is carried out at room temperature, extractive drying with PEG is in principle a very promising encapsulating technique for the food and flavour industries. Further study however is necessary regarding extraction times, the required ratio of extractant to product and the suitability of the process for various liquid foods and additives, as these factors determine the economics and praticability of the process.

102

VI GENERAL CONCLUSIONS

A generalized treatment of the diffusion equations describing
the loss of water and aroma components during the drying of
liquid foods, including similarity analysis, has lead to so-
phisticated models for drying of slabs, cylinders and spheres.
From a large number of computer simulations based on these mo-
dels, and from approximating models simple correlations have
been derived for the length of the constant-rate period and the
aroma loss during this period, in dependence on process variab-
les. Both from computer-generated data and from experimental
data is has been shown that these correlations can be used
successfully for the prediction of aroma retention under diffe-
rent process conditions from a limited number of simple slab
drying experiments.
Based on the insights of the selective diffusion theory, two
new drying processes, double-stage spray drying and extractive
drying, have been explored. The aroma loss in these processes
is split-up in the aroma loss during diffusion in the absence
of internal circulation streams, the "diffusional loss", and
aroma losses due to other causes, the "additional loss". From
estimations made of the diffusional loss by means of the cor-
relations, a good insight has been obtained into the other
factors influencing aroma loss, and suggestions for improvement
of these processes can be given. Both drying techniques seem
to be applicable for the drying of aroma containing liquid foods.

SUMMARY

The retention of volatile aroma components is an important qua-
lity requirement for the drying of many liquid foods. From pre-
vious investigations followed that the transport of both water
and aroma components during at least a large part of the drying
process is controlled by molecular diffusion. The aroma loss
during drying can be distinguished in a loss during this diff-
usion period, the diffusional loss, and additional losses.

In the underlying study first a generalized treatment is given
of the diffusion theory for liquid foods, including a similari-
ty analysis. The transport of water and dissolved solids can
be described by a binary diffusion model, the transport of aro-
ma components with a ternary diffusion model. Calculations
based on these models for the drying of slabs and of spherical
particles show good agreement with experimental observations
from literature, and are suitable for the quantitative descrip-
tion of drying rate and aroma retention in drying systems.

For the use of the above-mentioned models it is necessary to
know the concentration- and temperature dependence of diffusion
coefficients, and specialized calculation methods are required.
The determination of these quantities and the implementation
of the calculation programs is time-consuming. In order to cir-
cumvent these difficulties in this thesis a simplified method
is developed for the prediction of aroma retention. This method
is based upon the experimental observation that aroma loss
mainly takes place during the constant-rate period. Starting
from some approximating theoretical models and a large number
of numerically calculated results of the exact diffusion models,
correlations have been found between the length of the constant-
rate period and the aroma loss during this period on one hand,
and process variables on the other hand. Both from theoretical
and experimental investigations follows that it is possible to
predict with good accuracy the aroma retention in drying drop-

lets and slabs from data, obtained from a few very simple slab drying experiments. For the model system water-maltodextrin with the model aroma components methanol, n-propanol and n-pentanol correlation constants were determined.

Furthermore an experimental investigation was made of the aroma retention in two new drying processes : double-stage spray drying and extractive drying. From an analysis of the additional losses during double-stage spray drying follows that this technique can lead to improved aroma retention, especially for highly concentrated feed solutions. Extractive drying is a suitable incapsulation method, provided the feed viscosity is high enough, and the dissolved solids have a high selectivity for water transport at low water concentrations.

SAMENVATTING

Bij het drogen van vele vloeibare voedingsmiddelen is het behoud
van vluchtige geur- en smaakstoffen een belangrijke kwaliteits-
eis. Uit vroeger onderzoek is gebleken dat het transport van
zowel water als aromacomponenten tijdens tenminste een groot
gedeelte van het droogproces bepaald wordt door moleculaire dif-
fusie. Het aromaverlies bij drogen kan onderscheiden worden in
een verlies tijdens deze diffusieperiode, het diffusieverlies,
en additionele verliezen.

In de onderhavige studie wordt allereerst een gegeneraliseerde
behandeling gegeven van de diffusietheorie voor vloeibare voe-
dingsmiddelen, inclusief een gelijkvormigheidsanalyse. Het trans-
port van water en opgeloste stof kan met een binair diffusie-
model worden beschreven, het transport van aromacomponenten met
een ternair diffusiemodel. Berekeningen aan de hand van deze
modellen voor het drogen van vlakke lagen en van bolvormige
deeltjes tonen een goede overeenkomst met experimentele waar-
nemingen uit de literatuur, en zijn geschikt om kwantitatief
droogsnelheid en aromabehoud in drogende systemen te beschrijven.

Voor het werken met bovengenoemde modellen is kennis omtrent
concentratie- en temperatuurafhankelijkheid van diffusiecoëffi-
cienten noodzakelijk, en zijn speciale rekenmethoden vereist.
Het bepalen van deze grootheden en het implementeren van de
rekenprogramma's is een tijdrovende zaak. Ten einde deze moeilijk-
heden te ondervangen is in dit proefschrift een vereenvoudigde
methode ontwikkeld om aromabehoud te voorspellen. Deze methode
is gebaseerd op de experimentele waarneming dat aromaverlies
hoofdzakelijk optreedt gedurende de periode van constante droog-
snelheid. Uitgaande van enige benaderende theoretische modellen
en een groot aantal numeriek berekende resultaten van de exacte
diffusiemodellen, zijn correlaties gevonden tussen de lengte
van de periode van constante droogsnelheid en het aromaverlies
tijdens deze periode enerzijds, en procesvariabelen anderzijds.
Zowel uit theoretisch als experimenteel onderzoek blijkt dat

het mogelijk is via deze correlaties met goede nauwkeurigheid aromabehoud van drogende druppels en lagen te voorspellen met gegevens, verkregen uit enige zeer eenvoudige laagdroogexperimenten. Voor het modelsysteem water-maltodextrine met als model-aromacomponenten methanol, n-propanol and n-pentanol werden correlatieconstantes bepaald.

Experimenteel werd verder het aromabehoud onderzocht in twee nieuwe droogprocessen: meerzone-sproeidrogen en extractief drogen. Uit een analyse van de additionele verliezen tijdens het meerzone-sproeidrogen blijkt dat deze techniek kan leiden tot beter aromabehoud, speciaal voor hooggeconcentreerde voedingen. Extractief drogen is een geschikte incapsuleringsmethode, mits de voeding van voldoende hoge viscositeit is, en de opgeloste stof een hoge selectiviteit voor watertransport vertoont bij lage waterconcentraties.

APPENDIX 1

SPECIFICATIONS OF MALTODEXTRIN

The maltodextrin used in this study is the same as used by Rulkens (8), as denoted by him as $MD20_{II}$. The composition as given by the supplier, AVéBé, the Netherlands, is:

    1.5 wt% glucose

    4.5 wt% maltose

    9.3 wt% disaccharides

    6.0 wt% tetrasaccharides

    4.5 wt% pentasaccharides

  74.2 wt% polysaccharides

From density measurements it was found that the partial specific volume of maltodextrin in aqueous solution may be taken constant in good approximation, and equal to 6.211×10^{-4} m^3/kg. This value corresponds also with density data of Menting (9).

APPENDIX 2

COMPARISON OF THE POSTULATES OF THE GENERALIZED STEFAN-
MAXWELL EQUATION AND THE THEORY OF IRREVERSIBLE THERMODYNAMICS

1. The generalized Stefan-Maxwell equation

Let a system be considered consisting of n components. According
to the basis of the Stefan-Maxwell equation, the force F_i exert-
ed on one mole of species i by the other components is given
by (39):

$$F_i = \sum_{j=1}^{n} f_{ij} \, C_j (u_j - u_i) \tag{1}$$

in which:

f_{ij} = mutual friction coefficient between components i and j
($Nm^2 s/mol^2$)

C_j = molar concentration of j (mol/m^3)

u = molar velocity (m/s)

For the friction coefficients must hold $f_{ij} = f_{ji}$ (2)

The f_{ij} are generally dependent on the concentrations of all
components and on temperature.

In the absence of external forces and of pressure and tempera-
ture gradients the force F_i equals the gradient of the chemical
potential:

$$F_i = \nabla \mu_i = RT \, \nabla \ln A_i \tag{3}$$

Substitution of (3) in (1) and multiplication by C_i gives:

$$C_i \, \nabla \ln A_i = \sum_{j=1}^{n} \frac{f_{ij}}{RT} C_i C_j (u_j - u_i) = \sum_{j=1}^{n} \frac{Cf_{ij}}{RT} (x_i J_j - x_j J_i) \tag{4}$$

in which:

x_i = mole fraction of i

C = total molar density (mol/m^3)

J_i = molar flux of i $(mol/m^2 s)$

Defining $\underline{D}^m_{ij} = \dfrac{RT}{Cf_{ij}}$ and substitution in (4) leads to the genera-
lized Stefan-Maxwell equation:

$$C_i \ \nabla \ell n \ A_i = \sum_{j=1}^{n} \frac{1}{\underline{D}^m_{ij}} (x_i J_j - x_j J_i) \qquad (5)$$

as presented by Lightfoot et al (39).

2. Theory of irreversible thermodynamics

The application of the theory of irreversible thermodynamics on
the field of isothermal multicomponent diffusion was first work-
ed out by Onsager (31), and has been reviewed and verified expe-
rimentally by Miller (32,33). The following derivations are given
by Miller.

The entropy production σ per unit volume in a system not too far
from equilibrium, is given by

$$T\sigma = \sum_k J_k \ X_k \qquad (6)$$

in which the J_k are fluxes of for instance heat, mass or electri-
city, and the X_k are generalized forces, such as gradients of
temperature, chemical potential or electric potential.
Experimentally it has been found in many cases that

$$J_i = \sum_j L_{ij} \ X_j \qquad (7)$$

or

$$X_j = \sum_i R_{ji} \ J_i \qquad (8)$$

in which the L_{ij} and R_{ji} are called the phenomenological coeffi-
cients and resistance coefficients respectively. On the basis
of statistical mechanics Onsager (74) derived that for independ-
ent fluxes and forces the following relations hold:

$$L_{ij} = L_{ji} \tag{9}$$

and consequently

$$R_{ij} = R_{ji} \tag{10}$$

known as the Onsager Reciprocal Relationships (ORR).

For an isothermal, isobaric n-component system without external forces equation (6) goes over in:

$$T\sigma = \sum_{j=1}^{n} J_j \nabla\mu_j \tag{11}$$

in which the J_j are molar fluxes.

As the fluxes J_j and the gradients $\nabla\mu_j$ are not independent the ORR will not have to hold in general for $X_j = \nabla\mu_j$. For a volume fixed frame of reference holds:

$$\sum_{i=1}^{n} J_i \overline{V}_i^{-m} = 0 \tag{12}$$

and

$$\sum_{i=1}^{n} C_i \nabla\mu_i = 0 \tag{13}$$

in which $\overline{V}_i^{-m}$ is the molar specific volume (m^3/mol).

In order to obtain independent fluxes and forces the flux J_n and the gradient $\nabla\mu_n$ are expressed in the fluxes J_i and gradients $\nabla\mu_i$ of the other components, which then gives:

$$T\sigma = \sum_{j=1}^{n-1} J_j Y_j \tag{14}$$

and

$$J_i = \sum_{j=1}^{n-1} L_{ij} Y_j \tag{15}$$

in which

$$Y_j = - \nabla \mu_j - \frac{\bar{V}_j^m}{C_n \bar{V}_n^m} \sum_{k=1}^{n-1} C_k \nabla \mu_k$$

$$= - \sum_{k=1}^{n-1} (\delta_{jk} + \frac{C_k \bar{V}_j^m}{C_n \bar{V}_n^m}) \nabla \mu_k \tag{16}$$

in which δ_{jk} is the Kronecker delta $\delta_{jk} \begin{vmatrix} = 1 & \text{for } j=k \\ = 0 & \text{for } j \neq k \end{vmatrix}$

The chemical potential gradient can be written as a function of the n-1 independent concentration gradients:

$$\nabla \mu_k = RT \nabla \ln A_k = RT \sum_{k=1}^{n-1} (\frac{\partial \ln A_k}{\partial C_\ell}) C_{i, i \neq \ell} \nabla C_\ell \tag{17}$$

or

$$\nabla \mu_k = RT \sum_{\ell=1}^{n-1} A'_{k\ell} \nabla C_\ell \tag{18}$$

Equation (15) can now be written as:

$$J_i = - \sum_{j=1}^{n-1} \{ L_{ij} \sum_{\ell=1}^{n-1} B_{jk} \nabla C_k \} \tag{19}$$

with

$$B_{jk} = RT \sum_{\ell=1}^{n-1} (\delta_{jk} + \frac{C'_\ell \bar{V}_j^m}{C_n \bar{V}_n^m}) A'_{\ell k} \tag{20}$$

By the substitution

$$D_{ij} = \sum_{k=1}^{n-1} L_{ik} B_{kj} \tag{21}$$

follows:

$$J_i = - \sum_{j=1}^{n-1} D_{ij} \nabla C_j \tag{22}$$

3. Relations between the generalized Stefan-Maxwell equation and the irreversible thermodynamics description

Lightfoot et al (37) present a relation between the $\underline{D}_{ij}^m$ and the L_{ij} which is very complicated. Here an expression will be derived for the resistance coefficients R_{ij} in terms of the friction

114

coefficients f_{ij}.

Substitution of (1) and (2) in (16) gives for the independent forces Y_j:

$$Y_j = -\sum_{i=1}^{n} f_{ji}\left(J_i - \frac{J_jC_i}{C_j}\right) - \sum_{k=1}^{n-1} \frac{C_k}{C_n}\frac{\bar{V}_j^m}{\bar{V}_n^m}\left\{\sum_{i=1}^{n} f_{ki}\left(J_i - \frac{J_kC_i}{C_k}\right)\right\} \quad (23)$$

After some algebraic manipulation follows:

$$Y_j = -\sum_{i=1}^{n-1} f_{ji} J_i - f_{jn}J_n + \frac{J_j}{C_j}\sum_{i=1}^{n} C_i f_{ji} - \frac{\bar{V}_j^m}{C_n \bar{V}_n^m}\sum_{k=1}^{n-1} C_k$$

$$\left\{\sum_{i=1}^{n-1} f_{ki} J_i\right\} - \frac{\bar{V}_k^m}{C_n \bar{V}_n^m}\sum_{k=1}^{n-1} C_k f_{kn} J_n + \frac{\bar{V}_j^m}{C_n \bar{V}_n^m}\sum_{i=1}^{n-1} J_i$$

$$\left\{\sum_{k=1}^{n-1} f_{ik} C_k\right\} + \frac{\bar{V}_j^m}{C_n \bar{V}_n^m}\sum_{i=1}^{n-1} J_i f_{in} C_i \quad (24)$$

After expression of J_n in terms of the other fluxes, for the coefficient R_{ji} of J_i is found:

$$R_{ji} = - f_{ij} + \frac{\bar{V}_i^m}{\bar{V}_n^m} f_{jn} + \frac{\bar{V}_j^m}{\bar{V}_n^m} f_{in} - \frac{\bar{V}_j^m}{\bar{V}_n^m}\sum_{k=1}^{n-1} \frac{C_k}{C_n}(f_{ki} - f_{ik})$$

$$+ \frac{\bar{V}_j^m \bar{V}_i^m}{(\bar{V}_n^m)^2}\sum_{k=1}^{n-1} \frac{C_k}{C_n} f_{kn} + \frac{\delta_{ji}}{C_j}\sum_{k=1}^{n} C_k f_{jk} \quad (25)$$

As $f_{ij} = f_{ji}$ follows:

$$R_{ij} = - f_{ji} + \frac{\bar{V}_i^m}{\bar{V}_n^m} f_{jn} + \frac{\bar{V}_j^m}{\bar{V}_n^m} f_{in} + \frac{\bar{V}_j^m \bar{V}_i^m}{(\bar{V}_n^m)^2}\sum_{k=1}^{n-1} \frac{C_k}{C_n} f_{kn}$$

$$+ \frac{\delta_{ji}}{C_j}\sum_{k=1}^{n} C_k f_{jk} \quad (26)$$

For the straight coefficient follows:

$$R_{ii} = 2 \frac{\bar{V}_i^m}{\bar{V}_n^m} f_{in} + (\frac{\bar{V}_i^m}{\bar{V}_n^m})^2 \sum_{k=1}^{n-1} \frac{C_k}{C_n} f_{kn} + \frac{1}{C_i} \sum_{\substack{k=1 \\ k \neq i}}^{n} C_k f_{ik} \qquad (27)$$

It is easily verified that $R_{ji} = R_{ij}$, and so the postulates of the generalized Stefan-Maxwell equation are fully in agreement with the theory of irreversible thermodynamics.

APPENDIX 3

PHYSICAL DATA USED IN COMPUTER SIMULATIONS FOR SLAB DRYING
AND DRYING OF DROPLETS

physical property	mathematical expression	dimension
water diffusion coefficient at 25 $^{\circ}$C	$D_{ww}^{25}=\exp\{-14-14/(1+\rho_w\overline{V}_w)\}$	(m^2/s)
activation energy for water diffusion	$E_w=4+6\exp(-6\rho_w\overline{V}_w)$	$(kcal/mole)$
straight aroma diffusion coefficient at 25 $^{\circ}$C	$D_{aa}^{25}=\exp\{-10-17/(0.7+\rho_w\overline{V}_w)\}$	(m^2/s)
activation energy for aroma diffusion	$E_a=4+16\exp(-6\rho_w\overline{V}_w)$	$(kcal/mole)$
cross aroma diffusion coefficient	$D_{aw}'=D_{aa}\dfrac{\partial\ln H_a}{\partial\rho_w}-D_{ww}\dfrac{\overline{V}_w}{1-\rho_w\overline{V}_w}$	$(m^5/kg\ s)$
water activity	$A_w=1-\exp(-10\rho_w\overline{V}_w)$	$(-)$
aroma activity	$A_a=H_a\rho_a$ $H_a=20+100\exp(-7.5\rho_w\overline{V}_w)$	$(-)$ (m^3/kg)

Table 1. Physical properties used in computer simulation of drying of processes in chapter III.

physical property	mathematical expression	dimension
water diffusion coefficient at 25 $^{\circ}$C	$D_{ww}^{25}=1.7\times10^{-9}\exp\{-2/(0.3+\rho_w\overline{V}_w)\}$	(m^2/s)
activation energy for water diffusion	$E_w=10-6\rho_w\overline{V}_w$	$(kcal/mole)$
straight aroma diffusion coefficient at 25 $^{\circ}$C	$D_{aa}^{25}=1.7\times10^{-9}\exp\{-0.4/(0.3+\rho_w V_w)\}$	(m^2/s)
activation energy for aroma diffusion	$E_a=12-8\rho_w V_w$	$(kcal/mole)$
cross aroma diffusion coefficient	see table 1	
water activity	see table 1	
aroma activity	see table 1	

Table 2. Physical properties used for simulation of slab-drying by Kerkhof et al (20) and in chapter II and III of this thesis

physical property	mathematical expression	dimension
water diffusion coefficient at 25 °C	$D_{ww}^{25}=\exp(-21.606-17.938\ X_s)$ [1]	(m^2/s)
activation energy for water diffusion	$E_w=4.5791+23.603\ X_s$ [1]	$(kcal/mole)$
straight aroma diffusion coefficient at 25 °C	$D_{aa}^{25}=\exp(-20.944+7.601\ X_s^2 - 33.256\ X_s)$	(m^2/s)
activation energy for aroma diffusion	$E_a=4.5 + 34.312\ X_s$	$(kcal/mole)$
Stefan aroma diffusion coefficients	Eq. (II-12) and $\underline{D}_{aw}=10\underline{D}_{as}$	(m^2/s)
water activity	$A_w=X_w\exp(-4.49X_s^2+5.53X_s^3)$ [1]	$(-)$
aroma activity	see table 1	

[1] for system maltose-water according to van der Lijn (*35,43*)

X_s, X_w=mole fraction of dissolved solids and water respectively

Table 3. Physical properties used for simulation of slab drying (this thesis) and droplet drying by Kerkhof and Schoeber (*27,22,28*).

T (K)	$\rho_{w,o}$ (kg/m^3)	R_o (m)	k' (m/s)	ε (m^2/s)	ϕ_c (s/m^2)	B_1 (-)	N_{pp} (-)	AR (-)	$D_{a,eff}$ (m^2/s)
298	800	10^{-3}	0.04	9.17×10^{-10}	3.39×10^8	0.733	0.42	0.82	7.5×10^{-11}
298	500	10^{-3}	0.01	2.29×10^{-10}	2.45×10^8	0.333	0.17	0.951	7.7×10^{-12}
318	800	10^{-3}	0.04	2.61×10^{-9}	8.54×10^7	0.733	0.30	0.887	1.2×10^{-10}

Table 1 Simulation of drying slabs. Physical properties from Appendix 3, table 2. Gas phase bulk humidity in all cases equal to zero.

correlation for ϕ_c	correlation for $D_{a,eff}$
$F_w^o = 6.03 \times 10^{-9}$ m^2/s	$D_a^o = 2.98 \times 10^{-10}$ m^2/s
$E = 6749$ cal/mole	$E_a = 4441$ cal/mole
$f_{ww} = 10.34$	$f_{aw} = 7.59$

Table 2 Correlation constants for data in table 1

$\rho_{w,o}$ (kg/m³)	F_w (m²/s)	B_1	$D_{a,eff}$ (m²/s)	ε_{is} (m²/s)
500	1.28×10^{-11}	0.333	7.7×10^{-12}	3.84×10^{-11}
600	3.60×10^{-11}	0.467	1.64×10^{-11}	7.71×10^{-11}
700	1.01×10^{-10}	0.600	3.39×10^{-11}	1.68×10^{-10}
800	2.85×10^{-10}	0.733	7.21×10^{-11}	3.89×10^{-10}
900	8.02×10^{-10}	0.867	1.53×10^{-10}	9.25×10^{-10}

$RH^b = 0$ $\varepsilon = 2.29 \times 10^{-10}$ m²/s				$RH^b = 0,6$ $\varepsilon = 9.185 \times 10^{-11}$ m²/s		
$\rho_{w,o}$ (kg/m³)	relation for ϕ_c	ϕ_c (10^8 s/m²)	AR	relation for ϕ_c	ϕ_c (10^8 s/m²)	AR
500	(III-11)	2.44	0.95	(III-11)	15.2	0.88
600	(III-11)	6.86	0.88	(III-11)	42.8	0.70
700	(III-11)	19.3	0.71	(III-17)	65.4	0.47
800	(III-17)	32.0	0.46	(III-17)	79.9	0.20
900	(III-17)	37.9	0.19	(III-17)	94.5	0.02

Table 3   Prediction of the length of the constant-rate period and of aroma retention for drying slabs with correlation constants from table 2. Initial slab thickness $R_o = 10^{-3}$ m, gas phase mass transfer coefficient $k' = 10^{-2}$ m/s, slab temperature 25 °C.

T(K)	$\rho_{w,o}$ (kg/m³)	R_o (m)	k' (m/s)	ε (m²/s)	ϕ_c (s/m²)	B_1	N_{pp}	AR	$D_{a,eff}$ (m²/s)
298	700	10^{-3}	0.01	2.21×10^{-10}	8.94×10^8	0.42	0.47	0.484	2.35×10^{-10}
323	700	10^{-3}	0.01	8.00×10^{-10}	1.50×10^8	0.42	0.28	0.680	5.32×10^{-10}
298	900	10^{-2}	0.01	2.28×10^{-9}	1.45×10^8	0.81	0.41	0.568	9.98×10^{-10}

Table 4. Results of three slab drying simulations by computer. Physical constants as given in Appendix 2, table 3

correlation for ϕ_c	correlation for $D_{a,eff}$
$F_w^o = 5.12 \times 10^{-11}$ m²/s	$D_a^o = 7.03 \times 10^{-8}$ m²/s
$E = 6023$ cal/mole	$E_a = 6429$ cal/mole
$f_{ww} = 14.22$	$f_{aw} = 7.26$

Table 5. Correlation constants determined from data of table 4

APPENDIX 5

RESULTS OF SLAB DRYING EXPERIMENTS

Notation in the tables:

$\omega_{w,o}$	=	initial weight fraction of water
$\rho_{w,o}$	=	initial water concentration
T_o	=	stationary slab temperature
T_a	=	air temperature
W_o	=	initial weight of slab
R_o	=	initial slab thickness
$j_{w,o}^i$	=	stationary water flux determined from drying of agar-agar solutions
a	=	rate of slab temperature increase after stationary period
t_c	=	length of constant-rate period
AR	=	aroma retention
C_1, C_3, C_5	=	reference to methanol, n-propanol and n-pentanol respectively
N_{pp}	=	profile penetration number (Eq. (III-35))
$D_{a,eff}$	=	effective aroma diffusion coefficient
F_w	:	see Eq. (III-11)

nr	$\omega_{w,o}$	$\rho_{w,o}$ (kg/m^3)	T_o (°C)	T_a (°C)	W_o (10^{-3}kg)	R_o (10^{-3}m)	$j^i_{w,o}$ (10^{-4} kg/sm^2)	a (10^{-3} °C/s)	t_c (s)	AR c_1	AR c_3	AR c_5	N_{pp}
1a - 1	0.910	946	20.6	34.0	2.0893	2.84	3.28	1.0	4758	0.30	0.30	0.34	0.60
1a - 2	0.910	946	20.2	34.0	1.9923	2.71	3.28	1.0	3810	0.22	0.32	0.40	0.51
1a - 3	0.910	946	20.3	34.0	2.0586	2.80	3.28	1.0	3600	0.18	0.27	0.35	0.46
1b - 1	0.910	946	20.4	35.0	2.0113	2.74	4.92	1.4	1440	0.41	0.49	0.57	0.28
1b - 2	0.910	946	20.8	35.0	1.9617	2.67	4.92	1.5	1710	0.33	0.43	0.53	0.35
1b - 3	0.910	946	20.4	35.0	2.0133	2.74	4.92	1.7	1530	0.31	0.44	0.51	0.30
2a - 1	0.853	903	20.5	35.0	2.0281	2.71	4.78	1.7	1230	0.60	0.63	0.65	0.26
2a - 2	0.853	903	20.5	35.0	2.0635	2.76	4.78	1.7	1140	0.56	0.63	0.66	0.24
2b - 1	0.853	903	20.5	35.0	2.0778	2.78	3.05	0.9	3630	0.25	0.36	0.41	0.48
2b - 2	0.853	903	20.5	35.0	2.0598	2.75	3.05	0.8	3426	0.27	0.38	0.43	0.45
2b - 3	0.853	903	20.5	35.0	2.0875	2.79	3.05	0.8	3138	0.30	0.40	0.43	0.41
3a - 1	0.780	850	20.8	33.8	2.1984	2.85	3.85	2.3	1620	0.58	0.74	0.76	0.29
3a - 2	0.780	850	20.9	34.3	2.2150	2.87	3.85	3.0	1356	0.65	0.74	0.78	0.24
3a - 3	0.780	850	20.6	34.9	2.1711	2.82	3.85	2.8	1212	0.63	0.74	0.83	0.22
3b - 1	0.780	850	19.8	32.9	2.1509	2.79	4.64	3.8	762	0.73	0.80	0.86	0.17
3b - 2	0.780	850	19.9	32.7	2.1503	2.79	4.64	3.9	918	0.71	0.80	0.84	0.20
3b - 3	0.780	850	20.0	32.5	2.1277	2.76	4.64	4.1	852	0.68	0.77	0.80	0.19
4a - 1	0.619	724	20.5	33.0	2.3508	2.84	2.95	6.5	600	--	--	--	0.12
4a - 2	0.619	724	20.5	33.0	2.3218	2.81	2.95	6.5	564	0.68	0.74	0.93	0.11
4b - 1	0.619	724	20.5	34.0	2.3885	2.89	3.67	7.5	630	--	--	--	0.15
4b - 2	0.619	724	20.5	34.0	2.4310	2.94	3.67	7.5	594	0.70	0.77	0.98	0.14
5 - 1	0.602	710	20.1	33.9	2.2758	2.73	4.05	10.4	378	0.87	0.92	0.99	0.11
5 - 2	0.602	710	20.0	33.5	2.3420	2.81	4.05	10.0	378	0.92	0.96	0.98	0.11
5 - 3	0.602	710	20.3	33.5	2.2224	2.66	4.05	8.3	366	0.93	0.94	0.98	0.11

Table 1. Results of slab-drying experiments at 20 °C.

nr	$\omega_{w,o}$	$\rho_{w,o}$ (kg/m^3)	T_o ($^{\circ}$C)	T_a ($^{\circ}$C)	W_o (10^{-3}kg)	R_o (10^{-3}m)	$j^i_{w,o}$ (10^{-4} kg/sm^2)	a (10^{-3} $^{\circ}$C/s)	t_c (s)	AR c_1	AR c_3	AR c_5	N_{pp}
6a - 1	0.896	932	29.8	57.5	2.0688	2.81	5.08	1.9	2130	0.35	0.42	0.45	0.44
6a - 2	0.896	932	28.8	57.5	2.0804	2.83	5.08	1.6	2484	--	--	--	0.50
6a - 3	0.896	932	28.8	57.5	2.1363	2.91	5.08	2.2	2148	0.22	0.32	0.39	0.42
6b - 1	0.896	932	30.8	60.0	2.0588	2.80	8.94	3.6	900	0.48	0.57	0.60	0.32
6b - 2	0.896	932	30.3	60.0	2.0895	2.84	8.94	3.7	996	0.42	0.52	0.55	0.35
7a - 1	0.756	832	30.8	57.5	2.1562	2.77	5.08	8.3	828	--	--	--	0.21
7a - 2	0.756	832	30.1	57.5	2.2282	2.87	5.08	8.3	702	--	--	--	0.17
7a - 3	0.756	832	29.7	57.5	2.1810	2.80	5.08	8.3	660	0.70	0.81	0.97	0.17
7b - 1	0.756	832	30.5	60.0	2.1604	2.87	8.94	21.0	270	--	--	--	0.12
7b - 2	0.756	832	29.3	60.0	2.1042	2.71	8.94	21.0	390	--	--	--	0.17
7b - 3	0.756	832	29.3	60.0	2.2434	2.89	8.94	21.0	480	--	--	--	0.21
8 - 1	0.680	774	30.6	44.6	2.2028	2.74	4.71	8.3	585	0.63	0.70	0.79	0.16
8 - 2	0.680	774	30.2	44.5	2.1982	2.73	4.71	8.0	633	--	--	--	0.18
8 - 3	0.680	774	30.7	44.6	2.1744	2.70	4.71	6.2	615	--	--	--	0.17
8 - 4	0.680	774	31.1	44.5	1.9779	2.46	4.71	6.3	624	0.63	0.65	0.78	0.19
8 - 5	0.680	774	30.3	44.9	2.3050	2.87	4.71	7.3	597	0.59	0.64	0.77	0.16

Table 2. Results of slab-drying experiments at 30°C.

nr	$\rho_{w,o}$ (kg/m^3)	T ($^{\circ}$C)	F_w (10^{-10} m^2/s)
1	942	20	3.84
2	903	20	3.12
3	851	20	1.98
4/5	724/710	20	0.60
6	932	30	5.94
7	832	30	2.00
8	774	30	1.35

Table 3. Experimentally determined F_w values from slab drying experiments of aqueous maltodextrin solutions.

nr	$\rho_{w,o}$ (kg/m^3)	T ($^{\circ}$C)	$D_{a,eff}$ $(10^{-10}$ m^2/s)		
			c_1	c_3	c_5
1a	942	20	9.67	7.79	6.23
1b	942	20	16.06	11.13	7.95
2a	903	20	8.74	6.78	5.89
2b	903	20	9.98	6.95	5.97
3a	851	20	6.57	3.09	2.01
3b	851	20	6.18	3.17	2.01
4a	724	20	11.03	7.28	0.53
4b/5	717	20	2.80	1.39	0.039
6a	932	30	15.26	11.44	9.57
6b	932	30	20.10	13.70	11.92
7a	832	30	7.64	3.07	0.076
8	774	30	14.2	10.84	4.54

Table 4. Effective aroma diffusion coefficients found from slab drying experiments for n-alcohols in aqueous maltodextrin solutions.

APPENDIX 6

DETERMINATION OF THE LENGTH OF THE CONSTANT-RATE PERIOD FROM SLAB DRYING EXPERIMENTS

During the period of constant slab temperature holds:

$$\gamma(T_a - T_o) = k'A(\rho_w'^{io} - \rho_w'^b)\Delta H_v \tag{1}$$

in which: γ = total heat transfer coefficient (J/sK)

T_a = air temperature (K)

T_o = stationary slab temperature (K)

A = slab surface area (m^2)

$\rho_w'^{io}$ = interfacial water concentration in gas phase at T_o (kg/m^3)

During heating-up the heat balance reads:

$$\gamma(T_a - T_o) = k'A(\rho_w'^i - \rho_w'^b)\Delta H_v + \overline{MC}_p \frac{dT}{dt} \tag{2}$$

in which: T = slab temperature (K)

$\overline{MC}_p$ = total heat capacity of slab and sample holder (J/K)

If a linear temperature increase may be assumed over the first part of the warming-up period:

$$\frac{dT}{dt} = a \tag{3}$$

it follows:

$$(T_a - T) = \frac{1}{\gamma}\{k'A(\rho_w'^i - \rho_w'^b)\Delta H_v + \overline{MC}_p a\} \tag{4}$$

For the interfacial gas phase water concentration can be written: $\rho_w'^i = A_w^i \rho_w'^*$ (5)

in which A_w^i = water activity at interface

$\rho_w'^*$= equilibrium gas phase water concentration with pure water at temperature T

As an approximation over the temperature range from 20 ^{o}C to 30 ^{o}C can be written:

$$\rho_w'^* = \alpha \exp(\lambda T_c) \tag{6}$$

with: $\alpha = 5.957 \times 10^{-3}$ kg/m^3

$\lambda = 0.0532$ ^{o}C^{-1}

$$T_c = \text{temperature in } {}^{\circ}C$$

For values of T not too far from T_o can be written:

$$\rho_w'^* = \rho_w'^{*O} + \frac{\partial \rho_w'^*}{\partial T} (T - T_o) \tag{7}$$

Combination of Eqs. (6) and (7) gives

$$\rho_w'^* = \rho_w'^{*O}\{1 + \lambda(T - T_o)\} \tag{8}$$

As from the sorption isotherm follows that for aqueous malto-dextrin solution the critical water concentration is independent of temperature, it follows that

$$\rho_w'^i = A_w^i \rho_w'^{*O}\{1 + \lambda(T - T_o)\} \tag{9}$$

Substitution of $A_w^i = 0.9$, and combining Eqs. (1), (2) and (9) and re-arrangement gives:

$$T_c - T_o = \frac{0.1 \, k'A\rho_w'^{*O}\Delta H_v + \overline{MC}_p a}{\gamma + 0.9 \, k'A\rho_w'^{*O}\Delta H_v \lambda} \tag{10}$$

in which T_c is the temperature at which $A_w^i = 0.9$.

Sample calculation

For the experiments in Chapter IV the following values were used:

$$(\overline{MC}_p)_{copper} = 0.195 \quad cal/{}^{\circ}C = 0.82 \, J/K$$

$$(\overline{MC}_p)_{perspex} = 0.6 \quad cal/{}^{\circ}C = 2.52 \, J/K$$

$$(\overline{MC}_p)_{slab} = 2 \quad cal/{}^{\circ}C = 8.4 \, J/K$$

The heat of evaporation of water is given by

$$\Delta H_v = 585 \, cal/g \text{ at } 20 \, {}^{\circ}C = 2.460 \times 10^6 \, J/kg$$

$$\Delta H_v = 580 \, cal/g \text{ at } 30 \, {}^{\circ}C = 2.440 \times 10^6 \, J/kg$$

The slab surface area is equal to $A = 7.07 \times 10^{-4} \, m^2$. The gas phase bulk water concentration was $\rho_w'^b = 1.5 \times 10^{-3} \, kg/m^3$. From the experiments with agar-agar solutions followed for $T_a = 33.75 \, {}^{\circ}C$ and $T_o = 20.8 \, {}^{\circ}C$ a water vapour flux of $3.85 \times 10^{-4} \, kg/m^2 s$. As $\rho_w'^{*O} = 1.69 \times 10^{-2} \, kg/m^3$, it follows that $k' = 0.025 \, m/s$.

From relation (1) then follows $\gamma = 5.12 \times 10^{-2}$ J/sK. The rate of temperature increase follows from experimental data, and is for instance equal to 2.3×10^{-3} $^{\circ}$C/s. Substitution in Eq. (10) then gives:

$$T_c - T_0 = 1.15 \ ^{\circ}C$$

From the temperature readings now follows the value of t_c.

APPENDIX 7

THE SLAB WITH CONSTANT DIFFUSION COEFFICIENT, THICKNESS AND SURFACE FLUX (CDTF - MODEL)

For a slab with constant thickness R_o, constant diffusion coefficient D, and constant surface flux J, the diffusion equation with boundary conditions reads :

$$\frac{\partial \rho_w}{\partial Fo} = \frac{\partial^2 \rho_w}{\partial y^2} \tag{1}$$

$$Fo = 0 \qquad 0 \leq y \leq 1 \qquad \rho_w = \rho_{w,o} \tag{2}$$

$$Fo > 0 \qquad y = 0 \qquad \frac{\partial \rho_w}{\partial y} = 0 \tag{3}$$

$$y = 1 \qquad -\frac{\partial \rho_w}{\partial y} = JR_o/D \tag{4}$$

The solution of this equation, as given in terms of heat diffusion by Luikov (71) reads in terms of the interfacial concentration :

$$\frac{D(\rho_{w,o} - \rho_w^i)}{JR_o} = Fo + \frac{1}{3} - \frac{2}{\pi^2} \sum_{n=1}^{\infty} \frac{1}{n^2} \exp(-n^2 \pi^2 Fo) \tag{5}$$

which for large values of Fo goes over in

$$\frac{D(\rho_{w,o} - \rho_w^i)}{JR_o} = Fo \tag{6}$$

and thus in that case for $\phi = Fo/D$ follows :

$$\phi = \frac{(\rho_{w,o} - \rho_w^i)}{JR_o} \tag{7}$$

For short times the solution can be alternatively written as :

$$\frac{D(\rho_{w,o} - \rho_w^i)}{2JR_o} = Fo^{\frac{1}{2}} \sum_{n=1}^{\infty} \left\{ ierfc \frac{(n-1)}{Fo^{\frac{1}{2}}} + ierfc \frac{n}{Fo^{\frac{1}{2}}} \right\} \tag{8}$$

130

which for small values of Fo reduces to :

$$\frac{D(\rho_{w,o} - \rho_w^i)}{2JR_o} = Fo^{\frac{1}{2}} \text{ ierfc }(0) \tag{9}$$

For ϕ now follows :

$$\phi = \frac{1}{(\text{ierfc}(0))^2} \frac{D(\rho_{w,o} - \rho_w^i)^2}{4(JR_o)^2} \tag{10}$$

SYMBOLS USED

A	:	activity
		slab surface area
A'_{kl}	:	$\dfrac{\partial \ln A_k}{\partial C_l}\bigg\vert_{C_{i,i\neq l}}$
AR	:	aroma retention
B_1, B_2	:	constants in Eq. (III-17) and (III-24) respectively
B_{jk}	:	see appendix 2, Eq. (20)
Bi	:	Biot number
C	:	molar concentration
C_1, C_3, C_5	:	notation for methanol, n-propanol, n-pentanol respectively
C_d	:	drag coefficient
C_p	:	specific heat
D, $\underline{D}$	:	diffusion coefficient
D'_{aw}	:	modified diffusion coefficient, see Eq. (II-10)
E	:	activation energy
F_i	:	force on component i
F_w	:	coefficient in correlation of constant-rate period, see Eq (III-11)
$F_w^{\,o}$	:	correlation constant
Fo	:	Fourier number
H_a	:	modified activity coefficient
ΔH_v	:	heat of phase transformation
J	:	molar flux
L_{add}, L_{diff}	:	relative additional and diffusional loss respectively
$\underline{L}_{ij}$	:	Onsager phenomenological coefficient
$\overline{MC}_p$	:	total heat capacity of sample + sample holder
N_{pp}	:	profile penetration number, see Eq. (III-35)
Nu	:	Nusselt number
Pr	:	Prandtl number
R	:	radius, gas constant
R_{ij}	:	Onsager resistance coefficients

Re	:	Reynolds number
RH	:	relative humidity
Sc	:	Schmidt number
Sh	:	Sherwood number
T	:	temperature
$\bar{V}$	:	partial specific volume
WR	:	relative water retention
X	:	force
Y	:	independent force
		reduced specimen dimension

a	:	heating rate
d	:	diameter
f_{ij}	:	friction coefficient (appendix 2)
f_{aw}, f_{ww}	:	correlation constants
$\bar{g}$	:	gravity vector
j_i	:	mass flux of i
j_H	:	heat flux
		Chilton-Colburn j-factor
k'	:	mass transfer coefficient
r	:	distance coordinate
t	:	time
u	:	concentration per unit of dissolved solids volume
		molar velocity
v	:	velocity
v,w	:	transformed coordinates, see Eq.(III-4) and (III-5)
w_a	:	relative aroma concentration
$\bar{w}$	:	relative velocity
$|\bar{w}|$	:	absolute magnitude of $\bar{w}$
x	:	mole fraction
y	:	reduced distance coordinate

α	:	see Eq. (IV-3)
α	:	constant in appendix 6, Eq. (6)
α'	:	heat transfer coefficient
β	:	see Eq. (III-43)
γ	:	total heat transfer coefficient

γ	: see Eq. (II-23)
ε	: reduced flux parameter $j_{w,o}^{i} R_o \bar{V}_w$, see Eq. (III-12)
λ	: thermal conductivity
μ	: chemical potential
	: dynamic viscosity
ν	: geometry factor
ρ	: mass concentration, density
σ	: transformed coordinate based on dissolved solids
	: entropy production
ϕ	: reduced time t/R_o^2
ω	: weight fraction
∂	: differential operator
∇	: gradient

Subscripts

a	: aroma, air
c	: at critical water concentration
eff	: effective
f	: film
H	: heat
is	: at intersection point
ln	: logarithmic average
0	: at t = 0
	: stationary
s	: dissolved solids
w	: water

Superscripts

b	: bulk
i	: with respect to velocity of interface
	: at interface
m	: molar
o	: at T_o
s	: at standard situation, in section IV.5.2
	: with respect to dissolved solids velocity

v	: with respect to volume averaged velocity
'	: continuous phase
*	: referring to pure water

135

REFERENCES

1 Thijssen,H.A.C. & Rulkens,W.H.,(1968),De Ingenieurs,80,Ch45

2 Bomben,J.L. & Merson,R.L.,(1969),66th Ann. Meeting of the AIChE,November 16-20,Washington DC

3 Thijssen,H.A.C.,(1972),3[d] Nordic Aroma Syponsium,June 6-8, Helsinki

4 Chandrasekaran,S.K. & King,C.J.,(1971),Chem.Eng.Progr.Symp. Ser.,67,(108),122

5 Sivetz,M. & Foote,M.E.,(1963),"Coffee Processing Technology", AVI Publ.Comp.,Westport,Connecticut

6 Reineccius,G.A. & Coulter,S.T.,(1969),J.Dairy Sci,52,1219

7 Rulkens,W.H. & Thijssen,H.A.C.,(1972),J.Fd.Technol.,7,95

8 Rulkens,W.H.,(1973),Ph.D.Thesis,Eindhoven University of Technology

9 Menting,L.H.C.,(1969),Ph.D.Thesis,Eindhoven University of Technology

10 Menting,L.H.C., Hoogstad,B. & Thijssen,H.A.C.,(1970),J.Fd. Technol.,5,127

11 Chandrasekaran,S.K. & King,C.J.,(1972),AIChEJ,18,520

12 Chandrasekaran,S.K.,(1970),Ph.D.Thesis,University of California,Berkeley

13 Kerkhof,P.J.A.M. & Thijssen,H.A.C.,(1974),J.Fd.Technol.

14 Rulkens,W.H. & Thijssen, H.A.C.,(1972),J.Fd.Technol.,7,79

15 Flink,J,(1969),Ph.D.Thesis,Massachusetts Institute of Technology

16 Flink,J. & Karel,M.,(1969),66th Ann.Meeting of the AIChE, November 16-20,Washington DC

17 Flink,J. & Karel,M.,(1970),J.Fd.Sci.,35,444

18 Flink,J. & Karel,M.,(1970),J.Agr.Food Chem.,12,295

19 Thijssen,H.A.C.,(1965),Inaugural Address,Eindhoven University of Technology

20 Kerkhof,P.J.A.M.,Rulkens,W.H. & van der Lijn,J.,(1972), Int. Symp. on Heat and Mass Transfer Problems in Food Engineering, October 24-27, Wageningen, The Netherlands

21 Kerkhof,P.J.A.M. & Schoeber,W.J.A.H.,(1974),"Advances in Pre-Concentration and Dehydration of Foods",Ed.A.Spicer,Appl.Sci.

136

Publ.Ltd.,London,349

22 Schoeber,W.J.A.H.,(1973),M.Sc.Thesis,Dept.of Chemical Engineering,Eindhoven University of Technology (in Dutch)

23 Bomben,J.L.,Bruin,S.,Thijssen,H.A.C. & Merson,R.L.,(1973) Adv.Fd.Res.,20,1

24 King,C.J. & Massaldi,H.A.,(1974),IVth Int.Congress of Food Science and Technology,September 23-27,Madrid

25 Massaldi,H.A. & King,C.J.,(1974),J.Fd.Technol.

26 van der Lijn,J.,Rulkens,W.H. & Kerkhof,P.J.A.M.,(1972),Int. Symp. on Heat and Mass Transfer Problems in Food Engineering, October 24-27,Wageningen, The Netherlands

27 Rulkens,W.H. & Thijssen,H.A.C.(1969),Trans.Inst.Chem.Engrs. 47,T292

28 Kerkhof,P.J.A.M.,(1973),Paper presented at Informal Meeting at the VIth Int.Course on Freeze Drying,June,Bürgenstock

29 Chandrasekaran,S.K. & King,C.J.,(1972),AIChEJ,18,513

30 Menting,L.H.C.,Hoogstad,B & Thijssen,H.A.C.,(1970),J.Fd. Technol.,5,111

31 de Groot,S.R. & Mazur,P.,(1963),"Non-equilibrium Thermodynamics",North-Holland Publ.,Amsterdam

32 Miller,D.G.,(1959),J.Phys.Chem.,63,570

33 Miller,D.G.,(1960),Chem.Revs.,60,15

34 Crank,J.,(1964),"The Mathematics of Diffusion",University Press,Oxford

35 van der Lijn,J.,(1975),Ph.D.Thesis,Agricultural University of Wageningen (to be published)

36 Schoeber,W.J.A.H. & Kerkhof,P.J.A.M., to be published

37 Lightfoot,E.N.,Cussler,E.L. & Rettig,R.L.,(1962),AIChEJ, 8,708

38 Buttery,R.G.,Ling,L.C. & Guadagni,D.G.,(1969),J.Agr.Fd. Chem.,17,385

39 Hirschfelder,J.O.,Curtiss,C.F. & Bird,R.B.,(1954),"Molecular Theory of Gases and Liquids", Wiley, New York

40 Bird,R.B., Stewart,W.E. & Lightfoot,E.N.,(1960),"Transport Phenonema",3[d] ed,Wiley,New York

41 Ranz,W.E. & Marshall,W.R.Jr.,(1952),Chem.Engng.Prog.,48,141 and 173

42 Claassens,M.L.M.,(1972),M.Sc.Thesis,Dept. of Chemical Engin-
   eering,Eindhoven University of Technology,(in Dutch)

43 van der Lijn,J.,(1972),personal communication

44 Schoeber,W.J.A.H. & Kerkhof,P.J.A.M., to be published

45 Kerkhof,P.J.A.M.,(1974),IVth Int.Congress of Food Science
   and Technology, September 23-27, Madrid

46 Perry,J.H. & Chilton,E.H.(1973),"Chemical Engineers Hand-
   book",5th ed.,McGrawHill Inc.,New York

47 Goorden,J.J.P.M.,(1974),M.Sc.Thesis,Dept.of Chemical Engin-
   eering,Eindhoven University of Technology (in Dutch)

48 Karel,M.,(1974),"Advances in Preconcentration and Dehydra-
   tion of Foods",Ed. A. Spicer,Appl.Sci.Publ.Ltd.,London,45

49 Karel,M.,(1973),CRC Critical Reviews of Food Technology,3,
   329

50 Labuza,T.P.,(1972),CRC Critical Reviews of Food Technology,
   2, 217

51 Kjaergaard,O.G.,(1974),"Advances in Preconcentration and
   Dehydration of Foods",Ed.A.Spicer,Appl.Sci.Publ.LTD,
   London, 321

52 Lazr,M.E.,(1956),Fd.Technol.Chicago,10,129

53 Bljumberg,R.E. et al,(1970),German Pat.Appl.,nr. 1667205

54 Meade,R.E.,(1971),Food Engineering,July, 88

55 Utag GmbH,(1971),Voedingsmiddelentechnologie,2,(50),12

56 Okada,K. & Kato,F.,(1972),US Pat.,nr. 3.596.699

57 Meade,R.E.,(1973),Food Technology,December,18

58 Herczog,J.T.,(1971),M.Sc.Thesis,Dept.of Chemical Engineering,
   Eindhoven University of Technology (in Dutch)

59 Balassa,L.L. & Brody,J.(1968),Food Eng.,November,88

60 Balassa,L.L. & Weiss,H.(1967),Soap & Chem.Spec.,December,163

61 Nack,H.,(1969),J.Soc.Cosmetic Chemists,21,85

62 Balassa,L.L.,(1971),CRC Critical Reviews in Food Technology,
   2, 245

63 Balchem Corporation,(1971),Dutch Pat.Appl.,nr. 7015116

64 van Delft,H.W.,(1972),M.Sc.Thesis, Dept.of Chemical Engineer-
   ing,Eindhoven University of Technology (in Dutch)

65 Ryden,J. & Albertson,P.A.,(1971),J.Coll.and Int.Sci.,37,219

138

66 Barker,J.J. & Treyball,R.E.,(1960),AIChEJ,6,289

67 Huige,N.J.J.,(1972),Ph.D.Thesis,Eindhoven University of Technology

68 Kayaert,G.,(1974),Ph.D.Thesis,University of Leuven, Belgium

69 Flink,J.M. & Gejl-Hansen,F.,(1972),J.Sci.Food Agric.,20,691

70 Weast,R.C.,(1970),"Handbook of Chemistry and Physics",50th ed, Chemical Rubber Company, Clevelang

71 Luikov,A.V.,(1968),"Analytical Heat Diffusion Theory",Academic Press,New York

72 Carslaw,H.S. & Jaeger,J.C.,(1959),"Conduction of Heat in Solids",Clarendon Press,Oxford

73 Schoeber,W.J.A.H.,(1976),Ph.D.Thesis,Eindhoven University of Technology (in preparation)

74 Onsager,L.,(1945),Ann.New York Acad.Sci.,46,241

STELLINGEN

1. De betekenis van de techniek van de Laplace en Fourier trans-
   formaties op proceskundig terrein komt in het basisprogramma
   voor de opleiding tot scheikundig ingenieur aan de THE onvol-
   doende tot uitdrukking.

2. Uit eigen berekeningen (1) is vast komen te staan, dat de door
   Sjenitzer (2) aangegeven methode voor het berekenen van de
   fractionele verdamping van druppels als functie van de afgeleg-
   de weg in sproeidrogers kan leiden tot grote onnauwkeurigheden.

   (1) Kerkhof, P.J.A.M. & Schoeber, W.J.A.H. (1974),
   "Advances in Preconcentration and Dehydration of Foods", Ed.A.
   Spicer, Appl.Sci.Publ.,London, 349
   (2) Sjenitzer, F.,(1952),Chem.Eng.Sci.,$\underline{1}$,101

3. De door van der Sluijs (3) gegeven interpretatie van zijn expe-
   rimenten, dat er geen stofoverdrachtslimitering optreedt bij de
   continue tegenstroomhydrolyse van vetten in gepakte kolommen,
   is niet juist. Het verdient aanbeveling door nader onderzoek na
   te gaan in hoeverre deze onjuiste interpretatie de bruikbaar-
   heid van zijn ontwerpregels voor industriële installaties
   beïnvloedt.

   (3) Sluijs, W.van der, (1967), Proefschrift THE, 94,113

4. Het gebruik van de door Adolphi (4) gedefinieerde overdrachts-
   coëfficiënt in tegenstroomuitwisselaars dient afgeraden te
   worden, aangezien de effecten van menging en lokale overdracht
   hierin niet gescheiden worden.

   (4) Adolphi, G., (1962),Chem.Techn.,$\underline{14}$,516

5. In hun beschouwingen over het probleem van instationaire
   diffusie in en rond een stilstaande bol in een oneindig medium,
   is door Plöcker en Schmidt-Traub (5) een tijdsafhankelijke
   stoftransportcoëfficiënt gedefinieerd op basis van de momentane

stofflux en de initiële drijvende kracht. De gangbare definitie
van de stoftransportcoëfficiënt aan de hand van de momentane
drijvende kracht verdient echter de voorkeur, zowel op basis
van de fysische interpretatie, als vanwege het gedrag van de
stoftransportcoëfficiënt bij langere tijd.

(5) Plöcker, U.J. & Schmidt-Traub, H.,(1972), Chem.
Ing. Techn.,44,(5), 313

6. Uit eigen onderzoek (6) is gebleken dat de warmteoverdracht aan
bollen onder snel periodiek wisselende externe overdrachtscoëf-
ficiënten beschreven kan worden met een effectief Biot getal,
onafhankelijk van de wisselingsfrequentie.

(6) Nistelrooij, H.J.M. van & Lucassen, I.M.J.J.,(1974),
Praktikumrapport Fysische Technologie, THE

7. De door Karel (7) gehanteerde vergelijking voor de verdeling
van water in een drogende aardappelschijf is onjuist. Zijn
hierop gebaseerde berekeningen van bruinkleuring tijdens dit
droogproces zijn dan ook aanvechtbaar.

(7) Karel, M. (1974), "Advances in Preconcentration and
Dehydration of Foods", Ed.A.Spicer, p.45

8. Het verdient aanbeveling om operatieve handelingen op huis-
dieren, zoals castratie en couperen, uitsluitend toe te staan
in geval van medische indikatie.

20-6-1975   P.J.A.M. Kerkhof